ENVIRONMENTAL STUDIES

Greenhouse gas emissions from African lakes are no longer a blind spot

Alberto V. Borges[1]*, Loris Deirmendjian[1]†, Steven Bouillon[2], William Okello[3], Thibault Lambert[1]‡, Fleur A. E. Roland[1], Vao F. Razanamahandry[2], Ny Riavo G. Voarintsoa[2]§, François Darchambeau[1]¶, Ismael A. Kimirei[4], Jean-Pierre Descy[1], George H. Allen[5], Cédric Morana[1,2]

Natural lakes are thought to be globally important sources of greenhouse gases (CO_2, CH_4, and N_2O) to the atmosphere although nearly no data have been previously reported from Africa. We collected CO_2, CH_4, and N_2O data in 24 African lakes that accounted for 49% of total lacustrine surface area of the African continent and covered a wide range of morphology and productivity. The surface water concentrations of dissolved CO_2 were much lower than values attributed in current literature to tropical lakes and lower than in boreal systems because of a higher productivity. In contrast, surface water–dissolved CH_4 concentrations were generally higher than in boreal systems. The lowest CO_2 and the highest CH_4 concentrations were observed in the more shallow and productive lakes. Emissions of CO_2 may likely have been substantially overestimated by a factor between 9 and 18 in African lakes and between 6 and 26 in pan-tropical lakes.

INTRODUCTION

A better understanding of the aquatic biogeochemical cycle of greenhouse gases (GHGs; CO_2, CH_4, and N_2O) and a more precise estimate of GHGs emissions at regional and global scales are essential to implement realistic pathways to attenuate climate change and assess the effectiveness of mitigation strategies. The emission of GHGs from inland waters (streams, rivers, lakes, and reservoirs) to the atmosphere could be important for global budgets (*1*–*5*), although estimates are very poorly constrained. For lakes, this is due to a general low data coverage of GHGs that is additionally geographically skewed, with an overrepresentation in global datasets of North America and Scandinavia, while tropical regions are much less covered. Tropical lakes (representing 13% of the global lake surface area) accounted for 34% of the global lake CO_2 emission, although they were represented by only 1.5% of the CO_2 dataset used in the global estimate of a zonally explicit scaling study of lacustrine CO_2 fluxes (*4*). Data used for tropical regions had been obtained mainly in South America but were virtually nonexistent in African systems, although they contributed to a third of the estimated tropical lacustrine CO_2 emissions.

This lack of data in tropical lakes is a major impediment for global extrapolations because cycling of GHGs in tropical lakes cannot be readily understood from the principles that apply to temperate and boreal systems. Annually integrated primary production is potentially three times higher in tropical lakes (per unit of area) than in their temperate and boreal counterparts (based on theoretical considerations) (*6*). This is due to light and temperature conditions that are favorable for phytoplankton development year-round in tropical lakes but only during spring-summer in boreal and temperate lakes (*6*). In tropical lakes, a less vertically stable water column is favorable to nutrient inputs from deep to surface waters, but in temperate and boreal lakes, strong thermal vertical gradients in summer (when light conditions are most favorable) limit vertical nutrient inputs. Another notable difference is the higher content (by a factor of ~2) of dissolved organic carbon (DOC) in surface soils in boreal regions in North America and Scandinavia (where the bulk of lacustrine CO_2 data have been acquired so far) compared to tropical regions, even in rainforests (*7*). High DOC content in surface soils should enhance the hydrological transfer of DOC from soils to lakes and lead to an increase of the CO_2 content that usually correlates to DOC concentration in boreal lakes (*2*, *8*). Conversely, enhanced heterotrophic activity due to higher year-round temperatures in tropical lakes has been assumed to support high aquatic CO_2 production and emission to the atmosphere (*9*, *10*). The East African rift valley is the second major locus of large lakes on Earth after North America, yet it is nearly uncharted in terms of their GHGs emissions.

RESULTS AND DISCUSSION

Humic content and lake morphology explain the interlake variability of GHGs

Data on dissolved concentrations of CO_2, CH_4, and N_2O were collected in surface waters of 24 natural lakes (Fig. 1 and tables S1 and S2), covering a wide range of altitude (9 to 2536 m), surface area (0.2 to 67,075 km^2), average depth (0.1 to 572 m), surface water temperature (19.4° to 34.9°C), physical structure (holomictic to meromictic), and catchment land cover (savannah versus rainforest). This wide range of morphological and physiographical attributes was reflected in an equally wide range in medians of the partial pressure of CO_2 (pCO_2) [11 to 3143 parts per million (ppm)], CH_4 concentration

[1]Chemical Oceanography Unit, University of Liège, Liège, Belgium. [2]Department of Earth and Environmental Sciences, KU Leuven, Leuven, Belgium. [3]Department of Limnology, National Fisheries Resource Research Institute, Jinja, Uganda. [4]Tanzania Fisheries Research Institute, Dar es Salaam, Tanzania [5]Department of Geography, Texas A&M University, College Station, TX, USA.
*Corresponding author. Email: alberto.borges@uliege.be
†Present address: Géosciences Environnement Toulouse UMR 5563 and UR 234 IRD, Université Paul-Sabatier, Toulouse, France.
‡Present address: Institute of Earth Surface Dynamics, University of Lausanne, Lausanne, Switzerland.
§Present address: Department of Earth and Atmospheric Science, University of Houston, Texas, USA.
¶Present address: Direction générale opérationnelle Agriculture, Ressources Naturelles et Environnement, Service Public de Wallonie, Namur, Belgium.

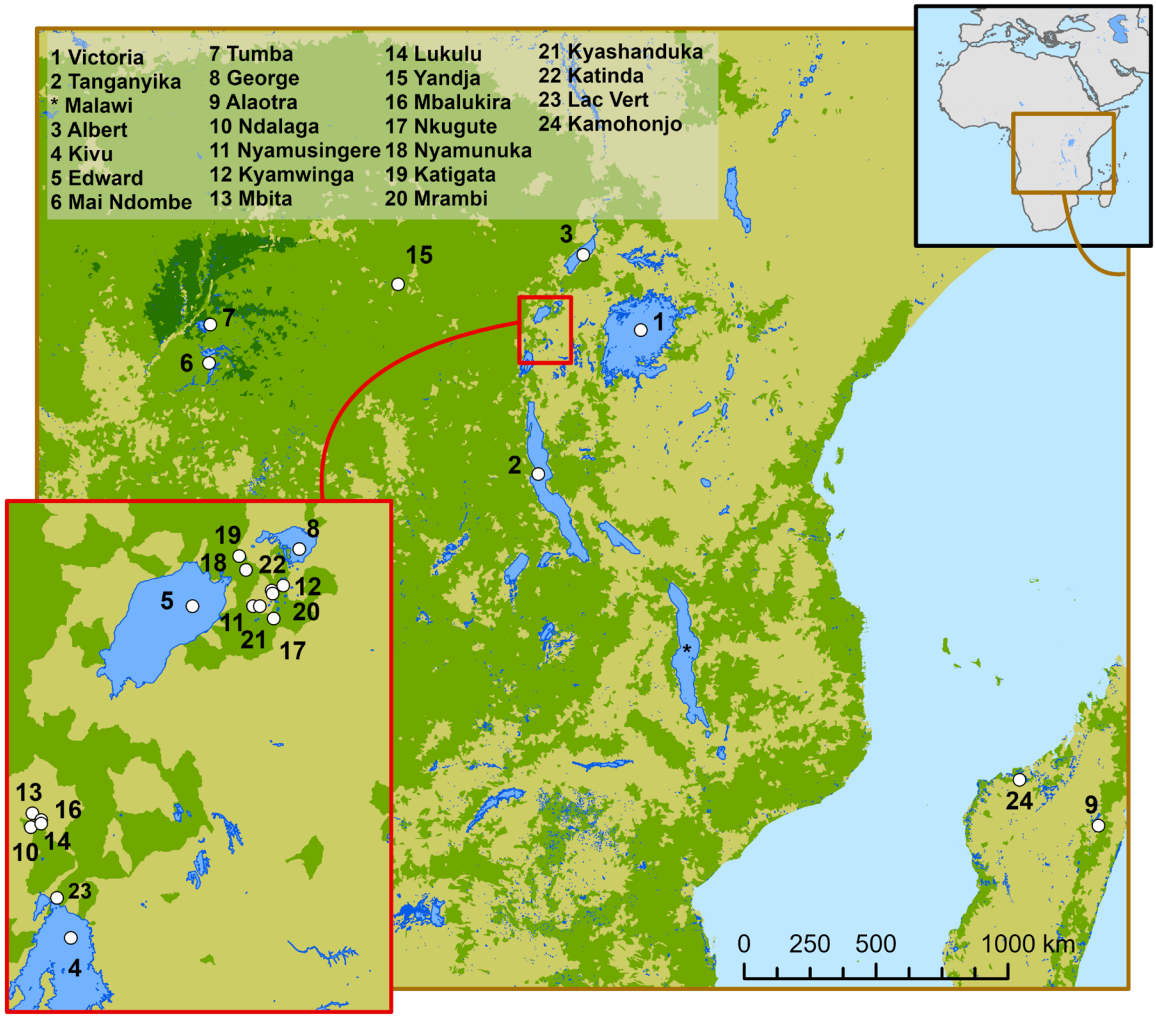

Fig. 1. Location of the 24 sampled African lakes, plus Lake Malawi (*48*). This dataset of CO_2, CH_4, and N_2O in surface waters covers a wide range of morphological conditions (surface area and depth), water column physical structure, catchment land cover, and lake productivity. Map indicates cover by savannah, forest, and flooded forest (from lightest to darkest shade of green).

(19 to 490,749 nM), N_2O saturation level (%N_2O) (8 to 381%), and phytoplankton biomass as indicated by the chlorophyll a (Chl-a) concentration (0.5 to 1,170 μg liter^{-1}).

We distinguished nonhumic lakes from humic lakes that are characterized by high concentrations of DOC and colored dissolved organic matter (CDOM) of terrigenous origin, characterized by low values of slope ratio (SR) (*11*). Consequently, we used the SR of CDOM (*11*) as a separation criterion and classified lakes with an SR < 1 as humic and lakes with an SR > 1 as nonhumic. In temperate and boreal lakes, these two types of lakes differ in terms of phytoplankton productivity and overall carbon cycling (*12*), and we hypothesize that they also behave differently in terms of the dynamics of GHGs (*13*).

The four sampled humic lakes (Mai Ndombe, Tumba, Alaotra, and Kamohonjo) showed higher pCO_2 and %N_2O and lower Chl-a values than the other (nonhumic) lakes at similar average depths and surface areas (Fig. 2). The pCO_2 and %N_2O values were negatively related to CDOM SR (Fig. 3 and fig. S1), showing that the content of these two GHGs increased with humic content of the sampled lakes. Dissolved CH_4 concentrations were unrelated to CDOM SR.

The average pCO_2 and %N_2O values in nonhumic lakes were positively related to both lake surface area and average depth, while CH_4 and Chl-a were negatively related to these morphological variables (Fig. 2). Surface waters were always oversaturated in CH_4 relative to the atmosphere. Among nonhumic lakes, smaller (shallower) lakes were generally undersaturated in CO_2 and N_2O relative to the atmosphere (i.e., acting as atmospheric sinks for both these gases), while larger (deeper) lakes were close to equilibrium with the atmosphere (slightly above or below saturation). Humic lakes, in contrast, were markedly oversaturated in CO_2 and N_2O (Fig. 2).

At the scale of individual lakes, CH_4 also followed a decreasing pattern as a function of depth (Fig. 4). At shallow depths (<10 m), the highest CH_4 values were observed in Lakes Victoria and Albert compared to Lakes Tanganyika and Edward. At depths >40 m, the CH_4 in surface waters of Lake Tanganyika was higher than Lakes Victoria and Albert (Fig. 4). This pattern was consistent with the meromictic nature of Lake Tanganyika that leads to very high concentrations of CH_4 in bottom anoxic waters, higher than in the holomictic Lakes Edward and Victoria (fig. S2), where CH_4 content in

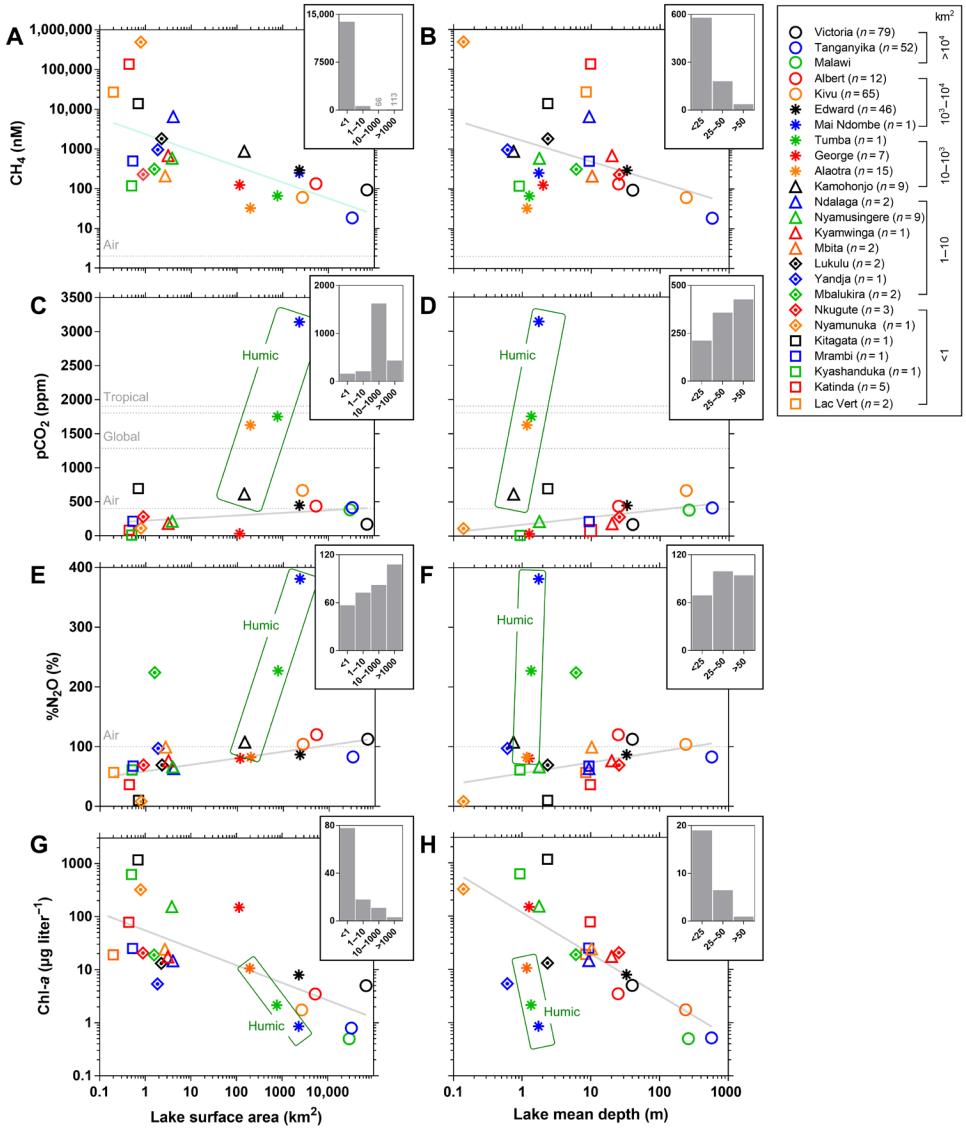

Fig. 2. Lake morphology controls CH_4, N_2O, and CO_2 in lacustrine surface waters. Surface water–dissolved CH_4 concentration (**A** and **B**), pCO_2 (**C** and **D**), N_2O saturation level (%N_2O) (**E** and **F**), and Chl-a concentration (**G** and **H**) in 24 African tropical lakes versus lake surface area and average depth. For lakes where multiple measurements were made, the symbol shows the median (*n* indicates the number of samplings, detailed in table S7). Insets show data binned (median) by classes of surface area or depth. Horizontal dotted lines indicate the atmospheric equilibrium of the three gases, additionally for CO_2 two average estimates for tropical (*4*, *7*) and global lakes (*1*). Solid lines are fits to the data (table S3) from which humic lakes were excluded for pCO_2 and %N_2O. Data of pCO_2 in Lake Malawi were obtained by another group but with a comparable high-quality method (equilibrator coupled to an infrared CO_2 analyzer) (*48*). CO_2 and %N_2O data in humic lakes were clustered but did not show a pattern with lake surface and mean depth, so the median was used to upscale the values at continental scale. CO_2 and %N_2O in nonhumic lakes were positively related to mean depth and these relations were used to scale the values at continental scale. CH_4 was negatively related to mean depth, irrespective of the lake type, and this relation was used to scale values at continental scale.

bottom waters strongly varies seasonally with changes in vertical thermal stratification and oxygenation levels (fig. S3).

A complex combination of sources and sinks of GHGs

The content of CO_2, CH_4, and N_2O in surface waters of lakes results from the balance of several sources and sinks that are specific to each gas (listed and explained in figs. S4 to S6). The relative importance of these sources and sinks varies as a function of external drivers (e.g., inputs of allochthonous organic matter and nutrients) and internal drivers (e.g., organic matter production and degradation), related to catchment proprieties (land cover), lake morphology (size and shape), and climate (precipitation). Lake surface area and depth are simple metrics and have been shown to be good predictors in boreal lakes of CO_2 and CH_4 concentrations [e.g., (*14*)], as well as of aquatic ecosystem metabolism (*15*) defined as the balance between production of autochthonous organic (primary production, *P*) and degradation of organic matter (respiration, *R*).

In nonhumic lakes, pCO_2 values were lower in the smallest and shallower lakes (Fig. 2). We interpret this pattern as resulting from higher phytoplankton biomass and *P* in shallower lakes, as shown

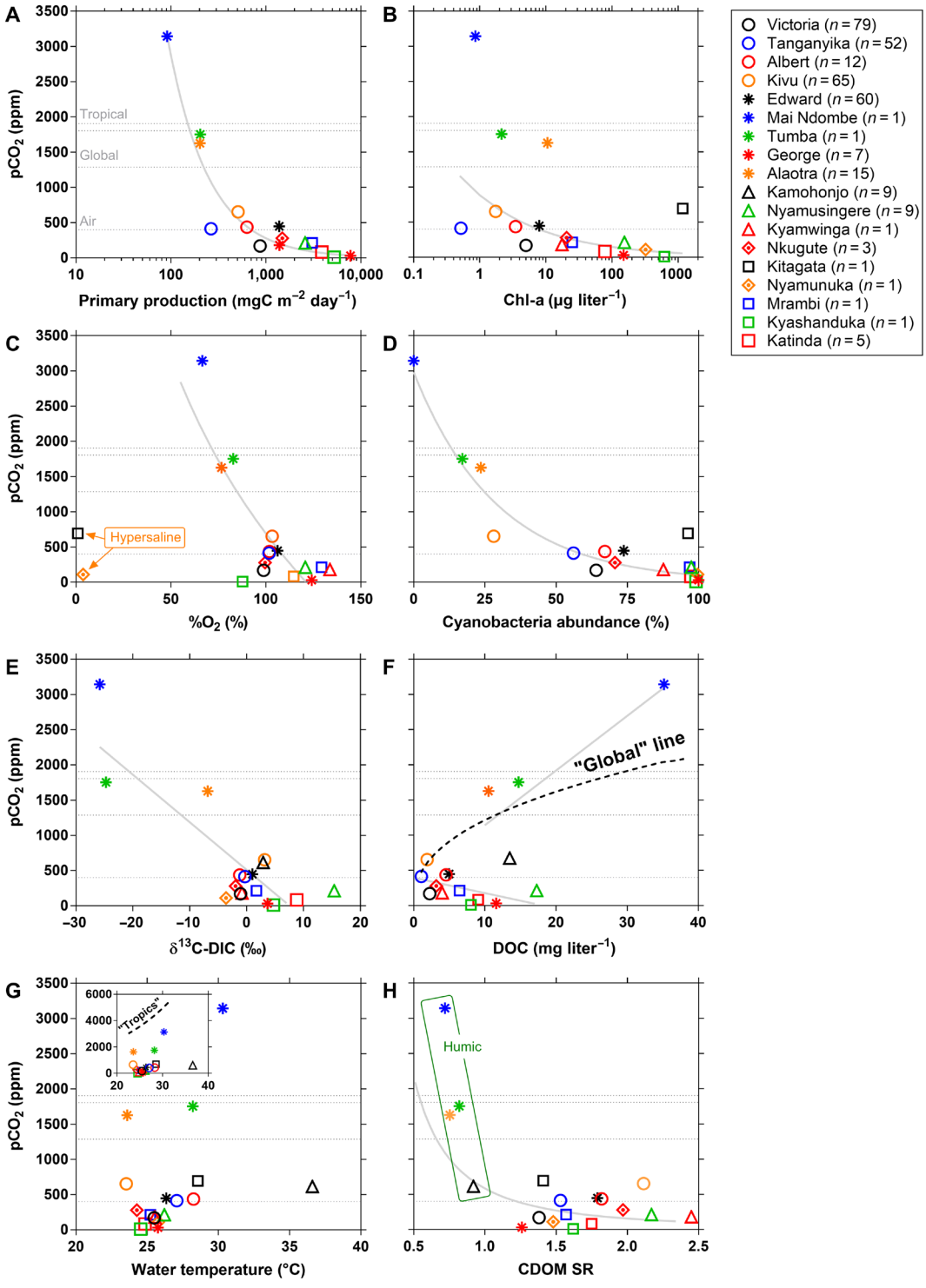

Fig. 3. CO_2 levels are highly variable among African lakes and patterns depend on primary production. Surface water pCO_2 in several African tropical lakes versus pelagic aquatic primary production (**A**), Chl-a concentration (**B**), oxygen saturation level ($\%O_2$) (**C**), cyanobacteria abundance (**D**), carbon stable isotope composition of dissolved inorganic carbon (δ^{13}C-DIC) (**E**), DOC (**F**), water temperature (**G**), and CDOM SR (**H**). Dotted lines and solid lines as in Fig. 2. The black dotted line gives the relation of pCO_2 versus DOC from a global dataset (*2*), while the black dotted line in the inset gives the relation of pCO_2 versus temperature from a dataset of tropical lakes (*9*). For lakes where multiple measurements were made, the symbol shows the median (*n* indicates the number of pCO_2 measurements).

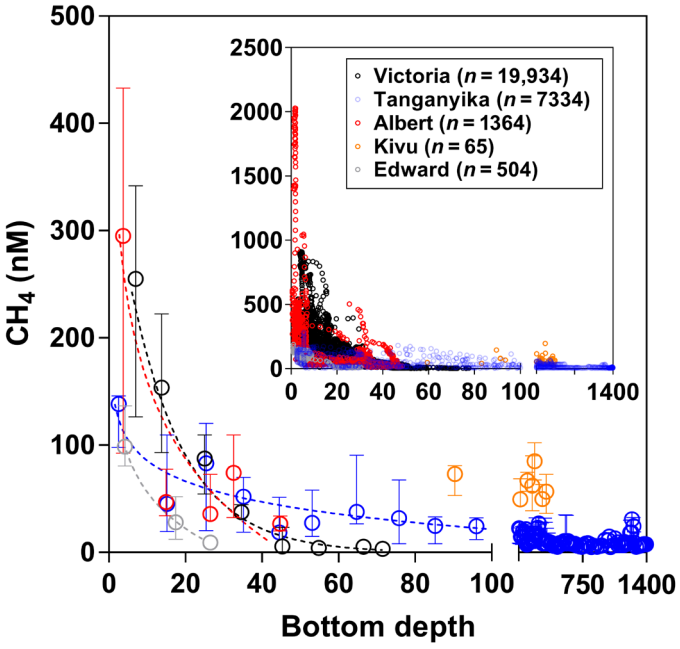

Fig. 4. CH_4 strongly varies as a function of bottom depth within lakes. Continuous measurements of dissolved CH_4 concentrations were made in Lakes Victoria, Tanganyika, Albert, Kivu, and Edward, with an equilibrator connected to a laser spectrometer except for Lake Kivu (compilation of 65 discrete samples measured by headspace with a gas chromatograph obtained during five cruises; *n* indicates the number of measurements). The inset shows the raw data, and the main panel shows the data binned by depth intervals of 10. Dotted lines are the curves fitted to data (table S3). Data bins per depth interval were combined with bathymetry maps to derive CH_4 (and pCO_2; not shown here) values spatially representative of the largest lakes, accounting for the strong horizontal gradients as a function of depth.

by the negative relation between Chl-a and depth (Fig. 2). This is probably due to the proximity of surface waters and the sediment in shallow lakes that allows a replenishment of surface waters in nutrients diffusing from the sediment (*15*). Nonhumic large lakes were characterized by lower phytoplankton biomass (Fig. 2) due to increasing depth and disconnection between surface (illuminated) waters and the nutrient-rich deeper waters. In parallel, the relative importance of terrestrial (allochthonous) organic and inorganic carbon inputs decreases relative to lake area and volume, hence having a lower impact on CO_2 levels in larger lakes (fig. S4). In larger lakes, higher gas transfer velocity (*k*) values (*16*) contribute to the equilibration of surface waters (this applies to the three gases). The combination of these putative drivers (see also fig. S4) could explain the general positive relationship between pCO_2 and lake size (surface area and depth) that we observed in nonhumic lakes (Fig. 2).

In humic lakes, high CDOM content decreases light penetration in the water column, strongly limiting phytoplankton growth and planktonic *P*, and the high content of terrestrial DOC should also sustain microbial degradation of organic matter (*12*). In addition, the sampled humic lakes were characterized by important wetland coverage (table S1) that should have sustained a large lateral input to the lakes of CO_2 from flooded soils (*17*). The combination of these putative drivers could explain the higher pCO_2 values observed in the humic lakes than in nonhumic lakes at similar depths or surface areas (Fig. 2); this interpretation agrees with the general patterns of pCO_2 and other variables shown in Fig. 3.

When combining data from both humic and nonhumic lakes, pCO_2 was negatively related to *P* and Chl-a (Fig. 3). In shallow lakes, extremely high Chl-a values were attained (Fig. 2) related to the occurrence of cyanobacteria. Numerous species of cyanobacteria can overcome nitrogen (N) limitation through N_2-fixation, as well as CO_2 limitation (by using HCO_3^- for photosynthesis) and light limitation because of higher light harvesting capabilities than most other phytoplankton groups (*18*). Together, these features provide cyanobacteria with a competitive advantage in warm, productive, and shallow waters over other phytoplankton groups (*18*). This could then possibly explain the general negative relationship between pCO_2 and the abundance of cyanobacteria observed in the sampled lakes (Fig. 3). Relations between pCO_2 and other variables can also be interpreted as resulting from a dominance of organic matter degradation in humic lakes and a stronger influence of carbon fixation by phytoplankton in nonhumic lakes. The negative relationship between pCO_2 and the carbon stable isotope composition of dissolved inorganic carbon (δ^{13}C-DIC) possibly resulted from a combination of two processes: (i) the input of CO_2 in humic lakes from the degradation of plant organic matter with mostly a C_3 photosynthetic pathway (woody plants and trees have $\delta^{13}C$ values of ~−27‰), leading to low δ^{13}C-DIC values and high pCO_2 values and (ii) the preferential removal of dissolved $^{12}CO_2$ by emission to the atmosphere and of the uptake of $^{12}CO_2$ by photosynthesis in nonhumic lakes leading to higher δ^{13}C-DIC values and low pCO_2 values. Note that there were no clear patterns between CO_2 levels and HCO_3^- levels in the sampled African lakes (fig. S7). $\%O_2$ levels can also be used as indicators of ecosystem metabolism, and in general, the lakes with low pCO_2 were also oversaturated in O_2, except in two hypersaline lakes (Kitagata and Nyamunuka) where $\%O_2$ values were very low and deviated from the general pCO_2-$\%O_2$ pattern, likely because of chemical consumption of O_2 from the oxidation of H_2S diffusing from the sediments to surface waters. Both the air-water gradient of pCO_2 (ΔpCO_2) and air-water CO_2 flux (FCO_2) showed an increasing sink of atmospheric CO_2 with lake net autotrophy, quantified by the ratio of planktonic *P* to *R* above 1 and a positive net ecosystem production (NEP = *P* − *R*) (Fig. 5). The lack of relation between pCO_2 in the sampled lakes and terrestrial vegetation biomass on the catchment (fig. S8) suggests two possible explanations: (i) The effects of the variations of lake size (Fig. 2 and fig. S4) have a stronger influence on CO_2 dynamics than the variations of the inputs of allochthonous carbon due to changes in terrestrial vegetation biomass, and/or (ii) internal processes independent of allochthonous carbon inputs also control CO_2 levels in these lakes, particularly planktonic *P* in nonhumic shallow lakes.

There were no clear differences between humic and nonhumic lakes in CH_4 as a function of lake surface area and mean lake depth (Fig. 2). The highest CH_4 concentrations were observed in the shallowest lakes (Fig. 2). This might reflect the relatively higher input of CH_4 from sediments to the water per unit of water volume in the shallowest lakes (fig. S5). Conversely, in the deeper and larger lakes, deeper mixed layers might promote microbial methane oxidation (MOX), while more marked thermal vertical stratification isolates the epilimnion (where CH_4 is removed by MOX and by the emission to the atmosphere) from the hypolimnion (where CH_4 accumulates) (fig. S5). In addition, shallower lakes were also the most productive (Fig. 2); hence, there should have been a larger delivery to the sediments of fresh organic matter from phytoplankton detritus. This, in turn, should lead to intense benthic organic matter

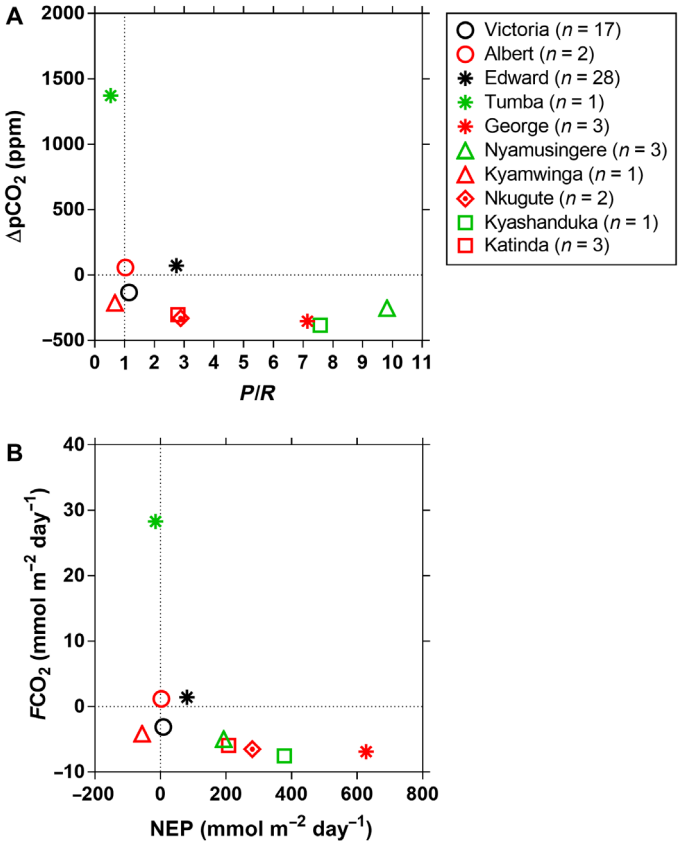

Fig. 5. Net ecosystem autotrophy drives a CO_2 sink in most of the studied African lakes. Variations in several African tropical lakes of the air-water gradient of the pCO_2 (ΔpCO_2) as a function of the ratio of aquatic pelagic primary production (*P*) and community respiration (*R*) (**A**) and the air-water CO_2 flux (FCO_2) as a function of NEP (**B**). $P/R > 1$ and NEP > 0 correspond to net autotrophy at the community level and is, in most cases, associated with being a sink of atmospheric CO_2 ($\Delta pCO_2 < 0$, $FCO_2 < 0$). For lakes where multiple measurements were made, the symbol shows the median (*n* indicates the number of measurements).

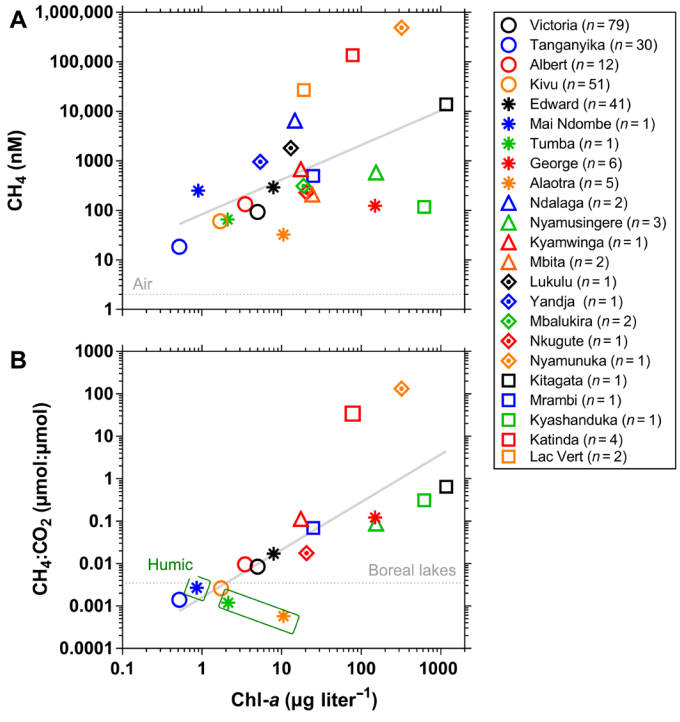

Fig. 6. CH_4 levels in surface waters of African lakes are driven by lacustrine productivity. Dissolved CH_4 concentrations (**A**) and ratio of dissolved CH_4 and CO_2 concentrations (**B**) versus Chl-a concentration in surface waters of several African tropical lakes. Horizontal dotted line represents the equilibrium with the atmosphere (top) and the average value for boreal lakes (*26*). Solid line is a fit to the data (table S3). For lakes where multiple measurements were made, the symbol shows the median (*n* indicates the number of measurements). For CH_4, no relation was observed with other measured variables. The positive relation of CH_4 and Chl-a should be interpreted as resulting from the dependence of CH_4 in surface waters from sedimentary CH_4 fluxes to the water column (*22*) that were higher in shallow and productive systems (fig. S9), while in stratified deep systems, the CH_4 removal by MOX led to low-surface CH_4 (*49*).

degradation including methanogenesis and, consequently, high sediment-water CH_4 fluxes (fig. S9). The combination of these putative drivers (fig. S5) could explain the general negative relation between CH_4 and lake depth and surface area that we report across different lakes (Fig. 2), as well as the variations with bathymetry within a single lake (Fig. 4). Furthermore, this might also explain the positive correlation between CH_4 and Chl-a (Fig. 6). Such a relation has been previously interpreted by some studies as resulting from the production of CH_4 in aerobic conditions (*19*), either directly (*20*) or indirectly (*21*) linked to phytoplankton metabolism. Although production of CH_4 in aerobic conditions linked to phytoplankton metabolism was shown to occur in five African lakes, the related input flux to the water column was orders of magnitude lower than sedimentary CH_4 inputs to the water column (*22*). In nonhumic lakes, high phytoplankton biomass also led to low CO_2 values that, combined with high CH_4, also resulted in an overall positive relation between the CH_4:CO_2 ratio and Chl-a (Fig. 6).

In nonhumic lakes, $\%N_2O$ was negatively related to lake depth (Fig. 2), being close to atmospheric equilibrium in the deeper lakes and below atmospheric equilibrium in the shallowest lakes. In these lakes with low dissolved inorganic N (DIN) levels, sedimentary denitrification could be involved in the uptake of N_2O from the water-column and explain the observed N_2O undersaturation (figs. S6 and S9). The N_2O undersaturation was more marked in the shallowest nonhumic lakes where intense sedimentary denitrification rates, sustained by high organic matter deposition on the sediments (phytoplankton detritus), should occur.

In humic lakes, N_2O was distinctly above atmospheric equilibrium (Fig. 2), indicating sedimentary or water column N_2O net production. In humic lakes, low phytoplankton *P* and microbial mineralization of organic matter led to relatively higher levels of DIN (*23*) that can sustain N_2O production (fig. S6). The combination of these putative drivers could explain the negative relations between $\%N_2O$ and primary production, Chl-a, and CDOM SR and the positive relation between $\%N_2O$ and DOC concentrations (fig. S1).

Comparison with boreal and other tropical lakes of GHGs

The increase of CH_4 and the decrease of CO_2 with phytoplankton biomass (Figs. 3 and 6) led to higher CH_4 and lower CO_2 values in surface waters in African lakes compared to boreal systems (Fig. 7) where phytoplankton biomass is typically low and seasonally restricted to spring and summer. Higher temperatures in tropical lakes compared to boreal lakes are also more favorable for methanogenesis

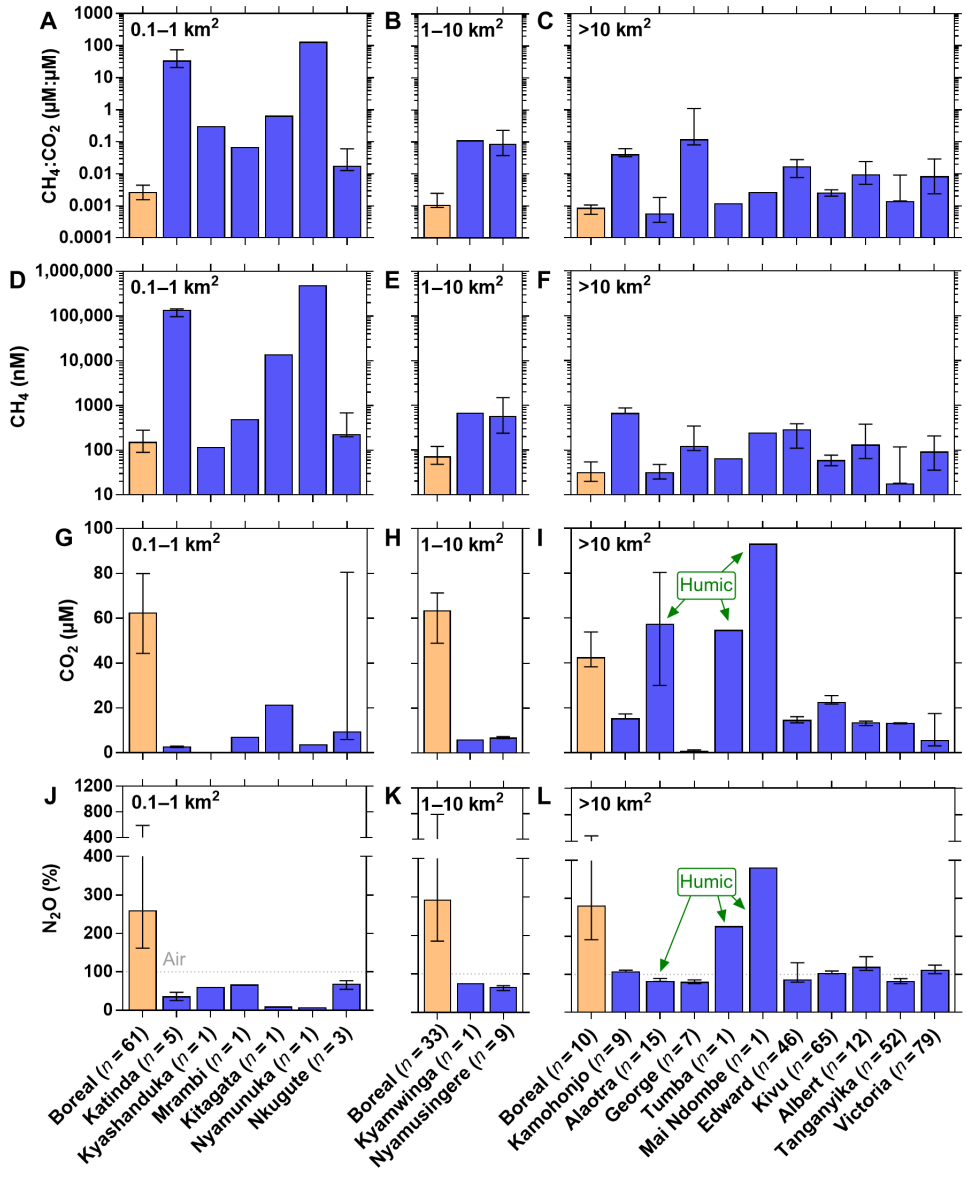

Fig. 7. CH_4 is higher and CO_2 is lower in African lakes than in boreal lakes. The ratio of dissolved CH_4 and CO_2 concentrations (**A** to **C**), dissolved CH_4 (**D** to **F**), CO_2 (**G** to **I**) concentrations, and N_2O saturation levels (%N_2O) (**J** to **L**) in surface waters of several African tropical lakes compared to paired CO_2 and CH_4 measurements ($n = 224$) in lakes located in the boreal climatic zone compiled from literature in (*26*) located in Finland, Canada, Siberia (latitude, >60°N) and %N_2O in Finland (*50*) sorted into three size classes (0.1 to 1 km^2, 1 to 10 km^2, and >10 km^2). Surface water temperature in boreal lakes was 9.8°C (median) versus 25.8°C in African lakes. Box indicates the median; bars indicate the first and third quartile. *n* indicates the number of data points.

(*24*). Comparatively higher soil DOC content at boreal latitudes (*7*) should also lead to a stronger enrichment in terrestrial DOC in boreal lakes compared to tropical lakes of similar size. As CO_2 increases with DOC in boreal lakes (*8*, *13*), this could also help explain why the CO_2 values in boreal lakes were higher than in African lakes (Fig. 7). Only in three African humic lakes was CO_2 higher than the median in large boreal lakes (Fig. 7). Boreal lakes were strongly oversaturated in %N_2O compared to tropical African lakes that were undersaturated for the smaller ones (surface area, <10 km^2), while larger ones (surface area, >10 km^2) were close to saturation, except for two humic ones in which %N_2O values were comparable to values in boreal lakes (Fig. 7).

The pCO_2 values in 22 lakes were lower than the values reported in the literature as representative for lakes globally (*1*) and the tropics (*4*, *9*) except for three of the humic lakes (Fig. 2). In addition, pCO_2 values in the sampled African lakes were below the relationship of pCO_2 as a function of temperature assumed to be representative of the tropics (Fig. 3G) (*9*), and most of our pCO_2 values were below the relationship for pCO_2 versus DOC for lakes globally (Fig. 3F) (*2*). In nonhumic lakes, pCO_2 was negatively related to DOC (Fig. 3F) most likely originating from phytoplankton exudates, as confirmed by the high CDOM SR values (Fig. 3H) and by the positive relation between DOC and Chl-a and cyanobacteria relative abundance (Fig. 8). In humic lakes, however, pCO_2 was positively related to

DOC as previously reported (*2*, *8*). Consequently, a positive correlation between pCO_2 and DOC does not seem to be a universal feature as frequently reported in literature (*2*, *8*), and in African lakes, it only applied to humic lakes. Note also that we report a positive relation between pCO_2 and lake surface area in nonhumic lakes (Fig. 2), although a negative relation between these variables has been repeatedly reported in boreal lakes at the local (*25*), regional (*8*, *14*), and global scale (*4*, *26*).

The surface area–weighted average pCO_2 for the sampled African lakes (plus Lake Malawi) of 400 ppm was only slightly above atmospheric equilibrium (388 ppm) and distinctly lower than the reported average pCO_2 values in South American tropical lakes (1804 to 2270 ppm) (*9*, *10*), which represent the bulk of data reported so far for tropical lakes. There could be several explanations for these differences, such as an overrepresentation of floodplain lakes and very small water bodies in the South American CO_2 datasets. The latter explanation is also consistent with a lower average pCO_2 value (1007 ppm) reported in 12 large (>500 km^2) tropical lakes (*27*). In addition, most of these studies were based on data that were indirectly calculated from pH and total alkalinity (TA), when it has been shown that this method is prone to extremely large errors due to measurement biases on both pH and TA and tends to strongly overestimate CO_2 levels particularly in humic lakes characteristic of floodplains (*28*).

GHG fluxes in African tropical and pan-tropical lakes

The FCO_2 and the air-water diffusive fluxes of CH_4 (FCH_4) and N_2O (FN_2O) were upscaled for tropical lakes (24°S to 24°N) with a surface area >0.1 km^2, at African and pan-tropical scales (Table 1). FCO_2, FN_2O, and diffusive FCH_4 per square meter were lower in nonhumic than humic lakes at African and pan-tropical scales (table S4). Lake Chad alone accounted for 47% of FCO_2, 87% of diffusive FCH_4, and 52% of FN_2O integrated for African humic lakes (table S4). For the initial upscaling, we used the surface area for Lake Chad of 18,752 km^2 given by HydroLAKES (*29*), although recent remote sensing data provide a much lower value of 2603 km^2 for the 1989–2017 period (*30*), reflecting its marked shrinkage since the 1980s due to climate change, as this lake is very shallow and located in an arid climatic zone. FCO_2, FCH_4, and FN_2O were recomputed using the more recent and more realistic surface area of Lake Chad (*30*), which we will consider hereafter as our nominal GHG flux values (Table 1).

The integrated FN_2O for pan-tropical lakes was 16 times lower than estimated from a global model (*31*). In African tropical lakes, the integrated FN_2O was negative, indicating a very small sink for atmospheric N_2O, while the global model (*31*) predicted a small source of N_2O to the atmosphere (Table 1). This global model computes N_2O (and FN_2O) from catchment N inputs and water

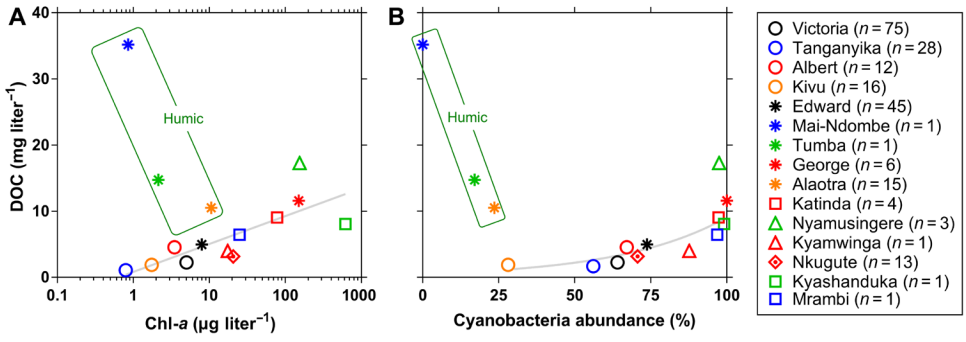

Fig. 8. Allochthonous versus autochthonous origin of DOC in African lakes depends on type (humic versus nonhumic). DOC versus Chl-a (**A**) concentration and versus cyanobacteria abundance (**B**) in surface waters of several African tropical lakes. Solid line is a fit to the data (table S3). For lakes where multiple measurements were made, the symbol shows the median (*n* indicates the number of measurements).

Table 1. Downward reevaluation of tropical lacustrine CO_2, CH_4, and N_2O emissions. Air-water flux of CO_2 (FCO_2), CH_4 (FCH_4, diffusive and ebullitive), and N_2O (FN_2O) integrated for African tropical and pan-tropical lakes (with a surface area >0.1 km^2) compared to previous estimates (details in table S4) (*1*, *3*, *4*, *9*, *31*, *47*). Values with a single asterisk (*) correspond to the scaling using the original HydroLAKES surface area (*29*), including an unrealistic surface area value of 18,752 km^2 for Lake Chad. Values with a double asterisk (**) were obtained with a more recent surface area value of 2603 km^2 for Lake Chad (*30*). n.a., not available.

		FCO_2	Diffusive FCH_4	Ebullitive FCH_4	FN_2O
		TgC year^{-1}	TgCH_4 year^{-1}	TgCH_4 year^{-1}	GgN_2O-N year^{-1}
African tropical lakes					
	This study (*)	**6.3 ± 1.9**	**1.3 ± 0.3**	**2.3 (0.8–5.5)**	**0.3 ± 0.2**
	This study (**)	**3.3 ± 1.0**	**0.4 ± 0.1**	**1.8 (0.6–4.1)**	**−0.1 ± 0.1**
	Previous studies	35.6	n.a.	n.a.	3.7
Pan-tropical lakes					
	This study (*)	**20.5 ± 10.7**	**1.6 ± 0.4**	**4.9 (1.7–11.4)**	**0.8 ± 1.1**
	This study (**)	**17.5 ± 9.5**	**0.7 ± 0.2**	**4.4 (1.5–10.0)**	**0.4 ± 0.7**
	Previous studies	103.1 to 441.6	3.1	22.2	6.5

residence time and accounts, also as a function of residence time, for the decrease of N_2O due to the reduction of N_2O to N_2, down to saturation but not below. The model cannot mathematically predict the undersaturation of N_2O that we observed in productive shallow lakes (Fig. 2) because it does not explicitly represent the denitrification process.

The integrated pan-tropical diffusive CH_4 emission was 4.5 lower than the one previously reported (*3*), and the difference was mostly related to the differences in total lake surface area values, as the diffusive FCH_4 per square meter was closer but still 2.5 times lower (table S4). We occasionally quantified ebullitive CH_4 emissions, found to be ~20 times higher than diffusive CH_4 emissions in two shallow productive lakes (George and Nyamusingire), but ebullitive and diffusive CH_4 fluxes were equivalent in deeper lakes (Edward and Victoria) (table S5). Combined with data reported mainly in South America (fig. S10), we estimated ebullitive CH_4 emissions of 1.8 [interquartile range (IQR): 0.6 to 4.1] $TgCH_4\ year^{-1}$ for African lakes and 4.4 (IQR: 1.5 to 10.0) $TgCH_4\ year^{-1}$ for pan-tropical lakes (Table 1 and table S6). The pan-tropical CH_4 ebullition emissions were six times lower than previously reported (*3*) because we only integrated the fluxes in the littoral zone (depth, <10 m) with a surface area totaling 135,206 km^2, while Bastviken *et al.* (*3*) integrated the fluxes over the total lacustrine area (585,536 km^2). The median ebullitive CH_4 flux per square meter that we upscaled [4.4 (IQR: 1.5 to 10.7) mmol $m^{-2}\ year^{-1}$] was close to the one used in (*3*) (6.5 ± 3.7 mmol $m^{-2}\ year^{-1}$). Yet, our CH_4 ebullition flux could be underestimated since it is based on open water lake values, while vegetated habitats have been shown to have very high emission rates (*32*). The pan-tropical lacustrine CH_4 emissions were dominated by ebullition compared to diffusion. The ratio of ebullitive to diffusive CH_4 lacustrine flux was ~6.3, close to the value of ~7.2 previously reported in (*3*), although the absolute numbers differ, as discussed above. Note that a downward reevaluation of CH_4 emissions from tropical lakes could contribute to partly close the gap of global CH_4 emission estimates based on the top-down approach (modeled from observations of atmospheric CH_4) and bottom-up approach (extrapolation per ecosystem of discrete flux estimates) (*33*).

Compared with previous reports, the integrated FCO_2 was 11 times lower for tropical African lakes (3.3 ± 1.0 $TgC\ year^{-1}$) and between 6 and 25 times lower for pan-tropical lakes (17.5 ± 9.1 $TgC\ year^{-1}$; Table 1 and table S4). The previously published CO_2 emission for large tropical lakes only (surface area larger than 500 km^2) of 5.4 $TgC\ year^{-1}$ (*27*) was also marginally higher than our own estimate for the same lake size class of 3.3 ± 1.7 $TgC\ year^{-1}$. This is related to the fact that FCO_2 per square meter was low or even negative in nonhumic lakes, although FCO_2 per square meter in humic lakes was similar to previous estimates (table S4). The pCO_2 values that we scaled were much lower than previously reported, between 1.8 and 4.3 times for African lakes and ~2.3 for pan-tropical lakes (table S4).

Integrated diffusive FCH_4 from African lakes (0.4 ± 0.1 $TgCH_4\ year^{-1}$) was lower than that from African rivers (~4.5 $TgCH_4\ year^{-1}$) (*34*). FCO_2 from African lakes (6 $TgC\ year^{-1}$) was also distinctly lower than that from African rivers (~300 $TgC\ year^{-1}$) (*34*). We conclude that African inland water CO_2 and CH_4 emissions are mainly lotic despite the fact that the total surface area of rivers and streams in Africa (68,560 km^2) is distinctly lower than that of tropical lakes (209,394 km^2). At the pan-tropical scale, lentic FCO_2 was also lower (18 $TgC\ year^{-1}$) than lotic FCO_2 (~1800 $TgC\ year^{-1}$) (*35*).

A large contribution to inland water CO_2 and CH_4 emissions from small water bodies (ponds) has been recently suggested (*26*) on the basis of data mainly collected in boreal systems (~190) and in a limited number of temperate systems (~40) but with no data for tropical systems. Small lakes, at tropical African and pan-tropical scales, were much more abundant than large lakes, although the relative surface area increased with lake size (Fig. 9). The relative surface area of large lakes (>1000 km^2) compared to the total was higher at the African scale (86%) than at the pan-tropical scale (63%). For humic African tropical lakes, FCO_2, diffusive FCH_4, and FN_2O regularly increased with lake size area (Fig. 9). In pan-tropical humic lakes, FCH_4, FCO_2, and FN_2O were more evenly distributed among size classes. For nonhumic lakes, diffusive FCH_4 tended to increase with lake size both at African and pan-tropical scales. For nonhumic lakes both at African and pan-tropical scales, the sink of atmospheric CO_2 increased with lake size but reverted to a source of CO_2 to the atmosphere for the largest size class. For nonhumic African and pan-tropical lakes, the sink of atmospheric N_2O also increased with lake size until the largest size class, for which the N_2O atmospheric sink decreased (Fig. 9).

Uncertainties in the computation and integration of GHG fluxes

Our strategy of data acquisition aimed first to describe interlake variations of GHG concentrations and, secondly, to describe the intralake spatial variations in the subset of the largest lakes (Victoria, Tanganyika, Albert, Kivu, and Edward). Consequently, the temporal variability was less constrained, particularly with regard to daily variations, since data were only acquired during daytime, as well as to seasonal variations, since lakes were only sampled repeatedly a few times (table S7).

Admittedly, diel variations were not represented explicitly in our estimates of CO_2 and CH_4 emissions from African lakes, but this should not radically change our overall conclusions that nonhumic lakes were low CO_2 sources or even sinks of atmospheric CO_2. We compared pCO_2 at dusk and dawn during the three cruises in Lake Victoria, and in only 11% of the comparisons of maximum diel amplitude of pCO_2 change (dusk-dawn difference) was there a change in the sign of ΔpCO_2 (direction of the flux) (fig. S11). In addition, the fact that data were mainly acquired during daytime should not have substantially underestimated the CO_2 emission rates because of supposedly much higher emission values during nighttime. On the contrary, diel measurement cycles in Lakes Kivu and Edward show that daytime CO_2 emissions were higher than nighttime because of higher daytime wind speed (fig. S12). This seemed to be a general feature in Lakes Victoria, Tanganyika, Kivu, and Edward (fig. S13). Furthermore, all previous estimates of CO_2 emissions from tropical lakes were presumably also based on daytime observations and did not account for the diel variations. Together, our conclusion that CO_2 emission estimates from tropical lakes are lower than those from previous studies remains valid. Daytime diffusive CH_4 emissions could be higher than nighttime values, possibly because of the photoinhibition of MOX (*22*), leading to higher CH_4 concentrations during daytime (also based on dusk-dawn comparisons of CH_4 in Lake Victoria; fig. S14) and higher daytime wind speed and k (fig. S13). Note that the difference between night- and daytime of CH_4 concentration inferred from dusk-dawn comparisons in Lake Victoria (fig. S14) was modest (median of −6 nM; range of −200 and 97 nM) compared to the range of spatial variations observed within Lake Victoria itself (3 to 911 nM; Fig. 4), as well as the range of CH_4 values across different lakes (19 to 490,749 nM; Fig. 2).

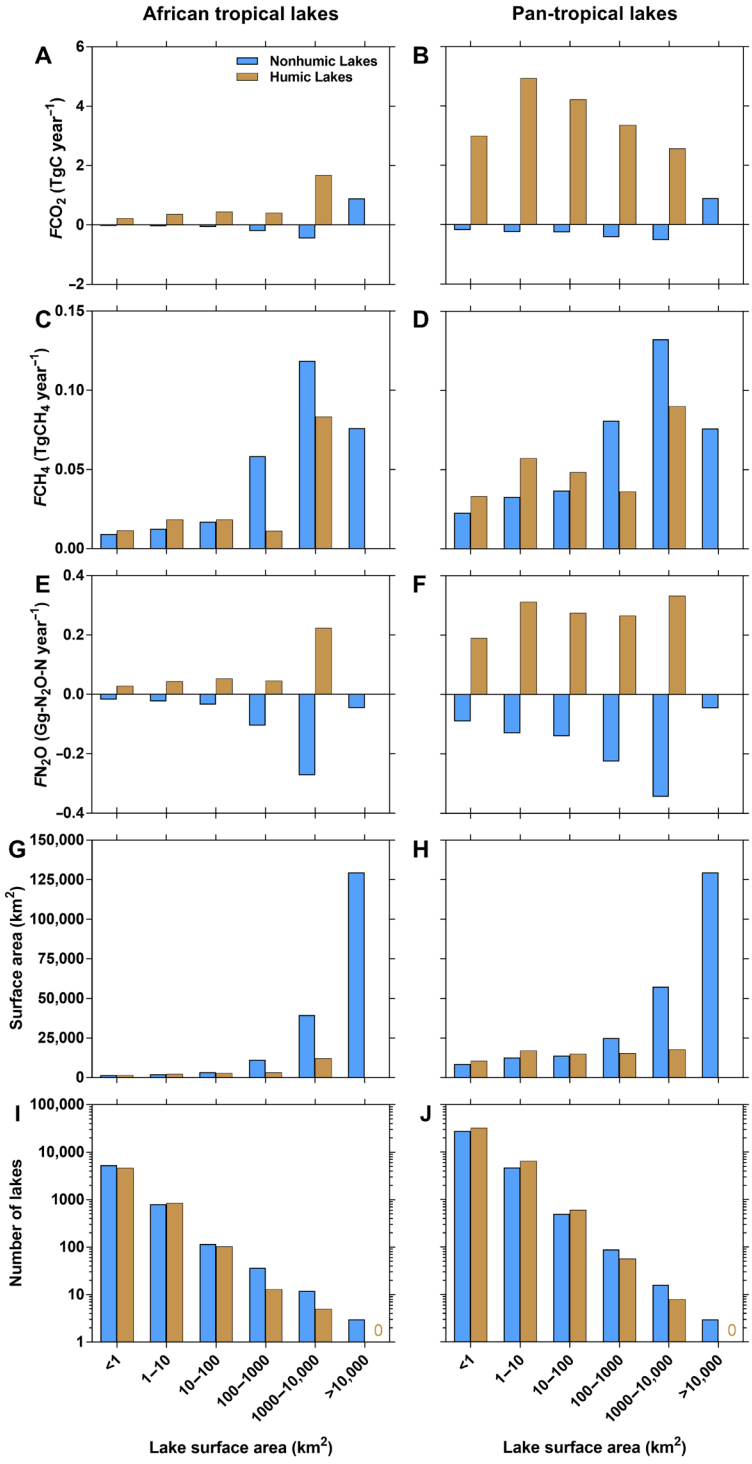

Fig. 9. Large contribution to CO_2, CH_4, and N_2O emissions from very large lakes. Air-water flux of CO_2 (FCO_2), CH_4 (FCH_4 diffusive), and N_2O (FN_2O) integrated for African tropical (**A**, **C**, and **E**) and pan-tropical lakes (**B**, **D**, and **F**) that were classified into humic and nonhumic, as well as surface area (**G** and **H**) and number of lakes per size classes (**I** and **J**) from HydroLAKES (*29*), except for Lake Chad for which the more recent and realistic surface area was applied (*30*).

Five lakes (Victoria, Tanganyika, Kivu, Edward, and George) were repeatedly sampled (table S7), allowing us to describe the amplitude of seasonal variations (fig. S15). The amplitude of seasonal variations of CH_4 was much stronger in shallower waters and more pronounced in holomictic comparted to meromictic lakes. Moreover, they followed the pattern of depth dependence of productivity as indicated by average Chl-a (fig. S15). Seasonal variations of pCO_2 were lower in the meromictic Lake Tanganyika and generally small and equivalent for all the other lakes, except for Lake Victoria, where seasonal pCO_2 changes were particularly strong. Seasonal variations

of pCO_2 in surface waters were attributable to the alternation of periods of vertical mixing and transport to surface of CO_2 from depth and periods of stratification with a decrease of CO_2 content in surface waters due to primary production. At an equivalent depth (30 m), the vertical gradients of pCO_2 were much stronger in Lake Victoria than in Lake Edward (fig. S16), explaining the corresponding higher amplitude of pCO_2 seasonal variations in Lake Victoria compared to Lake Edward (fig. S15). To derive GHG concentrations representative for each lake, before scaling of fluxes, we simply averaged all sampling periods for lakes Tanganyika, Kivu, Edward, and George where seasonal variations were small (fig. S15), while for Lake Victoria, the annual average was computed using a period of 2 months for the mixed conditions and period of 10 months for the stratified conditions (*36*).

The reliability of pan-tropical integration of GHGs partly depends on degree to which GHG data collected in African lakes are representative for tropical lakes in other continents. For CH_4, data collected in tropical lakes in other regions than Africa were generally comparable and consistent with the patterns in African lakes as a function of depth and surface area (fig. S17). This was also the case for pCO_2 in nonhumic lakes (fig. S18). Regarding humic lakes, pCO_2 collected in Amazonian floodplain lakes were comparable to data in African humic lakes for larger systems (surface area, >260 km^2) but higher for smaller systems (surface area, <260 km^2) (fig. S19). The fact that the difference was size dependent is probably attributable to the Amazonian floodplain lakes having a very strong hydrological connectivity with the Amazon River; during the high-water period, these floodplain lakes are entirely filled by river water with a very high CO_2 content and only become hydrological disconnected from the river during the low water period. The computation of the FCH_4 and FCO_2 at pan-tropical scale included the data from non-African tropical lakes (figs. S17 to S19). Note that median pCO_2 measured directly by equilibration in Amazon floodplain lakes (fig. S19) of 2880 ppm (IQR: 1752 to 3380, $n = 14$) was distinctly lower than median pCO_2 in Amazonian lakes calculated from pH and TA of 4860 ppm (IQR: 3858 to 9636, $n = 11$) reported in (*37*) and 8260 ppm (IQR: 3200 to 12,800, $n = 65$) reported in (*9*). These differences might be related to a systematic overestimation of pCO_2 computed from pH and TA in humic waters (*28*).

We tested three alternative scaling procedures for FCO_2 for African lakes since the FCO_2 estimates that we provide strongly diverge from previously published ones, unlike FCH_4 for which there is relatively more convergence (Table 1 and table S8). First, we simply upscaled the surface area–weighted average ΔpCO_2 of 12 ppm of all 25 lakes. A surface area–weighted average seemed more adequate than a simple average since the lake surface area in our dataset spans five orders of magnitude (table S1). This provided an integrated FCO_2 for African lakes of 0.3 TgC $year^{-1}$, about 11 times lower than our nominal estimate (Table 1), because of a predictable strong underestimation of the CO_2 emission from humic lakes since the largest lakes were nonhumic and have the strongest weight on the average. This supports our choice to separate humic and nonhumic lakes in our nominal scaling. Second, we used a ΔpCO_2 versus DOC relation (table S8) that was applied to a dataset of DOC calculated with a statistical model (*38*) for the lakes included in HydroLAKES (*29*). This predicted that African lakes acted collectively as a sink of atmospheric CO_2 of −4.2 TgC $year^{-1}$ because of a strong underestimation of the modeled DOC values compared to the measured DOC in the African lakes (fig. S20). The model seems to account realistically neither for autochthonous DOC inputs in productive nonhumic lakes nor for lateral inputs of DOC from wetlands in humic lakes (fig. S20). Third, we used a relation between ΔpCO_2 and lake surface area by separating humic and nonhumic lakes, although the relationship was positive for both lake types (table S8). This provided an integrated FCO_2 for African lakes of 5.7 ± 1.7 TgC $year^{-1}$ (table S8), higher but still relatively close to our nominal estimate of 3.3 ± 1.0 TgC $year^{-1}$ (Table 1). The positive relation between ΔpCO_2 and surface area in humic lakes was driven by the two largest lakes (Mai Ndombe and Tumba) that coincidentally were located in the Cuvette Centrale Congolaise, a giant wetland in the Congo basin that provides very high amounts of organic and inorganic carbon to streams (*17*). A positive relation between pCO_2 and surface area is in itself counterintuitive, as hydrological connectivity with wetlands and the rest of the catchment, and consequently lake CO_2 content, should be stronger in smaller water bodies (fig. S4), as also indicated by the comparison with Amazonian floodplain lakes (fig. S19). Our nominal estimate based on the scaling of the median ΔpCO_2 for humic lakes seems more robust given the low number of observations and clearly calls for more observations of GHGs dynamics in tropical humic lakes, which, in the future, should allow more elaborate scaling procedures.

A final additional possible limitation of our scaling approach is that HydroLAKES includes only lakes with a surface area larger than 0.1 km^2. Statistical extrapolations predict that lakes smaller than 0.1 km^2 are extremely numerous, yet they might only contribute marginally to total limnetic area based on an analysis of high-resolution satellite imagery (*39*).

The summed lake surface area of sampled African lakes (including Lake Malawi) accounts for 63% of the total tropical African lacustrine surface area that, in turn, accounts for 66% of the total surface area of tropical lakes larger than 0.1 km^2 (*29*), giving confidence in our pan-tropical scaling. We included in the scaling procedure a large-scale classification and separate scaling of humic and nonhumic lakes that seemed essential given the very different behavior of CO_2 and $\%N_2O$ in these two types of lakes and is in line with the idea that CDOM is a major factor controlling lake productivity and overall carbon cycling (*12*). Also in line with the idea that depth controls to a large extent productivity in lakes (*15*), we used relations between pCO_2 and lake morphology (depth), which should improve previous scaling efforts based on the simple extrapolation of the median of available values (*4*).

In recent literature, there is an inflationary tendency to publish increasingly higher CO_2 emissions from inland waters, the latest values (*40*) up to ~5000 TgC $year^{-1}$, distinctly higher than earlier estimates of ~700 TgC $year^{-1}$ (*41*). This might be unreasonable because CO_2 emissions from inland waters should be sustained by external carbon inputs, assumed to be provided by the terrestrial biosphere (*41*). It is becoming increasingly difficult to reconcile such high inland water CO_2 emissions with independent estimates of hydrological export of inorganic and organic carbon from land, given by the terrestrial science community. This hydrological export of CO_2 and DOC from soils to rivers is computed as a fraction of terrestrial net ecosystem exchange (NEE) defined as the difference between gross P and net ecosystem R (sum of autotrophic and heterotrophic R components) and is reported to vary between 3% for forests and 13% for grasslands (*42*). NEE as defined here differs from the long-term storage of carbon in terrestrial ecosystems, commonly called net biome production, corresponding to NEE

minus all the other losses of dead or living organic matter such as harvest, forest clearance, fire, and leaching of carbon to inland waters. Global grassland NEE is low (*43*), so assuming that the majority of carbon hydrological export is from forests (3% of NEE) (*42*), it should sustain a CO_2 emission of ~400 TgC $year^{-1}$, based on the terrestrial NEE of ~20,000 TgC $year^{-1}$ (*44*) and also taking into account the export of DOC from rivers to the ocean of ~200 TgC $year^{-1}$ (*45*). A way to address this large discrepancy and reconcile these independent estimates is to attribute a large part of CO_2 emissions from rivers to carbon inputs from wetlands rather than from "dry" terrestrial catchments, particularly in the tropics (*17*, *34*, *35*), as hydrological export of CO_2 and DOC from wetlands to inland waters is much higher than from dry land (*46*). In addition, there might be a need to reevaluate downward the global CO_2 emissions from inland waters, and this seems to be the case for tropical lakes, as shown here. This might also require challenging the longstanding paradigm of lakes as nearly universal sources of CO_2 sustained by prevailing net heterotrophy (*41*), as also shown here (Fig. 5).

MATERIALS AND METHODS

We focus exclusively on natural lakes, although we acquired data in five reservoirs in Zambia and Kenya that have been reported elsewhere (*51*, *52*). Natural lakes and reservoirs need to be treated separately, as the CO_2 and CH_4 emissions from reservoirs are sustained by the drowned former terrestrial biomass and strongly evolve with reservoir age (*53*). In addition, reservoirs only represent <13% of the surface area of lentic water bodies in Africa given by HydroLAKES (*29*). The sampled lakes can be considered as near-pristine, except Lake Victoria where the nearshore areas and bays are strongly eutrophicated, although a recent decrease since the 1990s in phytoplankton biomass has been reported (*54*).

Field sampling

We measured dissolved concentrations of CH_4 on 297 samples, N_2O on 241 samples, and pCO_2 on 287 samples collected in surface waters of 24 African lakes from 2007 to 2021 (table S7). The CO_2 and CH_4 data from four cruises in Lake Kivu were previously reported (*49*, *55*). All of the variables reported in this study were obtained with the same sampling and analytical protocols, providing a dataset that is methodologically consistent and of uniform quality. Sampling was done from small boats (fishermen boats or own inflatable boat) or larger ships for the two largest lakes (*Maman Benita* in Lake Tanganyika and *RV Hammerkop* in Lake Victoria). In small lakes, data were only acquired at one location (typically in the deepest central part of the lake), while in larger lakes, sampling was done at several locations, covering the depth gradient from the littoral zone to the deepest part of the lake. Sampling was done during daytime, from dawn to dusk in the case of continuous surface measurements in Lakes Victoria and Tanganyika, and typically from early morning to mid-afternoon in other lakes.

Sample handling and analysis

Depth at the sampling point was measured with a portable echosounder (Plastimo Echotest-II or Humminbird Helix 5 G2). Water temperature, conductivity, pH, and dissolved O_2 were measured with Yellow Springs Instrument (YSI) multiprobes (YSI 6600, YSI Pro Plus, and YSI EXO-2). The dissolved gases were measured with a uniform method based on a head-space technique, either directly in the field by infrared gas analysis (LI-COR Li-840 for CO_2) or upon return in the laboratory by gas chromatography (GC; for CH_4 and N_2O). Water was collected with a Niskin bottle below the surface (<0.5 m), and two 60-ml borosilicate serum bottles (Wheaton) for the determination of CH_4 and N_2O were filled with a silicone tubing, allowed to overflow, poisoned with a saturated solution of $HgCl_2$ (100 μl), sealed with butyl stoppers, crimped with aluminum caps, and stored at ambient temperature in the dark (*34*). Samples for the determination of pCO_2 were collected from the Niskin bottle in four 60-ml polypropylene syringes where 30 ml of sample water was equilibrated with 30 ml of ambient air (5 min of vigorous manual shaking) (*34*). The pCO_2 in ambient air and in the equilibrated gas phase was determined with a Li-840 calibrated with N_2 and a suite of CO_2:N_2 commercial mixtures (Air Liquide Belgium) with mixing ratios of 388-, 813-, 3788-, and 8300-ppm CO_2. The overall precision of pCO_2 measurements was ±2.0%. Concentrations of CH_4 and N_2O were determined via the headspace equilibration technique (20-ml N_2 headspace in 60-ml serum bottles) and measured by GC with flame ionization detection (GC-FID) and electron capture detection (GC-ECD) with an SRI 8610C GC-FID-ECD calibrated with CH_4:CO_2:N_2O:N_2 mixtures (Air Liquide Belgium) of 1-, 10-, 30-, 509-, and 2011-ppm CH_4 and of 0.2-, 2.0-, and 6.0-ppm N_2O and using the solubility coefficients of CH_4 (*56*) and N_2O (*57*). The precision of measurements was ±3.9% for CH_4 and ±3.2% for N_2O. During six cruises in Lakes Victoria, Tanganyika, Edward, and Albert (fig. S21), we also measured pCO_2 and the partial pressure of CH_4 (pCH_4) with a Los Gatos Research (LGR) off-axis integrated cavity output spectroscopy analyzer (Ultraportable Greenhouse Gas Analyzer with extended range for CH_4) coupled to an equilibrator. The reading of pCO_2 and pCH_4 from the LGR was compared in the home laboratory to the values from CH_4:CO_2:N_2 mixtures (Air Liquide Belgium) of 1-, 10-, 30-, 509-, and 2011-ppm CH_4 and 431-, 1088-, 4385-, and 22,029-ppm CO_2. The instrument did not show detectable drift between the start and the end of the fieldwork, and the factory calibration gave satisfactory readings against standards. This allowed a total of 29,127 surface measurements of pCO_2 and CH_4 (table S7). During these cruises, the pCO_2 and CH_4 were also measured with a headspace technique and measured with an infra-red gas analyzer (IRGA) and GC, respectively, on samples collected with a Niskin bottle. These measurements were consistent with the measurements obtained with the LGR analyzer coupled to the equilibrator (fig. S22). In Lake Edward, continuous unattended measurements of pCO_2 were carried out for 45 hours (fig. S12) using a custom-made equilibration system mounted on a floater inspired from (*58*) incorporating a Senseair ELG CO_2 analyzer.

Samples for δ^{13}C-DIC were collected from the Niskin bottle with a silicone tube in 12-ml Exetainer vials (Labco) and poisoned with 50 μl of a saturated solution of $HgCl_2$. Measurements were made with an elemental analyzer–isotope ratio mass spectrometer (Thermo FlashHT or Carlo Erba EA1110 with DeltaV Advantage). Calibration was performed with certified standards (NBS-19 or IAEA-CO-1, and LSVEC). Reproducibility of measurement based on duplicate injections of samples was typically better than ±0.2 ‰.

Water was filtered on Whatman glass fiber filters (GF/F grade; porosity, 0.7 μm; diameter, 47 mm) for phytoplankton pigments analyzed on 90% acetone extracts by high-performance liquid chromatography (HPLC) with a Waters HPLC chain (fluorescence and photodiode detectors), with a reproducibility for Chl-a of ±0.5% and a detection limit of 0.01 μg $liter^{-1}$. The abundance of

phytoplankton classes including the cyanobacteria was derived with CHEMTAX (*59*).

The water filtered through GF/F Whatman glass fiber filters was collected and further filtered through polyethersulfone syringe encapsulated filters (porosity, 0.2 μm) for samples to DOC, CDOM, NO_3^-, NO_2^- and NH_4^+, and TA. Samples to determine DOC were stored at 4°C and in the dark in 40-ml brown borosilicate vials with polytetrafluoroethylene (PTFE)–coated septa and poisoned with 50 μl of H_3PO_4 (85%), and DOC concentration was determined with a wet oxidation total organic carbon analyzer (IO Analytical Aurora 1030W), with a typical reproducibility better than ±5%. Samples to determine CDOM were stored at 4°C and in the dark in 20-ml brown borosilicate vials with PTFE-coated septa. Absorbance spectra were measured from 190 to 900 nm at 1-nm increments with a PerkinElmer UV/Vis 650S spectrophotometer using a 1-cm quartz cuvette, and SR was computed according to the work in (*11*). Samples for the determination of NO_3^-, NO_2^-, and NH_4^+ were collected in 50-ml polypropylene vials and stored frozen (−20°C). NO_3^- and NO_2^- were determined with the sulfanilamide colorimetric with the vanadium reduction method (*60*), and NH_4^+ with the dichloroisocyanurate-salicylate-nitroprussiate colorimetric method (*61*). Detection limits were 0.3, 0.01, and 0.15 μM for NH_4^+, NO_2^-, and NO_3^-, respectively. Precisions were ±0.02, ±0.02, and ±0.1 μM for NH_4^+, NO_2^-, and NO_3^-, respectively. Samples for TA were stored at ambient temperature in 55-ml polyethylene vials, and measurements were carried out by open-cell titration with 0.1 M HCl, and data were quality checked with certified reference material obtained from Andrew Dickson (Scripps Institution of Oceanography, University of California, San Diego, CA, USA), with a typical reproducibility better than ±3 μmol kg^{-1}. HCO_3^- was computed from TA and pCO_2 measurements using the carbonic acid dissociation constants for freshwater and the CO2SYS package.

P was measured during 2-hour incubations along a gradient of light intensity using ^{13}C-HCO_3^- as a tracer, as described in detail elsewhere (*22*). For Lake Mai Ndombe, *P* was calculated with a statistical model using Secchi disk depth and Chl-a concentration developed for the Congo River network (*17*). Pelagic community *R* was determined from the decrease of O_2 measured with an optical O_2 probe (YSI ProODO) in 60-ml biological oxygen demand bottles (Wheaton) over ~24-hour incubation periods (*17*).

Air-water flux computation and upscaling

The general approach to scale FCO_2, FCH_4, and FN_2O for tropical lakes (24°N to 24°S) at African and pan-tropical scales was as follows: (i) classification of lakes in HydroLAKES into humic and nonhumic lakes based on wetland coverage derived from GIESM-D15 (*62*); (ii) computation of air-water CO_2, N_2O, and CH_4 concentration gradients based on relations with lake mean depth for each lake in HydroLAKES (*29*), using two different approaches for humic and nonhumic lakes (for CO_2 and N_2O); (iii) computation of FCO_2, FN_2O, and FCH_4 fluxes per square meter from the respective air-water concentration gradients, water temperature [derived for each lake from a relation with air temperature derived from WorldClim (*63*)], and the *k* computed from a parameterization as a function of wind speed (*64*) itself derived for individual lakes in HydroLAKES from WorldClim (*63*); and (iv) integration of the fluxes from fluxes per square meter for each lake and the respective surface area from HydroLAKES (*29*). Two versions of the scaling were made: one using the original HydroLAKES surface area data with an unrealistic surface area value of 18,752 km^2 for Lake Chad and another using a more recent surface area value of 2603 km^2 for Lake Chad (*30*).

HydroLAKES (*29*) is a global database of lake morphology for lakes with a surface area ≥ 0.1 km^2, which incorporates lake mean depth. We classified the objects in HydroLAKES for natural lakes (unregulated, category 1; regulated, category 3; excluding reservoirs, category 2) into strongly humic lakes and nonhumic lakes. We hypothesized that wetlands fringing lakes were the major source of humic DOM to the lakes, and CDOM SR was negatively correlated with wetland presence on the catchment extracted from GIEMS-D15 (*62*). On the basis of the regression of CDOM SR as a function of % wetland

CDOM SR = 1.85 − 0.0765 × %wetland (r^2 = 0.57, P = 0.0003, n = 18).

We computed the threshold value of wetland coverage of 8.1% to classify humic (CDOM SR < 1) and nonhumic (CDOM SR > 1) lakes. For each lake in HydroLAKES, the watershed was extracted from HydroSHEDS (*65*) allowing us, in turn, to extract the wetland coverage on the watershed from GIEMS-D15 (*62*). GIEMS-D15 data were unavailable for 707 tropical lakes totaling a surface area of 395 km^2 (~0.1% of total) of which 92 lakes in the African continent totaling a surface of 29 km^2 (~0.01% of total), and these lakes were excluded from the analysis. While this approach is admittedly coarse, it is a first attempt to classify lakes into humic and nonhumic classes that have been shown to be important in driving CO_2 concentrations rather than simply extrapolating a central value of CO_2 concentration either globally (*1*, *2*) or zonally (*4*). In addition, the general approach is conceptually consistent with the independent evidence showing that the presence of wetlands is important in sustaining high CO_2 concentrations in temperate and boreal lakes (*13*, *66*).

The annual average of both the wind speed and the air temperature was also extracted for each lake from WorldClim (*63*). The surface lake water temperature was computed from air temperature using a linear regression as a function of the latitude of the difference of air and water temperature in 76 tropical lakes from a recent global compilation (fig. S23) (*67*)

Air temperature − water temperature = 0.1001 * LAT − 3.66 (n = 76; r^2 = 0.2; P < 0.0001)where LAT is absolute latitude (in degrees).

The derived lake surface temperature compared satisfactorily to our average measured data, except for two of the warmest lakes (fig. S24). Excluding these two outliers, the root mean square value was ±1.3°C.

For large lakes where data distribution covered a depth gradient (Albert, Edward, Tanganyika, and Victoria), the GHG data were binned by depth and the average for the whole lake was calculated from bathymetry maps. For Lakes Edward and Albert, bathymetry was digitized from (*68*); for Lake Tanganyika, digital bathymetry was provided by TCarta, and for Lake Victoria, bathymetry was available from (*69*). For the lakes where sampling was obtained during various cruises, the spatially integrated averages based on bathymetry were averaged to provide an annual mean. The period of different cruises were chosen to cover contrasted periods of the year in terms of vertical mixing that typically follow the alternation of the rainy and the dry seasons. The seasonal variations tended to be relatively modest in most lakes, except for Lake Victoria that showed much higher pCO_2 values during the cruise during the dry season when vertically mixed conditions were observed (*54*)

compared to two other cruises when stratified condition prevailed (*54*). For Lake Victoria, we then averaged the data considering that the period of vertical mixing lasted 2 months (*36*) and stratified conditions lasted 10 months per year.

For nonhumic African lakes, ΔpCO_2 and $\%N_2O$ were computed from lake mean depth according to

$\Delta pCO_2 = 147.3 \times \log(\text{mean depth}) - 250.3$ ($r^2 = 0.29$, $P = 0.0399$, $n = 15$)

$\%N_2O = 18.321 \times \log(\text{mean depth}) + 55.4$ ($r^2 = 0.30$, $P = 0.0153$, $n = 19$)

The same relation between $\%N_2O$ and mean depth was used for the pan-tropical lake upscaling (in the absence of additional N_2O data in other tropical lakes), but for ΔpCO_2, we added two data points (fig. S18) for the pan-tropical nonhumic lake upscaling, according to

$\Delta pCO_2 = 133.41 \times \log(\text{mean depth}) - 231.5$ ($r^2 = 0.24$, $P = 0.0446$, $n = 17$)

For humic lakes, there was no relation between ΔpCO_2 and $\%N_2O$ and lake mean depth, so we used the median ΔpCO_2 value of 1302 ppm and the median $\%N_2O$ value of 167.2%. The same median of $\%N_2O$ value was used for the pan-tropical humic lake upscaling (in the absence of additional N_2O data in other tropical lakes). For the pan-tropical upscaling of FCO_2 in humic lakes, we included 14 additional data points from Amazon floodplain lakes (fig. S19), and we used a median ΔpCO_2 of 2657 ppm for lakes <260 km^2 and a median ΔpCO_2 of 1373 ppm for lakes >260 km^2.

No clear differences in CH_4 concentration as a function of depth was observed between humic and nonhumic lakes, so a single overall relation was applied to all African lakes

$\log(CH_4) = -0.6226 \times \log(\text{mean depth}) + 3.29$ ($r^2 = 0.18$, $P = 0.0391$, $n = 24$)

For the pan-tropical upscaling, we included 35 additional CH_4 data points (fig. S17) using the following relation

$\log(CH_4) = -0.4123 \times \log(\text{mean depth}) + 2.807$ ($r^2 = 0.12$, $P = 0.0086$, $n = 59$)

The flux (F) of GHGs between surface waters and the atmosphere was computed according to

$F = k.\Delta G$

where k is the gas transfer velocity (centimeters per hour) and ΔG is the air-water gradient of dissolved concentration of a given gas.

We computed k for each lake in HydroLAKES as a function of wind speed using a parameterization based on the compilation of tracer-based estimates of k in 11 lakes with a wide range of morphological characteristics such as maximum depth (Dozmary pool, 0.7 m; Pyramid lake, 109 m) and surface area (Dozmary pool, 0.14 km^2; Pyramid lake, 487 km^2) (*64*). While k is parameterized as a function of wind speed, this does imply that this parameterization only accounts for the effect on k of turbulence generated by wind shear. This parameterization intrinsically integrates at least partly other sources of turbulence such as convection due to nighttime cooling (*70*) or the modulation of k by fetch limitation (*16*, *71*) because the parameterization is built on compilation of numerous tracer measurements (lasting typically 1 to 2 weeks) in several lakes covering a wide range of size and depth, thus integrating all the drivers of k in lakes. In lakes, k is known to show a fetch dependence that seems to be a function of lake surface area (*16*, *71*), which has led to the use of a constant k with a different value for several lake size classes to scale CO_2 fluxes globally in lakes (*4*). The k value specific to each lake size class was calculated from the compilation of k values derived from tracer experiments in temperate or boreal systems (*4*). However, wind speed is zonally variable as a function of latitude, with tropical landmasses showing distinctly lower values than higher-latitude areas (fig. S25). Consequently, the area-averaged k based on the k-wind relationship (*64*) that we computed and used in the scaling was about 1.6 times lower than the k values computed from the k–surface area classes tabulated in (*4*) both at tropical African (3.0 cm $hour^{-1}$ versus 4.7 cm $hour^{-1}$) and pan-tropical (2.9 cm $hour^{-1}$ versus 4.6 cm $hour^{-1}$) scales. The pan-tropical area-averaged k based on the k-wind relationship (2.9 cm $hour^{-1}$) (*64*) was also lower than the one used in (*47*) (4.0 cm $hour^{-1}$), although there is no indication in (*47*) on how this average value was derived.

Error analysis on the GHG flux computation and upscaling was carried out by error propagation of the GHG concentration measurements, the k value estimates, and the classification into humic and nonhumic lakes using a Monte Carlo simulation with 10,000 iterations. The uncertainty on pCO_2, CH_4, and N_2O was arbitrarily set at ±25% to account for the uncertainty arising from the representativeness of available data to capture all spatial and temporal scales of variability and also including the uncertainty of measurements of ±2.0% for pCO_2, ±3.9% for CH_4, and ±3.2% for N_2O. The uncertainty on k derived from tracer experiments was evaluated to ±30% on the basis of the reported (*64*) variability across different lakes of k at low wind speeds, characteristic of low-latitude land masses (fig. S25). The uncertainty on the lake surface temperature was ±1.3°C (fig. S24). The uncertainty on the classification into humic and nonhumic lakes was arbitrarily set at ±25%.

Ebullitive FCH_4 was scaled for both humic and nonhumic lakes using a median of 5.7 (IQR: 2.1 to 14.6) mmol m^{-2} day^{-1} for the littoral zone between depth of 0 and 4 m and a median of 5.2 (IQR: 1.7 to 8.7) mmol m^{-2} day^{-1} for the littoral zone between 4 and 10 m derived from a compilation of 23 data in tropical lakes including our own four measurements in African lakes (fig. S10). This was motivated by the fact that ebullitive FCH_4 shows a strong depth dependence and is usually confined to shallow depths in boreal and temperate lakes (*72*, *73*). The lake surface area corresponding to the two depth interval regions of the littoral zone (0 to 4 m and 4 to 10 m) was derived from morphometric relations based on maximum depth (*74*) that was itself derived from the mean depth reported in HydroLAKES (*29*) using a ratio of average depth over maximum depth of 0.464 (*75*).

Statistical analysis

Linear regressions were tested at 0.05 level (r^2 and P) using GraphPad Prism (version 7).

SUPPLEMENTARY MATERIALS

Supplementary material for this article is available at https://science.org/doi/10.1126/sciadv.abi8716

REFERENCES AND NOTES

1. J. J. Cole, N. F. Caraco, G. W. Kling, T. K. Kratz, Carbon dioxide supersaturation in the surface waters of lakes. *Science* **265**, 1568–1570 (1994).
2. S. Sobek, L. J. Tranvik, J. J. Cole, Temperature independence of carbon dioxide supersaturation in global lakes. *Global Biogeochem. Cycles* **19**, GB2003 (2005).
3. D. Bastviken, L. J. Tranvik, J. A. Downing, P. M. Crill, A. Enrich-Prast, Freshwater methane emissions offset the continental carbon sink. *Science* **331**, 50–50 (2011).
4. P. A. Raymond, J. Hartmann, R. Lauerwald, S. Sobek, C. McDonald, M. Hoover, D. Butman, R. Striegl, E. Mayorga, C. Humborg, P. Kortelainen, H. Dürr, M. Meybeck, P. Ciais, P. Guth, Global carbon dioxide emissions from inland waters. *Nature* **503**, 355–359 (2013).

5. T. DelSontro, J. J. Beaulieu, J. A. Downing, Greenhouse gas emissions from lakes and impoundments: Upscaling in the face of global change. *Limnol. Oceanogr. Lett.* **3**, 64–75 (2018).
6. W. M. Lewis Jr., Tropical limnology. *Annu. Rev. Ecol. Syst.* **18**, 159–184 (1987).
7. J. Langeveld, A. F. Bouwman, W. J. van Hoek, L. Vilmin, A. H. W. Beusen, J. M. Mogollón, J. J. Middelburg, Estimating dissolved carbon concentrations in global soils: A global database and model. *SN Appl. Sci.* **2**, 1626 (2020).
8. J. F. Lapierre, P. A. del Giorgio, Geographical and environmental drivers of regional differences in the lake pCO_2 versus DOC relationship across northern landscapes. *J. Geophys. Res.* **117**, G03015 (2012).
9. H. Marotta, C. M. Duarte, S. Sobek, A. Enrich-Prast, Large CO_2 disequilibria in tropical lakes. *Global Biogeochem. Cycles* **23**, GB4022 (2009).
10. S. Kosten, F. Roland, D. M. L. Da Motta Marques, E. H. Van Nes, N. Mazzeo, L. da S. L. Sternberg, M. Scheffer, J. J. Cole, Climate-dependent CO_2 emissions from lakes. *Global Biogeochem. Cycles* **24**, GB2007 (2010).
11. J. R. Helms, A. Stubbins, J. D. Ritchie, E. C. Minor, D. J. Kieber, K. Mopper, Absorption spectral slopes and slope ratios as indicators of molecular weight, source, and photobleaching of chromophoric dissolved organic matter. *Limnol.Oceanogr.* **53**, 955–969 (2008).
12. P. A. del Giorgio, R. H. Peters, Patterns in planktonic *P:R* ratios in lakes: Influence of lake trophy and dissolved organic carbon. *Limnol. Oceanogr.* **39**, 772–787 (1994).
13. S. Sobek, G. Algesten, A.-K. Bergström, M. Jansson, L. Tranvik, The catchment and climate regulation of pCO_2 in boreal lakes. *Glob. Change Biol.* **9**, 630–641 (2003).
14. J. P. Casas-Ruiz, J. Jakobsson, P. A. del Giorgio, The role of lake morphometry in modulating surface water carbon concentrations in boreal lakes. *Environ. Res. Lett.* **16**, 074037 (2021).
15. K. Sand-Jensen, P. A. Staehr, Scaling of pelagic metabolism to size, trophy and forest cover in small Danish lakes. *Ecosystems* **10**, 128–142 (2007).
16. R. Wanninkhof, Relationship between wind speed and gas exchange over the ocean. *J. Geophys. Res.* **97**, 7373–7382 (1992).
17. A. V. Borges, F. Darchambeau, T. Lambert, C. Morana, G. H. Allen, E. Tambwe, A. Toengaho Sembaito, T. Mambo, J. Nlandu Wabakhangazi, J.-P. Descy, C. R. Teodoru, S. Bouillon, Variations in dissolved greenhouse gases (CO_2, CH_4, N_2O) in the Congo River network overwhelmingly driven by fluvial-wetland connectivity. *Biogeosciences* **16**, 3801–3834 (2019).
18. C. S. Reynolds, *The Ecology of Phytoplankton* (Cambridge Univ. Press, 2006).
19. M. J. Bogard, P. A. del Giorgio, L. Boutet, M. C. G. Chaves, Y. T. Prairie, A. Merante, A. M. Derry, Oxic water column methanogenesis as a major component of aquatic CH_4 fluxes. *Nat. Commun.* **5**, 5350 (2014).
20. M. Bižić, T. Klintzsch, D. Ionescu, M. Y. Hindiyeh, M. Günthel, A. M. Muro-Pastor, W. Eckert, T. Urich, F. Keppler, H.-P. Grossart, Aquatic and terrestrial cyanobacteria produce methane. *Sci. Adv.* **6**, eaax5343 (2020).
21. H.-P. Grossart, K. Frindte, C. Dziallas, W. Eckert, K. W. Tang, Microbial methane production in oxygenated water column of an oligotrophic lake. *Proc. Natl. Acad. Sci. U.S.A.* **108**, 19657–19661 (2011).
22. C. Morana, S. Bouillon, V. Nolla-Ardèvol, F. A. E. Roland, W. Okello, J.-P. Descy, A. Nankabirwa, E. Nabafu, D. Springael, A. V. Borges, Methane paradox in tropical lakes? Sedimentary fluxes rather than pelagic production in oxic conditions sustain methanotrophy and emissions to the atmosphere. *Biogeosciences* **17**, 5209–5221 (2020).
23. R. I. Jones, The influence of humic substances on lacustrine planktonic food chains. *Hydrobiologia* **229**, 73–91 (1992).
24. G. Yvon-Durocher, A. P. Allen, D. Bastviken, R. Conrad, C. Gudasz, A. St-Pierre, N. Thanh-Duc, P. A. del Giorgio, Methane fluxes show consistent temperature dependence across microbial to ecosystem scales. *Nature* **507**, 488–491 (2014).
25. P. Kankaala, J. Huotari, T. Tulonen, A. Ojala, Lake-size dependent physical forcing drives carbon dioxide and methane effluxes from lakes in a boreal landscape. *Limnol. Oceanogr.* **58**, 1915–1930 (2013).
26. M. A. Holgerson, P. A. Raymond, Large contribution to inland water CO_2 and CH_4 emissions from very small ponds. *Nat. Geosci.* **9**, 222–226 (2016).
27. S. R. Alin, T. C. Johnson, Carbon cycling in large lakes of the world: A synthesis of production, burial, and lake-atmosphere exchange estimates. *Global Biogeochem. Cycles* **21**, GB3002 (2007).
28. G. Abril, S. Bouillon, F. Darchambeau, C. R. Teodoru, T. R. Marwick, F. Tamooh, F. O. Omengo, N. Geeraert, L. Deirmendjian, P. Polsenaere, A. V. Borges, Technical note: Large overestimation of pCO_2 calculated from pH and alkalinity in acidic, organic-rich freshwaters. *Biogeosciences* **12**, 67–78 (2015).
29. M. L. Messager, B. Lehner, G. Grill, I. Nedeva, O. Schmitt, Estimating the volume and age of water stored in global lakes using a geo-statistical approach. *Nat. Commun.* **7**, 13603 (2016).
30. B. Pham-Duc, F. Sylvestre, F. Papa, F. Frappart, C. Bouchez, J.-F. Crétaux, The Lake Chad hydrology under current climate change. *Sci. Rep.* **10**, 5498 (2020).
31. R. Lauerwald, P. Regnier, V. Figueiredo, A. Enrich-Prast, D. Bastviken, B. Lehner, T. Maavara, P. Raymond, Natural lakes are a minor global source of N_2O to the atmosphere. *Global Biogeochem. Cycles* **33**, 1564–1581 (2019).
32. J. M. Melack, L. L. Hess, M. Gastil, B. R. Forsberg, S. K. Hamilton, I. B. T. Lima, E. M. L. M. Novo, Regionalization of methane emissions in the Amazon Basin with microwave remote sensing. *Glob. Change Biol.* **10**, 530–544 (2004).
33. M. Saunois, P. Bousquet, B. Poulter, A. Peregon, P. Ciais, J. G. Canadell, E. J. Dlugokencky, G. Etiope, D. Bastviken, S. Houweling, G. Janssens-Maenhout, F. N. Tubiello, S. Castaldi, R. B. Jackson, M. Alexe, V. K. Arora, D. J. Beerling, P. Bergamaschi, D. R. Blake, G. Brailsford, V. Brovkin, L. Bruhwiler, C. Crevoisier, P. Crill, K. Covey, C. Curry, C. Frankenberg, N. Gedney, L. Höglund-Isaksson, M. Ishizawa, A. Ito, F. Joos, H.-S. Kim, T. Kleinen, P. Krummel, J.-F. Lamarque, R. Langenfelds, R. Locatelli, T. Machida, S. Maksyutov, K. C. Mc Donald, J. Marshall, J. R. Melton, I. Morino, V. Naik, S. O'Doherty, F.-J. W. Parmentier, P. K. Patra, C. Peng, S. Peng, G. P. Peters, I. Pison, C. Prigent, R. Prinn, M. Ramonet, W. J. Riley, M. Saito, M. Santini, R. Schroeder, I. J. Simpson, R. Spahni, P. Steele, A. Takizawa, B. F. Thornton, H. Tian, Y. Tohjima, N. Viovy, A. Voulgarakis, M. van Weele, G. R. van der Werf, R. Weiss, C. Wiedinmyer, D. J. Wilton, A. Wiltshire, D. Worthy, D. Wunch, X. Xu, Y. Yoshida, B. Zhang, Z. Zhang, Q. Zhu, The global methane budget. *Earth Syst. Sci. Data* **8**, 697–751 (2016).
34. A. V. Borges, F. Darchambeau, C. R. Teodoru, T. R. Marwick, F. Tamooh, N. Geeraert, F. O. Omengo, F. Guérin, T. Lambert, C. Morana, E. Okuku, S. Bouillon, Globally significant greenhouse gas emissions from African inland waters. *Nat. Geosci.* **8**, 637–642 (2015).
35. A. V. Borges, G. Abril, F. Darchambeau, C. R. Teodoru, J. Deborde, L. O. Vidal, T. Lambert, S. Bouillon, Divergent biophysical controls of aquatic CO_2 and CH_4 in the World's two largest rivers. *Sci. Rep.* **5**, 15614 (2015).
36. J. F. Talling, The annual cycle of stratification and phytoplankton growth in Lake Victoria (East Africa). *Int. Rev. gesamten Hydrobiol., Syst. Beih.* **51**, 545–621 (1966).
37. L. Pinho, C. M. Duarte, H. Marotta, A. Enrich-Prast, Temperature dependence of the relationship between pCO_2 and dissolved organic carbon in lakes. *Biogeosciences* **13**, 865–871 (2016).
38. K. Toming, J. Kotta, E. Uuemaa, S. Sobek, T. Kutser, L. J. Tranvik, Predicting lake dissolved organic carbon at a global scale. *Sci. Rep.* **10**, 8471 (2020).
39. C. Verpoorter, T. Kutser, D. A. Seekell, L. J. Tranvik, A global inventory of lakes based on high-resolution satellite imagery. *Geophys. Res. Lett.* **41**, 6396–6402 (2014).
40. T. W. Drake, P. A. Raymond, R. G. M. Spencer, Terrestrial carbon inputs to inland waters: A current synthesis of estimates and uncertainty. *Limnol. Oceanogr. Lett.* **3**, 132–142 (2018).
41. J. J. Cole, Y. T. Prairie, N. F. Caraco, W. H. McDowell, L. J. Tranvik, R. G. Striegl, C. M. Duarte, P. Kortelainen, J. A. Downing, J. J. Middelburg, J. Melack, Plumbing the global carbon cycle: Integrating inland waters into the terrestrial carbon budget. *Ecosystems* **10**, 172–185 (2007).
42. R. Kindler, J. Siemens, K. Kaiser, D. C. Walmsley, C. Bernhofer, N. Buchmann, P. Cellier, W. Eugster, G. Gleixner, T. Grunwald, A. Heim, A. Ibrom, S. K. Jones, M. Jones, K. Klumpp, W. Kutsch, L. K. Steenberg, S. Lehuger, B. Loubet, R. McKenzie, E. Moors, B. Osborne, K. Pilegaard, C. Rebmann, M. Saunders, M. W. I. Schmidt, M. Schrumpf, J. Seyfferth, U. Skiba, J.-F. Soussana, M. A. Sutton, C. Tefs, B. Vowinckel, M. J. Zeeman, M. Kaupenjohann, Dissolved carbon leaching from soil is a crucial component of net ecosystem carbon balance. *Glob. Change Biol.* **17**, 1167–1185 (2011).
43. W. Liang, W. Zhang, Z. Jin, J. Yan, Y. Lü, S. Wang, B. Fu, S. Li, Q. Ji, F. Gou, S. Fu, S. An, F. Wang, Estimation of global grassland net ecosystem carbon exchange using a model tree ensemble approach. *J. Geophys. Res. Biogeosci.* **125**, e2019JG005034 (2020).
44. J. Zeng, T. Matsunaga, Z.-H. Tan, N. Saigusa, T. Shirai, Y. Tang, S. Peng, Y. Fukuda, Global terrestrial carbon fluxes of 1999–2019 estimated by upscaling eddy covariance data with a random forest. *Sci. Data* **7**, 313 (2020).
45. W. Ludwig, J. L. Probst, S. Kempe, Predicting the oceanic input of organic carbon by continental erosion. *Global Biogeochem. Cycles* **10**, 23–41 (1996).
46. G. Abril, A. V. Borges, Ideas and perspectives: Carbon leaks from flooded land: Do we need to replumb the inland water active pipe? *Biogeosciences* **16**, 769–784 (2019).
47. A. K. Aufdenkampe, E. Mayorga, P. A. Raymond, J. M. Melack, S. C. Doney, S. R. Alin, R. E. Aalto, K. Yoo, Riverine coupling of biogeochemical cycles between land, oceans, and atmosphere. *Front. Ecol. Environ.* **9**, 53–60 (2011).
48. M. J. Ngochera, H. A. Bootsma, Spatial and temporal dynamics of pCO_2 and CO_2 flux in tropical Lake Malawi. *Limnol. Oceanogr.* **65**, 1594–1607 (2020).
49. A. V. Borges, G. Abril, B. Delille, J.-P. Descy, F. Darchambeau, Diffusive methane emissions to the atmosphere from Lake Kivu (Eastern Africa). *J. Geophys. Res.* **116**, G03032 (2011).
50. P. Kortelainen, T. Larmola, M. Rantakari, S. Juutinen, J. Alm, P. J. Martikainen, Lakes as nitrous oxide sources in the boreal landscape. *Glob. Change Biol.* **26**, 1432–1445 (2020).
51. E. O. Okuku, S. Bouillon, M. Tole, A. V. Borges, Diffusive emissions of methane and nitrous oxide from a cascade of tropical hydropower reservoirs in Kenya. *Lakes Reserv.* **24**, 127–135 (2019).

52. C. R. Teodoru, F. C. Nyoni, A. V. Borges, F. Darchambeau, I. Nyambe, S. Bouillon, Spatial variability and temporal dynamics of greenhouse gas (CO_2, CH_4, N_2O) concentrations and fluxes along the Zambezi River mainstem and major tributaries. *Biogeosciences* **12**, 2431–2453 (2015).
53. G. Abril, F. Guérin, S. Richard, R. Delmas, C. Galy-Lacaux, P. Gosse, A. Tremblay, L. Varfalvy, M. Aurelio Dos Santos, B. Matvienko, Carbon dioxide and methane emissions and the carbon budget of a 10-year old tropical reservoir (Petit Saut, French Guiana). *Global Biogeochem. Cycles* **19**, GB4007 (2005).
54. L. Deirmendjian, J.-P. Descy, C. Morana, W. Okello, M. P. Stoyneva-Gärtner, S. Bouillon, A. V. Borges, Limnological changes in Lake Victoria since the mid-20th century. *Freshw. Biol.* **66**, 1630–1647 (2021).
55. A. V. Borges, C. Morana, S. Bouillon, P. Servais, J.-P. Descy, F. Darchambeau, Carbon cycling of Lake Kivu (East Africa): Net autotrophy in the epilimnion and emission of CO_2 to the atmosphere sustained by geogenic inputs. *PLOS ONE* **9**, e109500 (2014).
56. S. Yamamoto, J. B. Alcauskas, T. E. Crozier, Solubility of methane in distilled water and seawater. *J. Chem. Eng. Data* **21**, 78–80 (1976).
57. R. F. Weiss, B. A. Price, Nitrous oxide solubility in water and seawater. *Mar. Chem.* **8**, 347–359 (1980).
58. C. W. Hunt, L. Snyder, J. E. Salisbury, D. Vandemark, W. H. McDowell, SIPCO2: A simple, inexpensive surface water pCO_2 sensor. *Limnol. Oceanogr. Methods* **15**, 291–301 (2017).
59. M. D. Mackey, D. J. Mackey, H. W. Higgins, S. W. Wright, CHEMTAX—A program for estimating class abundances from chemical markers: Application to HPLC measurements of phytoplankton. *Mar. Ecol. Progr. Ser.* **144**, 265–283 (1996).
60. APHA, *Standard Methods For The Examination Of Water And Wastewater* (American Public Health Association, 1998).
61. Standing Committee Of Analysts, *Ammonia in Waters: Methods for the Examination of Waters and Associated Materials* (H.M.S.O., 1981), 16 pp.
62. E. Fluet-Chouinard, B. Lehner, L.-M. Rebelo, F. Papa, S. K. Hamilton, Development of a global inundation map at high spatial resolution from topographic downscaling of coarse-scale remote sensing data. *Remote Sens Environ.* **158**, 348–361 (2015).
63. S. E. Fick, R. J. Hijmans, WorldClim 2: New 1km spatial resolution climate surfaces for global land areas. *Int. J. Climatol.* **37**, 4302–4315 (2017).
64. J. J. Cole, N. F. Caraco, Atmospheric exchange of carbon dioxide in a low-wind oligotrophic lake measured by the addition of SF_6. *Limnol. Oceanogr.* **43**, 647–656 (1998).
65. B. Lehner, K. Verdin, A. Jarvis, New global hydrography derived from spaceborne elevation data. *Eos* **89**, 93–94 (2008).
66. J.-F. Lapierre, D. A. Seekell, C. T. Filstrup, S. M. Collins, C. Emi Fergus, P. A. Soranno, K. S. Cheruvelil, Continental-scale variation in controls of summer CO_2 in United States lakes. *J. Geophys. Res. Biogeosci.* **122**, 875–885 (2017).
67. S. C. Maberly, R. A. O'Donnell, R. I. Woolway, M. E. J. Cutler, M. Gong, I. D. Jones, C. J. Merchant, C. A. Miller, E. Politi, E. M. Scott, S. J. Thackeray, A. N. Tyler, Global lake thermal regions shift under climate change. *Nat. Commun.* **11**, 1232 (2020).
68. J. Verbeke, Recherches écologiques sur la faune des grands lacs de l'est du Congo belge. Bulletin de l'Institut royal des Sciences naturelles de Belgique : Résultats scientifiques de l'exploration hydrobiologique (1952-1954) des lacs Kivu, Edouard et Albert (1957).
69. S. E. Hamilton, "Creation of a bathymetric map of Lake Victoria, Africa" (2016); http://dx.doi.org/10.7910/DVN/SOEKNR.
70. S. MacIntyre, A. T. Crowe, A. Cortés, L. Arneborg, Turbulence in a small arctic pond. *Limnol. Oceanogr.* **63**, 2337–2358 (2018).
71. D. Vachon, Y. T. Prairie, The ecosystem size and shape dependence of gas transfer velocity versus wind speed relationships in lakes. *Can. J. Fish. Aquat. Sci.* **70**, 1757–1764 (2013).
72. T. DelSontro, L. Boutet, A. St-Pierre, P. A. del Giorgio, Y. T. Prairie, Methane ebullition and diffusion from northern ponds and lakes regulated by the interaction between temperature and system productivity. *Limnol. Oceanogr.* **61**, S62–S77 (2016).
73. M. Wik, P. M. Crill, R. K. Varner, D. Bastviken, Multiyear measurements of ebullitive methane flux from three subarctic lakes. *J. Geophys. Res. Biogeosci.* **118**, 1307–1321 (2013).
74. J. Håkan, A. A. Brolin, L. Håkanson, New approaches to the modelling of lake basin morphometry. *Environ. Model. Assess.* **12**, 213–228 (2007).
75. R. G. Wetzel, *Limnology: Lake & River Ecosystems* (Academic Press, ed. 3, 2001), p. 429.
76. P. A. del Giorgio, J. J. Cole, N. F. Caraco, R. H. Peters, Linking planktonic biomass and metabolism to net gas fluxes in northern temperate lakes. *Ecology* **80**, 1422–1431 (1999).
77. K. Finlay, P. R. Leavitt, A. Patoine, B. Wissel, Magnitudes and controls of organic and inorganic carbon flux through a chain of hardwater lakes on the northern Great Plains. *Limnol. Oceanogr.* **55**, 1551–1564 (2010).
78. H. Marotta, C. M. Duarte, L. Pinho, A. Enrich-Prast, Rainfall leads to increased pCO_2 in Brazilian coastal lakes. *Biogeosciences* **7**, 1607–1614 (2010).
79. M. A. Xenopoulos, D. M. Lodge, J. Frentress, T. A. Kreps, S. D. Bridgham, E. Grossman, C. J. Jackson, Regional comparisons of watershed determinants of dissolved organic carbon in temperate lakes from the Upper Great Lakes region and selected regions globally. *Limnol. Oceanogr.* **48**, 2321–2334 (2003).
80. J. A. Zwart, Z. J. Hanson, J. Vanderwall, D. Bolster, A. Hamlet, S. E. Jones, Spatially explicit, regional-scale simulation of lake carbon fluxes. *Global Biogeochem. Cycles* **32**, 1276–1293 (2018).
81. P. A. Staehr, L. Baastrup-Spohr, K. Sand-Jensen, C. Stedmon, Lake metabolism scales with lake morphometry and catchment conditions. *Aquat. Sci.* **74**, 155–169 (2012).
82. J. P. Casas-Ruiz, R. H. S. Hutchins, P. A. del Giorgio, Total aquatic carbon emissions across the boreal biome of Québec driven by watershed slope. *J. Geophys. Res. Biogeosci.* **126**, e2020JG005863 (2021).
83. G. W. Kling, Comparative transparency, depth of mixing, and stability of stratification in lakes of Cameroon, West Africa. *Limnol. Oceanogr.* **33**, 27–40 (1988).
84. E. G. Stets, D. Butman, C. P. McDonald, S. M. Stackpoole, M. D. DeGrandpre, R. G. Striegl, Carbonate buffering and metabolic controls on carbon dioxide in rivers. *Global Biogeochem. Cycles* **31**, 663–677 (2017).
85. J. Schenk, H. O. Sawakuchi, A. K. Sieczko, G. Pajala, D. Rudberg, E. Hagberg, K. Fors, H. Laudon, J. Karlsson, D. Bastviken, Methane in lakes: Variability in stable carbon isotopic composition and the potential importance of groundwater input. *Front. Earth Sci.* **9**, 722215 (2021).
86. W. E. West, K. P. Creamer, S. E. Jones, Productivity and depth regulate lake contributions to atmospheric methane. *Limnol. Oceanogr.* **61**, S51–S61 (2016).
87. D. Bastviken, J. Cole, M. Pace, L. Tranvik, Methane emissions from lakes: Dependence of lake characteristics, two regional assessments, and a global estimate. *Global Biogeochem. Cycles* **18**, GB4009 (2004).
88. F. A. E. Roland, F. Darchambeau, C. Morana, A. V. Borges, Nitrous oxide and methane seasonal variability in the epilimnion of a large tropical meromictic lake (Lake Kivu, East-Africa). *Aquat. Sci.* **79**, 209–218 (2017).
89. K. Desrosiers, T. DelSontro, P. A. del Giorgio, Disproportionate contribution of vegetated habitats to the CH_4 and CO_2 budgets of a boreal lake. *Ecosystems* , (2021).
90. E. S. Oliveira Junior, T. J. H. M. van Bergen, J. Nauta, A. Budiša, R. C. H. Aben, S. T. J. Weideveld, C. A. de Souza, C. C. Muniz, J. Roelofs, L. P. M. Lamers, S. Kosten, Water hyacinth's effect on greenhouse gas fluxes: A field study in a wide variety of tropical water bodies. *Ecosystems* **24**, 988–1004 (2021).
91. J. E. Fernández, F. Peeters, H. Hofmann, On the methane paradox: Transport from shallow water zones rather than in situ methanogenesis is the major source of CH4in the open surface water of lakes. *J. Geophys. Res. Biogeosci.* **121**, 2717–2726 (2016).
92. T. DelSontro, P. A. del Giorgio, Y. T. Prairie, No longer a paradox: The interaction between physical transport and biological processes explains the spatial distribution of surface water methane within and across lakes. *Ecosystems* **21**, 1073–1087 (2018).
93. H. Wang, L. Yang, W. Wang, J. Lu, C. Yin, Nitrous oxide (N_2O) fluxes and their relationships with water-sediment characteristics in a hyper-eutrophic shallow lake, China. *J. Geophys. Res.* **112**, G01005 (2007).
94. C. Soued, P. A. del Giorgio, R. Maranger, Nitrous oxide sinks and emissions in boreal aquatic networks in Quebec. *Nat. Geosci.* **9**, 116–120 (2015).
95. M. Mengis, R. Gächter, B. Wehrli, Sources and sinks of nitrous oxide (N_2O) in deep lakes. *Biogeochemistry* **38**, 281–301 (1997).
96. K. Finlay, P. R. Leavitt, B. Wissel, Y. T. Prairie, Regulation of spatial and temporal variability of carbon flux in six hard-water lakes of the northern Great Plains. *Limnol. Oceanogr.* **54**, 2553–2564 (2009).
97. A. Baccini, N. Laporte, S. J. Goetz, M. Sun, H. Dong, A first map of tropical Africa's above-ground biomass derived from satellite imagery. *Environ. Res. Lett.* **3**, 045011 (2008).
98. P. Mayaux, E. Bartholomé, S. Fritz, A. Belward, A new land-cover map of Africa for the year 2000. *J. Biogeogr.* **31**, 861–877 (2004).
99. D. Bastviken, A. L. Santoro, H. Marotta, L. Q. Pinho, D. F. Calheiros, P. Crill, A. Enrich-Prast, Methane emissions from Pantanal, South America, during the low water season: Toward more comprehensive sampling. *Environ. Sci. Technol.* **44**, 5450–5455 (2010).
100. P. M. Barbosa, J. M. Melack, J. H. F. Amaral, S. MacIntyre, D. Kasper, A. Cortés, V. F. Farjalla, B. R. Forsberg, Dissolved methane concentrations and fluxes to the atmosphere from a tropical floodplain lake. *Biogeochemistry* **148**, 129–151 (2020).
101. P. M. Crill, K. B. Bartlett, J. O. Wilson, D. I. Sebacher, R. C. Harriss, J. M. Melack, S. MacIntyre, L. Lesack, L. Smith-Morrill, Tropospheric methane from an Amazonian floodplain lake. *J. Geophys. Res.* **93**, 1564–1570 (1988).
102. D. Engle, J. M. Melack, Methane emissions from an Amazon floodplain lake: Enhanced release during episodic mixing and during falling water. *Biogeochemistry* **51**, 71–90 (2000).
103. A. H. Devol, J. E. Richey, W. A. Clark, S. L. King, L. A. Martinelli, Methane emissions to the troposphere from the Amazon Floodplain. *J. Geophys. Res.* **93**, 1583–1592 (1988).
104. L. K. Smith, W. M. Lewis, J. P. Chanton, G. Cronin, S. K. Hamilton, Methane emissions from the Orinoco River floodplain, Venezuela. *Biogeochemistry* **51**, 113–140 (2000).

105. K. Attermeyer, S. Flury, R. Jayakumar, P. Fiener, K. Steger, V. Arya, F. Wilken, R. van Geldern, K. Premke, Invasive floating macrophytes reduce greenhouse gas emissions from a small tropical lake. *Sci. Rep.* **6**, 20424 (2016).
106. P. M. Barbosa, V. F. Farjalla, J. M. Melack, J. H. F. Amaral, J. S. da Silva, B. R. Forsberg, High rates of methane oxidation in an Amazon floodplain lake. *Biogeochemistry* **137**, 351–365 (2018).
107. R. E. Hecky, R. Mugidde, P. S. Ramlal, M. R. Talbot, G. W. Kling, Multiple stressors cause rapid ecosystem change in Lake Victoria. *Freshw. Biol.* **55**, 19–42 (2010).
108. P. M. Barbosa, J. M. Melack, V. F. Farjalla, J. H. F. Amaral, V. Scofield, B. R. Forsberg, Diffusive methane fluxes from Negro, Solimões and Madeira rivers and fringing lakes in the Amazon basin. *Limnol. Oceanogr.* **61**, S221–S237 (2016).
109. G. Abril, J.-M. Martinez, L. F. Artigas, P. Moreira-Turcq, M. F. Benedetti, L. Vidal, T. Meziane, J.-H. Kim, M. C. Bernardes, N. Savoye, J. Deborde, P. Albéric, M. F. L. Souza, E. L. Souza, F. Roland, Amazon river carbon dioxide outgassing fuelled by wetlands. *Nature* **505**, 395–398 (2014).
110. B. Panneer Selvam, S. Natchimuthu, L. Arunachalam, D. Bastviken, Methane and carbon dioxide emissions from inland waters in India - implications for large scale greenhouse gas balances. *Glob. Change Biol.* **20**, 3397–3407 (2014).
111. M. U. Mendoza-Pascual, M. Itoh, J. I. Aguilar, K. S. A. R. Padilla, R. D. S. Papa, N. Okuda, Controlling factors of methane dynamics in tropical lakes of different depths. *J. Geophys. Res. Biogeosci.* **126**, e2020JG005828 (2021).
112. D. Tonetta, P. A. Staehr, B. Obrador, L. P. Mello Brandão, L. Silva Brighenti, M. Mello Petrucio, F. A. Rodrigues Barbosa, J. F. Bezerra-Neto, Effects of nutrients and organic matter inputs in the gases CO_2 and O_2: A mesocosm study in a tropical lake. *Limnologica* **69**, 1–9 (2018).
113. P. A. Macklin, I. G. N. A. Suryaputra, D. T. Maher, I. R. Santos, Carbon dioxide dynamics in a lake and a reservoir on a tropical island (Bali, Indonesia). *PLOS ONE* **13**, e0198678 (2018).
114. P. Albéric, M. A. P. Pérez, P. Moreira-Turcq, M. F. Benedetti, S. Bouillon, G. Abril, Variation of the isotopic composition of dissolved organic carbon during the runoff cycle in the Amazon River and the floodplains. *C. R. Geosci.* **350**, 65–75 (2018).
115. J. H. F. Amaral, J. M. Melack, P. M. Barbosa, S. MacIntyre, D. Kasper, A. Cortés, T. S. Freire Silva, R. Nunes de Sousa, B. R. Forsberg, Carbon dioxide fluxes to the atmosphere from waters within flooded forests in the Amazon basin. *J. Geophys. Res. Biogeosci.* **125**, e2019JG005293 (2020).
116. M. Call, C. J. Sanders, A. Enrich-Prast, L. Sanders, H. Marotta, I. R. Santos, D. T. Maher, Radon-traced pore-water as a potential source of CO_2 and CH_4 to receding black and clear water environments in the Amazon Basin. *Limnol. Oceanogr. Lett.* **3**, 375–383 (2018).
117. S. Sobek, L. J. Tranvik, , Y. P. Prairie, P. Kortelainen, J. J. Cole, Patterns and regulation of dissolved organic carbon: An analysis of 7,500 widely distributed lakes. *Limnol. Oceanogr.* **52**, 1208–1219 (2007).
118. M. Frankignoulle, A. Borges, R. Biondo, A new design of equilibrator to monitor carbon dioxide in highly dynamic and turbid environments. *Water Res.* **35**, 1344–1347 (2001).
119. G. W. Kling, M. A. Clark, G. N. Wagner, H. R. Compton, A. M. Humphrey, J. D. Devine, W. C. Evans, J. P. Lockwood, M. L. Tuttle, E. J. Koenigsberg, The 1986 Lake Nyos gas disaster in Cameroon, West Africa. *Science* **236**, 169–175 (1987).

Acknowledgments: We are grateful to crews of *RV Hammerkop* and the *Maman Benita* for support during the sampling expeditions in Lakes Victoria and Tanganyika; to C. M. Balagizi for help during the sampling of the Masisi lakes; to the team from the Institut Supérieur Pédagogique Bukavu for help during the sampling in Lake Kivu; to the Katwe marine police officers, A. Nankabirwa and E. Nabafu for help during sampling in Lakes Edward and George; to M.-V. Commarieu, B. Leporcq, Z. Kelemen, and T. Bousmanne for analytical support; to TCarta for the GIS of Lake Tanganyika bathymetry; and to four anonymous reviewers for comments on the initial submission. L.D., C.M., and F.A.E.R. are postdoctoral researchers at the FNRS, and A.V.B. is a Research Director at the FNRS. **Funding:** This work was supported by Belgian Federal Science Policy Office grant SD/AR/02A, Belgian Federal Science Policy Office grant BR/154/A1/HIPE, Fonds National de la Recherche Scientifique grant 2.4.598.07, Fonds National de la Recherche Scientifique grant 2.4.515.11, Fonds National de la Recherche Scientifique grant T.0246.13, Fonds National de la Recherche Scientifique grant J.0009.15, Fonds National de la Recherche Scientifique grant U.N024.17, Fonds National de la Recherche Scientifique grant T.0156.18, Fonds National de la Recherche Scientifique grant J.0013.19, Fonds National de la Recherche Scientifique grant T.0027.20, Fonds National de la Recherche Scientifique grant J.0015.21, EU Marie Skłodowska Curie Fellowship grant H2020-MSCA-IF-2017 no. 796707, KU Leuven Special Research Fund, Fonds Wetenschappelijk Onderzoek, Fonds Agathon de Potter, and Fonds Léopold III pour l'Exploration et la Conservation de la Nature. **Author contributions:** Conceptualization: A.V.B. Sample collection: A.V.B., L.D., S.B., W.O., T.L., F.A.E.R., V.F.R., N.R.G.V., F.D., I.A.K., and C.M. Sample analysis: A.V.B., L.D., S.B., T.L., F.A.E.R., V.F.R., N.R.G.V., F.D., J.-P.D., and C.M. GIS data extraction and analysis: A.V.B., L.D., T.L., G.H.A., and C.M. Writing (original draft): A.V.B. Writing (review and editing): L.D., S.B., W.O., T.L., F.A.E.R., V.F.R., N.R.G.V., F.D., I.A.K., J.-P.D., G.H.A., and C.M. **Competing interests:** The authors declare that they have no competing interests. **Data and materials availability:** The CO_2, CH_4, and N_2O data can be downloaded from https://doi.org/10.5281/zenodo.6025626. All data needed to evaluate the conclusions in the paper are present in the paper and/or the Supplementary Materials.

Submitted 6 April 2021
Accepted 9 May 2022
Published 24 June 2022
10.1126/sciadv.abi8716

ScienceAdvances

Greenhouse gas emissions from African lakes are no longer a blind spot

Alberto V. BorgesLoris DeirmendjianSteven BouillonWilliam OkelloThibault LambertFleur A. E. RolandVao F. RazanamahandryNy Riavo G. VoarintsoaFrançois DarchambeauIsmael A. KimireiJean-Pierre DescyGeorge H. AllenCédric Morana

Sci. Adv., 8 (25), eabi8716.

Science Advances
AAAS

Supplementary Materials for

Greenhouse gas emissions from African lakes are no longer a blind spot

Alberto V. Borges *et al.*

Corresponding author: Alberto V. Borges, alberto.borges@uliege.be

Sci. Adv. **8**, eabi8716 (2022)
DOI: 10.1126/sciadv.abi8716

This PDF file includes:

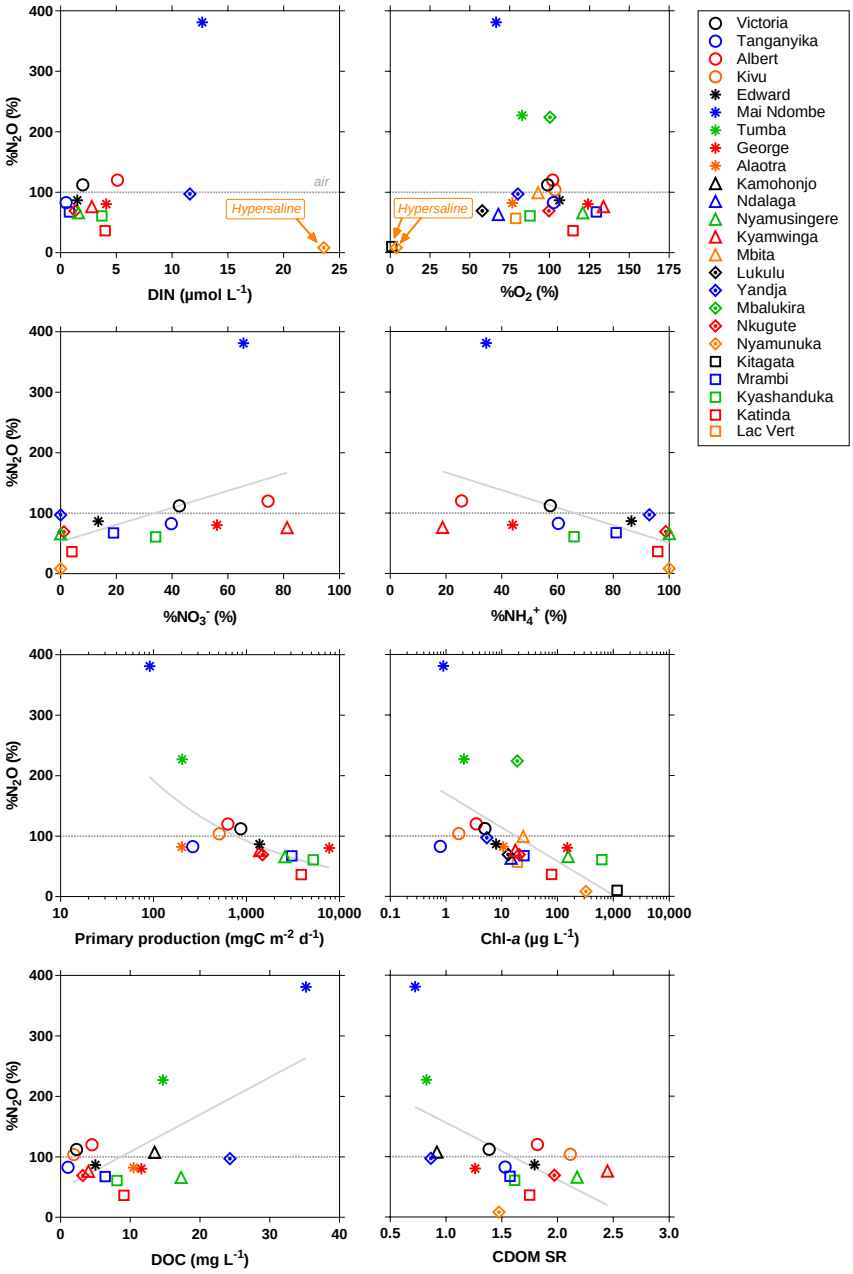

Fig. S1.

N_2O saturation level (%N_2O) versus dissolved inorganic nitrogen (DIN=NO_3^- + NH_4^+), oxygen saturation level (%O_2), relative abundance of NO_3^- (%NO_3^- =NO_3^- / (NO_3^- + NH_4^+) x 100), relative abundance of NH_4^+ (% NH_4^+ =NH_4^+ / (NO_3^- + NH_4^+) x 100), primary production, chlorophyll-a (Chl-a) concentration, dissolved organic carbon (DOC) and colored dissolved organic matter slope ratio (CDOM SR) in several African tropical lakes. Horizontal dotted line indicates saturation with the atmosphere, and solid lines are fitted to the data (Table S3). Humic Lake Mai Ndombe had a high DIN concentration associated with high %N_2O, while hypersaline lake Nyamunuka had even higher DIN but nearly no N_2O due to strong denitrification related to the nearly anoxic water column. For non-humic lakes, the positive relation between %N_2O with the relative abundance of NO_3^- (%NO_3^-) and the negative relation with the relative abundance of NH_4^+ (%NH_4^+) confirm the hypothesis of N_2O removal by denitrification in low %NO_3^- lakes, and N_2O production by nitrification in high %NO_3^- lakes.

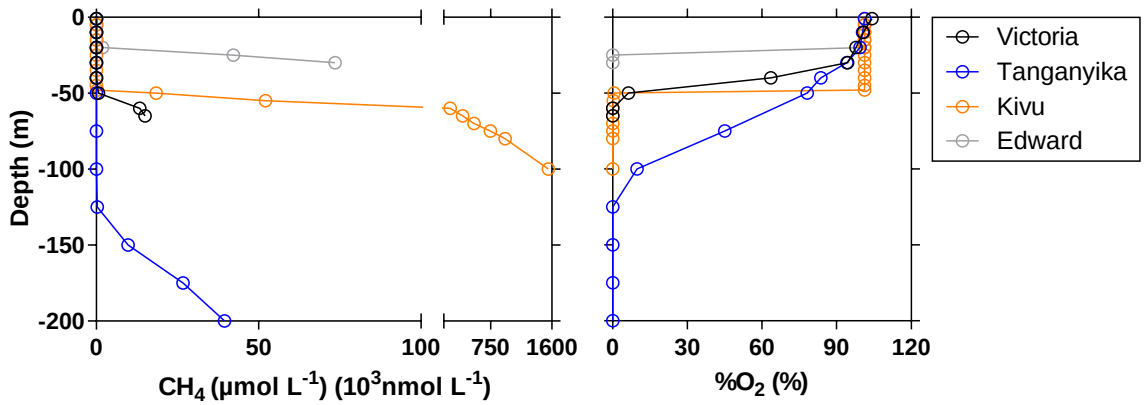

Fig. S2.

Examples of vertical profiles of CH_4 concentration and oxygen saturation level ($\%O_2$) in Lakes Victoria, Tanganyika, Kivu and Edward. Lakes Tanganyika and Kivu are permanently stratified (meromictic) where anoxic bottom water is a permanent feature. Lakes Victoria and Edward are seasonally stratified (holomictic) anoxic bottom water only occurs seasonally (Fig. S3). The meromictic nature sustains a constant upward flux of CH_4 from bottom to surface waters, and methane oxidation (MOX) in surface waters might be limited by sunlight (*22*) in Lakes Tanganyika and Kivu characterized by deeper photic depths. In the holomictic lakes such as Victoria and Edward, the seasonal mixing led to full oxygenation to bottom waters and strong CH_4 removal by MOX, preventing the accumulation of extremely large quantities of CH_4 in anoxic bottom waters during the stratified period, as observed in the meromictic lakes (Fig. S3). Note that Lake Kivu is characterized by much higher CH_4 concentrations in the hypolimnion than Lake Tanganyika, which might explain higher CH_4 concentrations in surface waters in Lake Kivu than in Lake Tanganyika at similar bottom depth (Fig. 4).

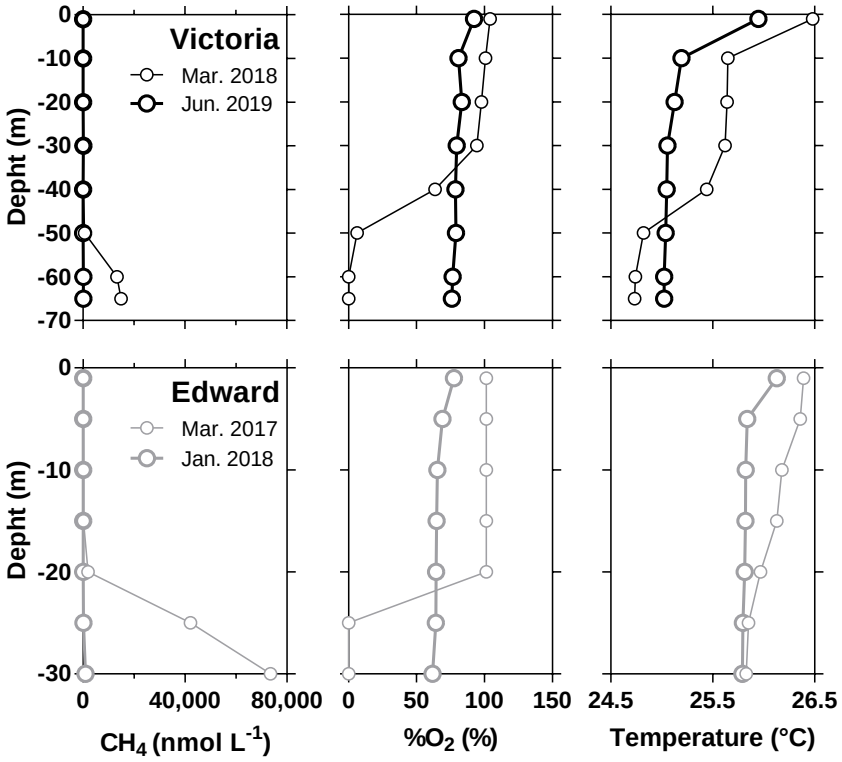

Fig. S3.

Examples of vertical profiles of CH_4 concentration, oxygen saturation level ($\%O_2$) and water temperature in holomictic Lakes Victoria and Edward, during contrasting periods of the year (vertically mixed and stratified).

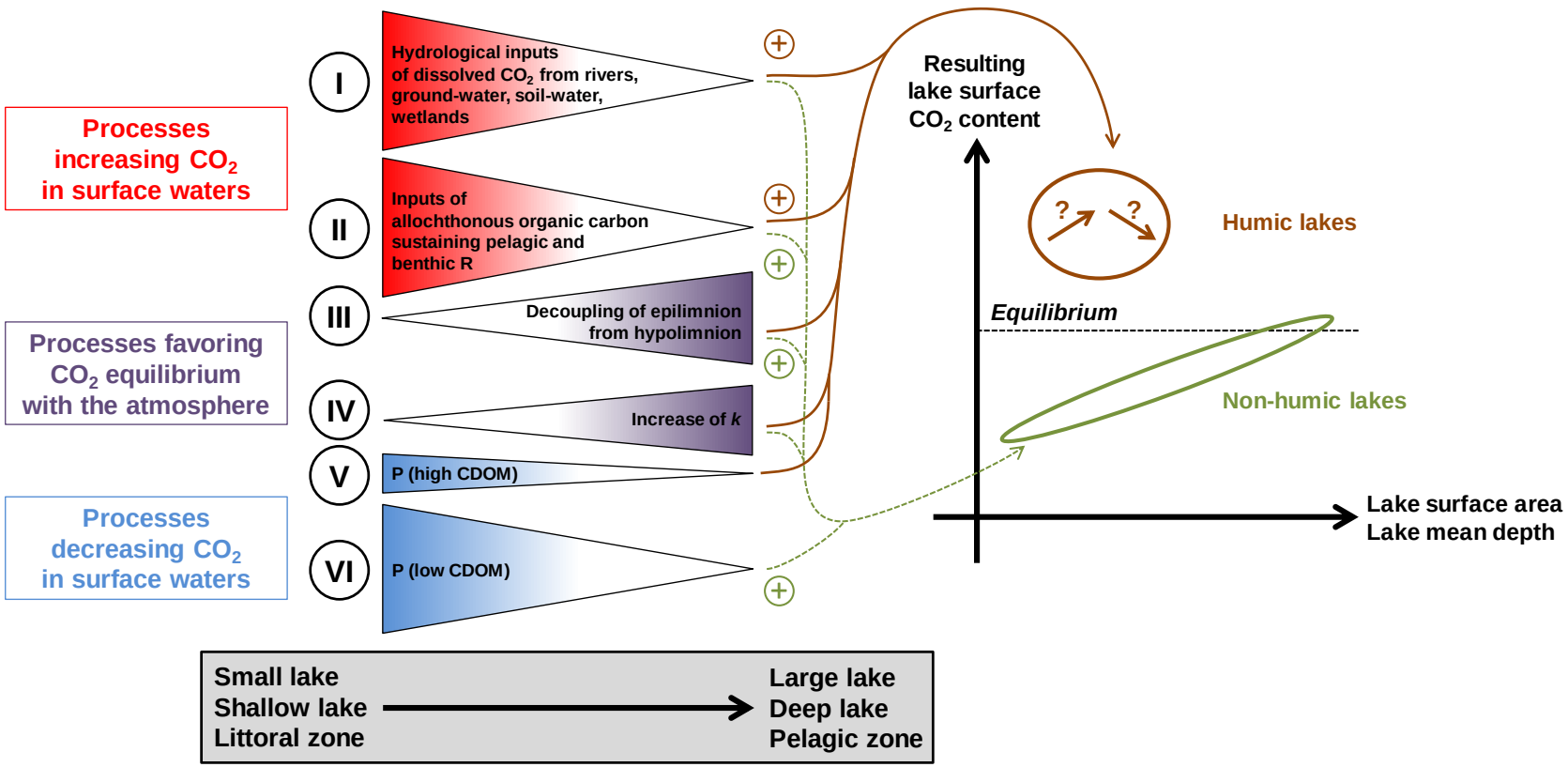

Fig. S4.

Conceptual diagram summarizing the processes that increase or decrease CO_2 in surface waters of lakes as a function of lake size (surface area and depth). The CO_2 content in surface waters of lakes results from the balance of sources and sinks of CO_2 that are in part linked to organic carbon processing within the lake (metabolic status at ecosystem scale, that is, the balance between gross primary production (P) and ecosystem respiration (R)) (*76*), in part linked to hydrological inputs of CO_2 from rivers, surface runoff, soil-water and ground-water (*77*,*78*), and in part related to the exchange of CO_2 with the atmosphere. Part of the heterotrophic degradation of organic matter (leading to the production of CO_2 and contributing to R) is sustained by allochthonous inputs of dissolved (DOC) and particulate (POC) organic carbon from the catchment and riparian wetlands (*15*). The relative intensity of external inputs of

DOC, POC and CO_2 depend on a complex combination of land cover on the catchment, catchment slope, lake size and precipitation (*15*). Inputs of DOC and humic content are strongly promoted by the presence of riparian wetlands on the catchment (*79*). The relative importance of internal processing of allochthonous organic carbon inputs depends on water residence time that is itself a function of the fraction of hydrologic export as evaporation (*80*) and scale with lake size. Overall, most processes affecting CO_2 dynamics in lakes directly or indirectly scale with lake size, leading to documented inter-lake variations as function of lake average depth and lake surface area (*8,14,15,25,26,81*), and intra-lake variations as a function of bathymetry, from the shallow (littoral) to deeper (pelagic) zones. Small lakes have a greater connectivity and potential exchange of organic and inorganic carbon with the riparian wetlands and surrounding terrestrial landscape along its periphery relative to lake surface area than large lakes. Hence, hydrological inputs of CO_2 (I) and organic matter (II) should be relatively higher in smaller lakes than in larger lakes (*15,81*). The fraction of organic matter that is mineralized within a lake or that is on the contrary exported depends on hydrologic residence time that is function of the ratio of water loss by evaporation to river outflow, that itself scales with the ratio of watershed area to lake area (*80*) or possibly also slope of the catchment (*82*). The relative contribution of CO_2 hydrologic inputs to CO_2 generated by organic matter degradation strongly declines with increasing water residence time (*80*). In general, larger and/or deeper lakes tend to have longer water residence times than smaller ones. Similarly, allochthonous inputs of nutrients should decline with increasing lake area and water depth, hence P should be higher in smaller/shallower lakes than larger/deeper lakes (V and VI) (*15,81*). Planktonic and benthic P will also be modulated by the content of colored dissolved organic matter (CDOM) that reduces light availability in the water column, decreasing P (*12*). Vertical water column density stratification (physical stability) increases with maximum depth of the lake (*83*). This will promote the decrease of CO_2 in the mixed layer and the increase of CO_2 in bottom waters due to the decoupling of CO_2 uptake in surface waters by phytoplankton carbon fixation and CO_2 release in bottom waters due to degradation of organic matter by microbes (mineralization) following the sedimentation of organic matter particles to depth (III). Higher water column stability also results in reduced upward turbulent flux of CO_2. Increasing lake size leads to an increase in fetch and enhanced turbulence generated by wind shear (*16*). This has two consequences: deeper mixed layers (*83*) and higher gas transfer velocities (*k*) (*16)* both promoting the equilibration of gases with the atmosphere (IV). Precipitation or dissolution of calcium carbonate leads, respectively, to a production or consumption of CO_2 ($2HCO_3^- + Ca^{2+} = CaCO_3 + CO_2 + H_2O$) although this process usually contributes marginally to changes in CO_2 content in surface lakes (*55*). CO_2 is in chemical equilibrium with HCO_3^- and CO_3^{2-} ($CO_2 + H_2O = HCO_3^- + H^+ = CO_3^{2-} + 2H^+$) and the higher the HCO_3^- and CO_3^{2-} content of water (hardness) the higher the buffering capacity (relative change of CO_2 concentration to a dissolved inorganic carbon (DIC) change in response to a biogeochemical uptake or release) (e.g. *84*). The left-hand side of the figure shows the processes that change CO_2 content and how their intensity changes with lake depth (between lakes or within a given lake) and/or lake surface area; the right hand-side of the figure shows the putative combination of processes that could explain the patterns observed in the sampled African lakes (Fig. 2). The “+” symbol indicates the processes we hypothesize as most important in regulating the observed patterns in African lakes. The “?” indicates that we could not determine a tendency based on available data (positive, negative or none at all).

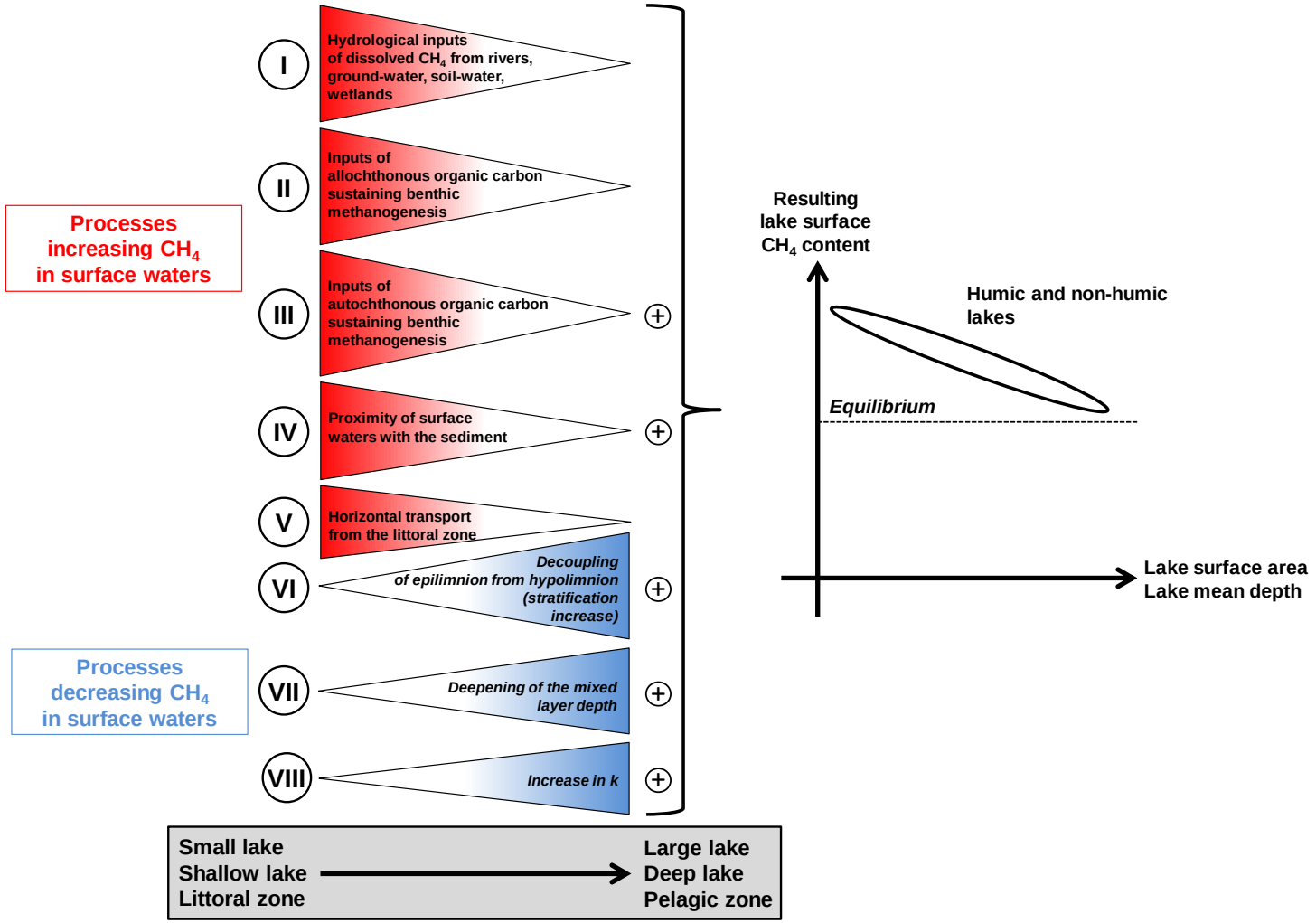

Fig. S5.

Conceptual diagram summarizing the processes that increase or decrease CH_4 in surface waters of lakes as a function of lake size (surface area and depth). The dissolved CH_4 concentration in surface waters of lakes results from the balance of sources and sinks of CH_4. CH_4 is mainly produced by

methanogenesis in sediments; CH_4 production in aerobic conditions related to phytoplankton metabolism has been shown to occur in African lakes although a marginal source compared to sedimentary sources (*22*). CH_4 produced in sediments can diffuse directly into the overlying water column, or accumulate as gas bubbles that can be released into the overlying water column (ebullition). Bubbles can reach the atmosphere or dissolve as they rise in water (partly or completely). The main processes that remove dissolved CH_4 in lakes are the emission of CH_4 to the atmosphere and the microbial CH_4 oxidation (MOX) either in oxic or anoxic conditions, at the sediment-water interface or in the water column. As for CO_2, hydrological inputs of CH_4 from rivers, surface runoff, soil-water and ground-water can contribute to CH_4 content in lakes (I) (*85*), although CH_4 is usually attributed mostly to internal production (*14*). The inputs of allochthonous (II) and autochthonous (III) organic matter to sediments stimulates sedimentary methanogenesis (*86*). This input of organic matter is higher in littoral zones of lakes than in deeper zones of lakes, as in small compared to larger lakes (*87*). Shallow water column also reduces the impact of CH_4 removal by MOX (IV), while the deepening of the mixed layer depth (VII) enhances the relative impact of MOX in CH_4 removal (*88*). Small lakes have a greater connectivity and potential exchange of organic matter and CH_4 with the riparian wetlands and surrounding terrestrial landscape along its periphery relative to lake surface area than large lakes. Shallower depths are favorable to methane ebullition (lower hydrostatic pressure countering release of bubbles), and the partial dissolution of rising bubbles will increase dissolved CH_4 concentration in surface waters (*87*). Additionally, small and shallow lakes can have higher production of phytoplankton or macrophytes supplying organic carbon to sediments and sustaining CH_4 production (*89,90*). Some of the CH_4 in the water column in the more central part of lakes is transported horizontally from hot-spot production littoral zones (*91,92*) although the importance of this process decreases with the size of the lake (V). The increase of lake depth leads to enhanced stratification (*83*) and the decoupling of the hypolimnion where CH_4 diffusing from the sediment accumulates and the epilimnion where CH_4 decreases due to loss to the atmosphere or to removal by aerobic MOX (VI, VII). The increasing lake size leads to an increase in fetch and enhanced turbulence generated by wind shear, and higher gas transfer velocity (k) values (*16*) promoting the equilibration of gases with the atmosphere (VIII). The left-hand side of the figure shows the processes that change CH_4 content and how their intensity changes with lake depth (between lakes or within a given lake) and/or lake surface area, the right hand-side of the figure shows the putative combination of processes that can explain the patterns observed in the sampled African lakes (Fig. 2). The "+" symbol indicates the processes we hypothesize as most important in regulating the observed patterns in African lakes.

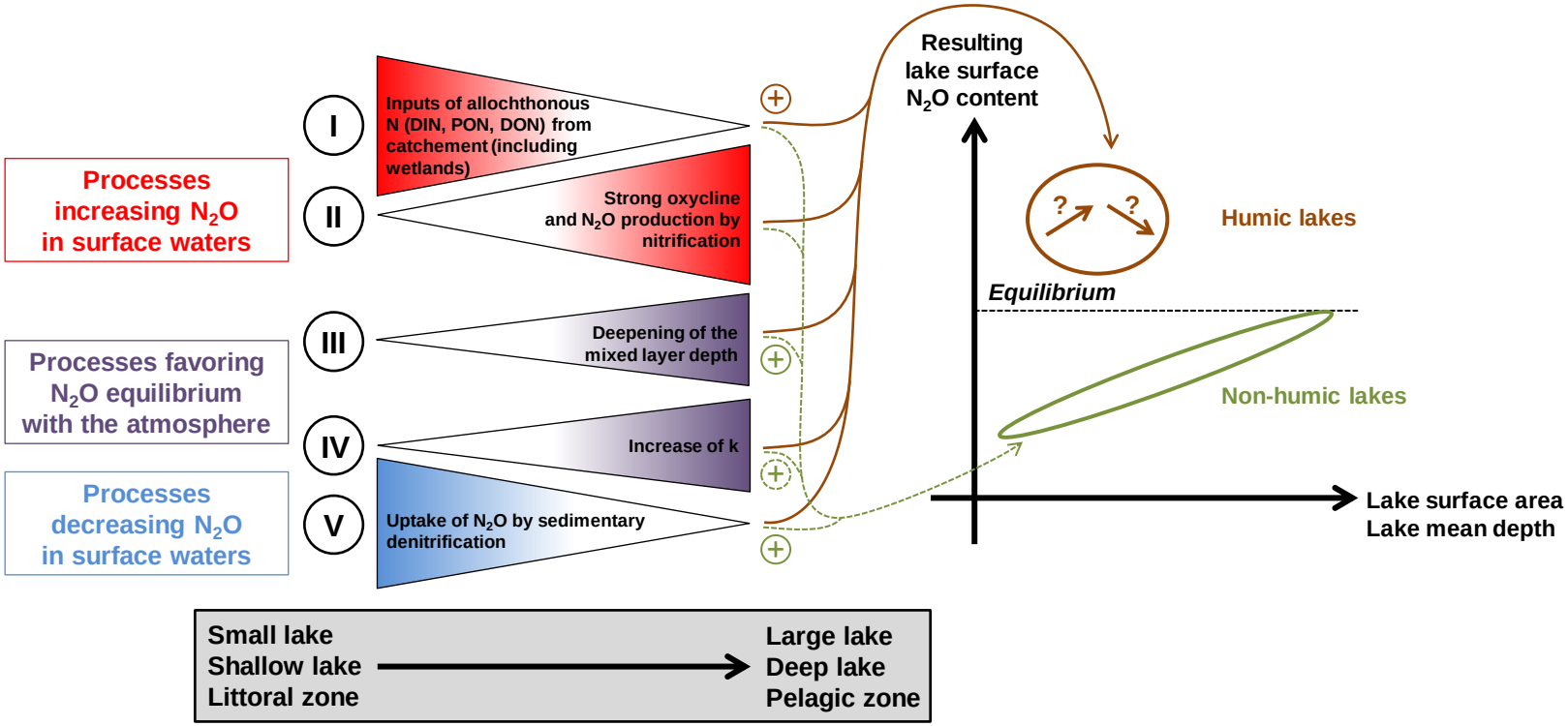

Fig. S6.

Conceptual diagram summarizing the processes that increase or decrease N_2O in surface waters of lakes as a function of lake size (surface area and depth). N_2O can be produced as a byproduct of nitrification (oxidation of NH_4^+ to NO_3^- in aerobic conditions). N_2O is also involved in the last step (reduction of N_2O to N_2) of denitrification (reduction of NO_3^- to N_2 in anaerobic conditions), so N_2O can accumulate in the case of incomplete reduction to N_2 (in presence of trace levels of O_2) or, alternatively, be removed by denitrifiers (in low NO_3^- conditions). The yield of N_2O produced by nitrification strongly increases with decreasing oxygen levels. Denitrification can occur in presence of trace levels of O_2 (<6 µmol L^{-1}), but in this case there is an inhibition of reduction to N_2 step and N_2O strongly accumulates. Hence, N_2O production (from nitrification or denitrification) tends to be highest from both processes at low O_2 levels, while strictly anoxic conditions promote the removal of N_2O by denitrification (reduction to N_2). Rates of nitrification and denitrification (and N_2O levels) increase with the levels of dissolved inorganic nitrogen (DIN) (*50,93,94*). Terrestrial DIN, dissolved (DON) and particulate (PON) organic nitrogen inputs stimulate N_2O production that should be higher in smaller lakes (I) (as for DOC and POC, see Fig. S4). In humic lakes, phytoplankton production is low but microbial mineralization of organic matter is high and can lead to relatively high levels of DIN (*23*). In larger or deeper lakes, a strong

stratification (*83*) will promote a more marked oxycline and a peak of N_2O related to nitrification (*95*) (II). If the hypolimnion becomes anoxic, N_2O can decrease due to denitrification (*88*,*95*). The equilibrium of N_2O with the atmosphere will be favored in larger lakes due to the deepening of the mixed layer, as well as the increase in the gas transfer velocity (*k*) (III, IV) (*16*,*83*). In shallower lakes, the impact of fluxes between the sediment and the water column will be strongest. In the sampled lakes, sedimentary denitrification is the most likely explanation for the water column under-saturation of N_2O (V) (refer to Fig. S9) although this has only been occasionally reported in boreal lakes that are strongly over-saturated in N_2O (*50*). The left-hand side of the figure shows the processes that change N_2O content and how their intensity changes with lake depth (between lakes or within a given lake) and/or lake surface area, the right hand-side of the figure shows the putative combination of processes that could explain the patterns observed in the sampled African lakes (Fig. 2). The "+" symbol indicates the processes we hypothesize as most important in regulating the observed patters in African lakes. The observed patterns of CO_2, CH_4 and N_2O are to some extent linked in the sampled non-humic lakes. Higher phytoplankton biomass in shallower lakes (littoral zones) leads to low CO_2 levels in surface waters, but also enhanced transfer of organic matter to sediments, consequently higher sedimentary organic matter degradation including methanogenesis possibly explaining the positive relationship between CH_4 dissolved concentration and chlorophyll-a (Chl-*a*) concentration (Fig. 6). The higher sediment denitrification (and uptake of N_2O from the water by the sediment) related to higher delivery of phytoplankton biomass to sediments might also explain the negative relationship between N_2O saturation levels and Chl-*a* (Fig. S1). The "?" indicates that we could not determine a tendency based on available data (positive, negative or none at all).

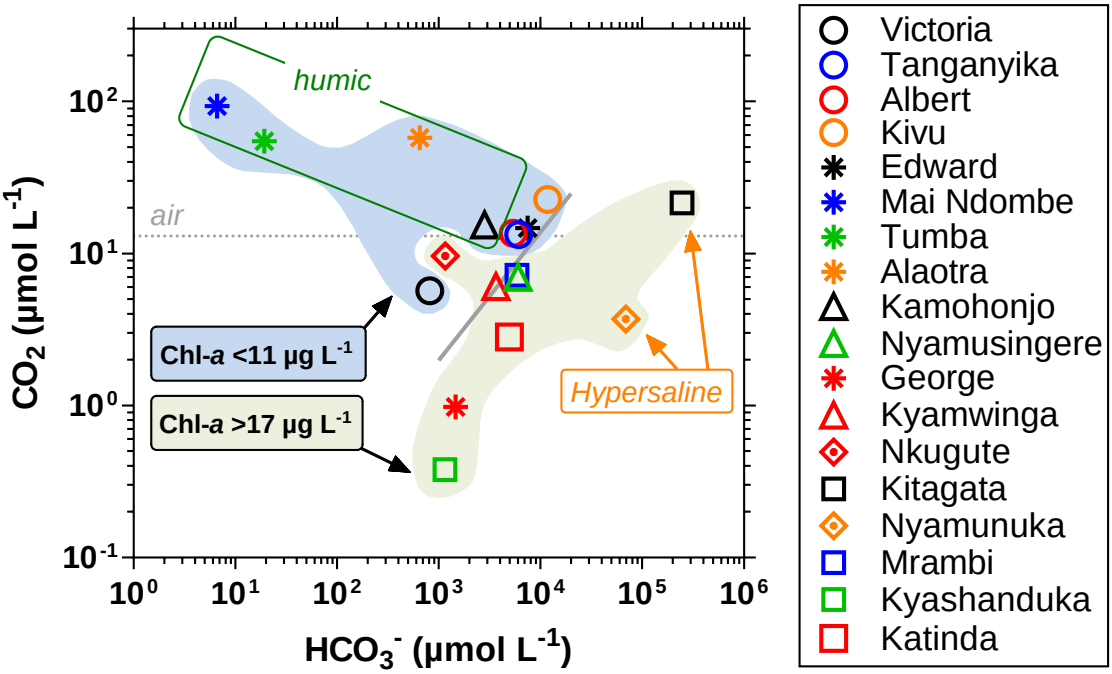

Fig. S7.

Dissolved CO_2 concentration *versus* HCO_3^- concentration in several African tropical lakes. The concentration of CO_2 did not show clear patterns with the concentration of HCO_3^- despite very large range of variation of both quantities. The two lakes with the highest CO_2 concentrations were located in the Congo River basin characterized by low rock weathering (*17*), hence, also characterized by the lowest HCO_3^- concentrations (Mai Ndombe, Tumba). The highest HCO_3^- concentrations were observed in the two hypersaline lakes (Nyamunuka and Kitagata). If the four humic lakes and the two hypersaline lakes are excluded, then CO_2 and HCO_3^- concentrations are positively correlated for the remaining 12 lakes. It is unclear if such a correlation implies a causality or is simply spurious. Yet, such a positive relationship is inconsistent with the hypothesis that CO_2 under-saturation in lakes is driven by high HCO_3^- and pH in hard-water lakes by opposition with soft-water lakes (*77*,*96*). In the sampled African lakes, CO_2 values above equilibrium were observed for Chlorophyll-a (Chl-*a*) concentrations below 11 µg L^{-1}, while CO_2 below equilibrium were observed for Chl-*a* above 17 µg L^{-1}. Solid line is the fit to the data (Table S3).

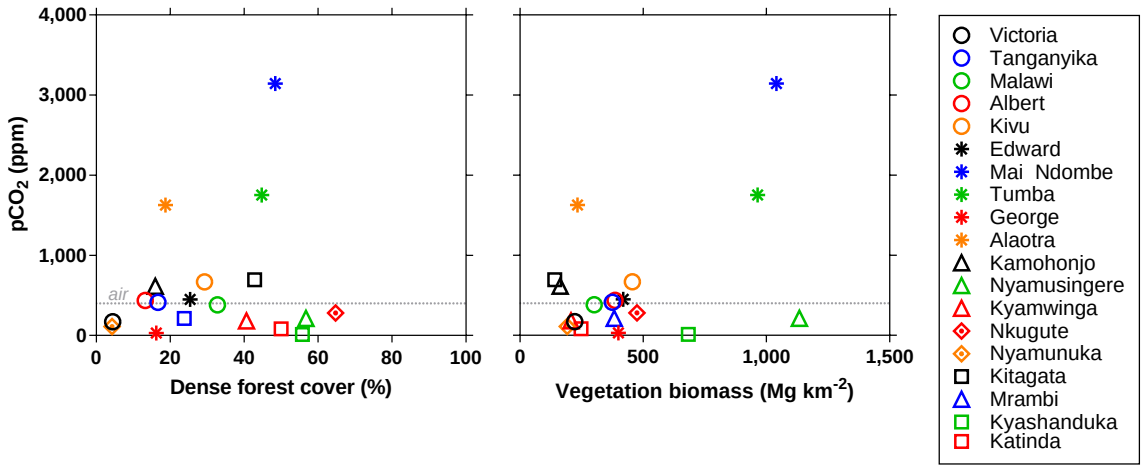

Fig. S8.

Surface partial pressure of CO_2 (pCO_2) versus dense forest cover and vegetation biomass on the catchment in several African tropical lakes. Vegetation biomass was extracted from pantropical national level carbon stock data-set (*97*), and dense forest cover from Global Land Cover 2000 database of Africa (*98*), using catchment delineation based on HydroSHEDS (*65*).

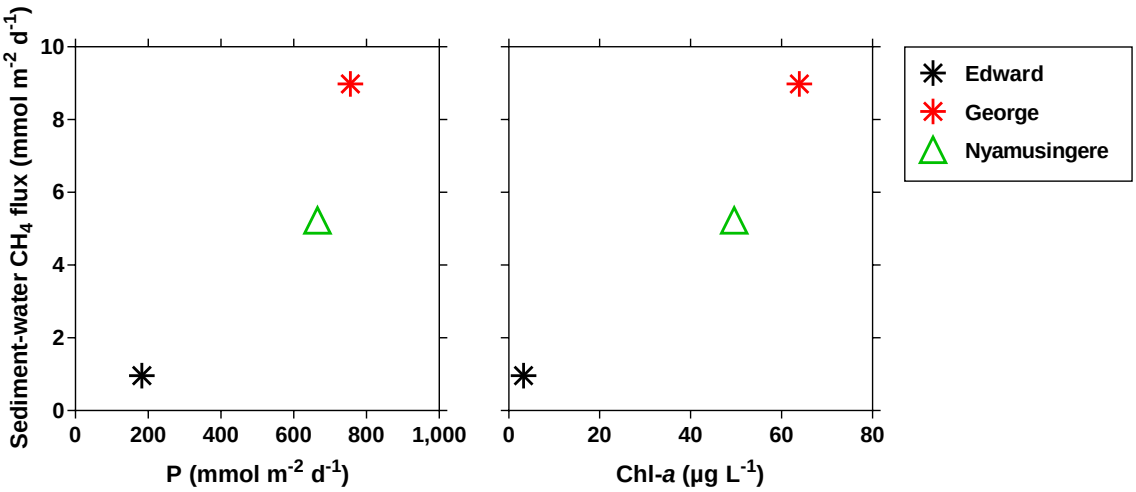

Fig. S9.

Sedimentary air-water diffusive CH_4 flux (*22*) versus primary production (P) and surface water chlorophyll-*a* (Chl-*a*) concentration in Lakes Edward, George and Nyamusingere. During the same incubations, a flux of N_2O from the water to the sediment was measured of -1.3 µmol m^{-2} d^{-1} in L. Edward, -0.7 µmol m^{-2} d^{-1} in L. George, and -4.0 µmol m^{-2} d^{-1} in L. Nyamusingere. While a negative flux is indicative of the removal of N_2O from the water column from sedimentary denitrification, no correlation was found with P nor Chl-*a*, indicating a more complex relation between sedimentary N_2O removal and organic matter delivery to the sediment.

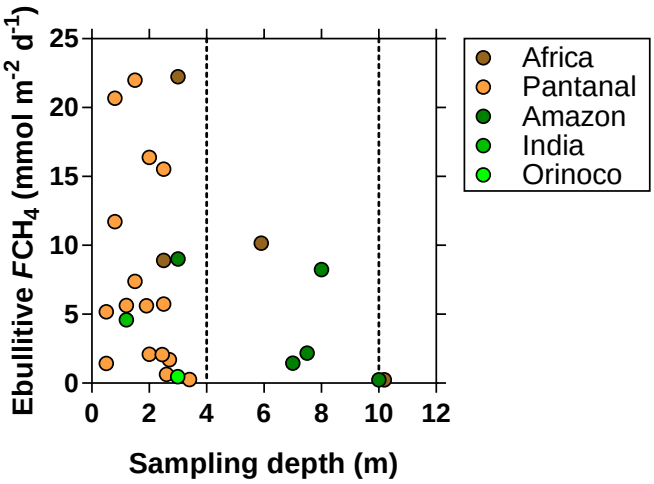

Fig. S10.

Ebullitive air-water flux of CH_4 (FCH_4) in African lakes (this study, Table S5), Pantanal lakes (*99*), Amazon floodplain lakes (*100-103*), Orinoco floodplain lakes (*104*), and one lake in India (*105*).

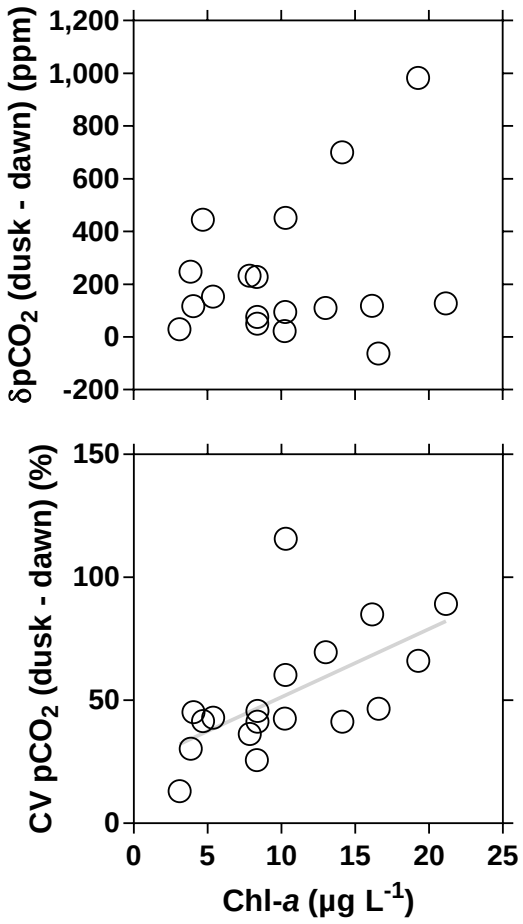

Fig. S11.

Difference of the partial pressure of CO_2 in surface waters (δpCO_2) and coefficient of variation (CV) of pCO_2 in surface waters between dusk and dawn (next day) as a function of chlorophyll-*a* (Chl-*a*) concentration in Lake Victoria during three cruises (Table S7). Sampling was carried out during daytime (dawn to dusk) and the ship anchored during the night. The difference between dusk and dawn (at the anchoring point) provides an estimate of the maximum daily amplitude. Solid line is fitted to the data (Table S3). The δpCO_2 values ranged between -63 and 983 ppm, with a median of 123 ppm and only in 2 cases out of 18 did the sign of the ΔpCO_2 (direction of FCO_2) change. These differences were consistent with diel variations of P and R and seemed to be related to phytoplankton biomass as indicated by the lower plot.

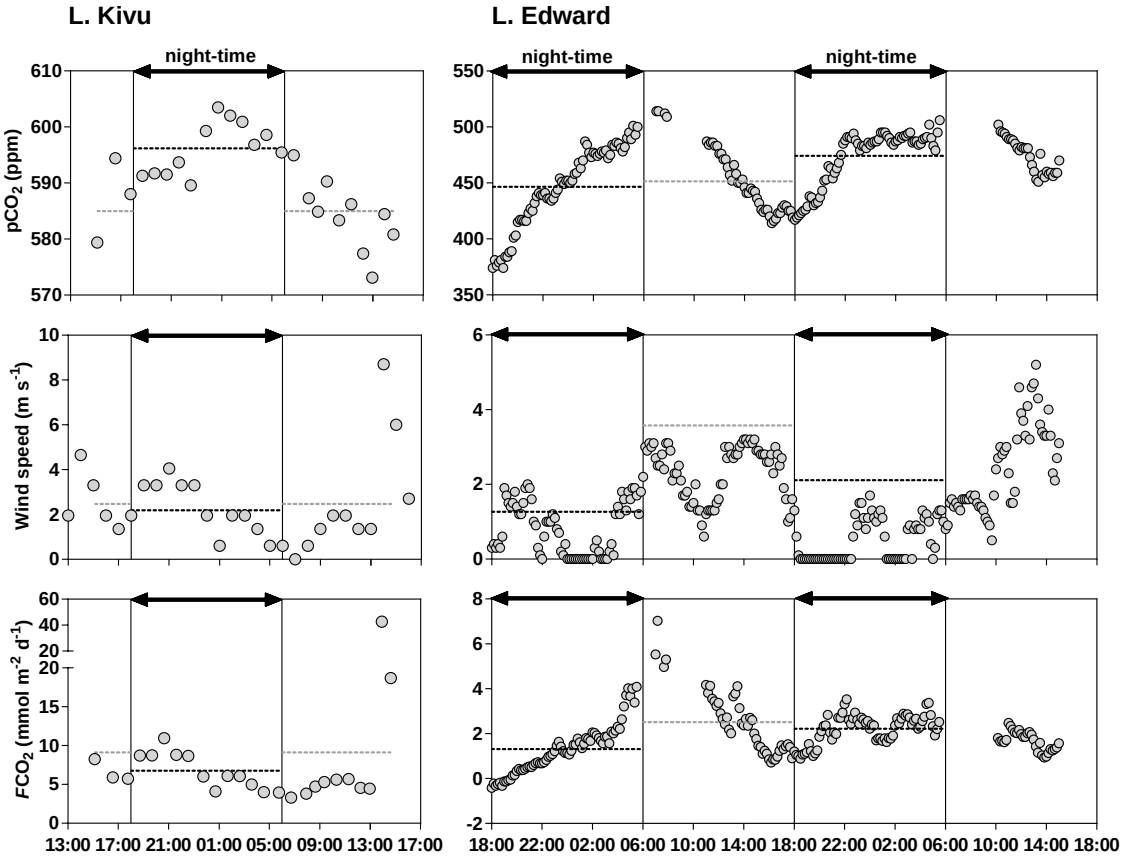

Fig. S12.

Diel variations of the partial pressure of CO_2 (pCO_2) in surface waters, wind speed and air-water CO_2 flux (FCO_2) in Lake Kivu (23/03/2007 (13:00) to 24/03/2007 (14:00), 60 min acquisition) and Lake Edward (20/01/2018 (18:00) to 22/01/2018 (15:00), 10 min acquisition). Grey horizontal dotted line indicates the day-time average, black horizontal dotted line indicates the night-time average.

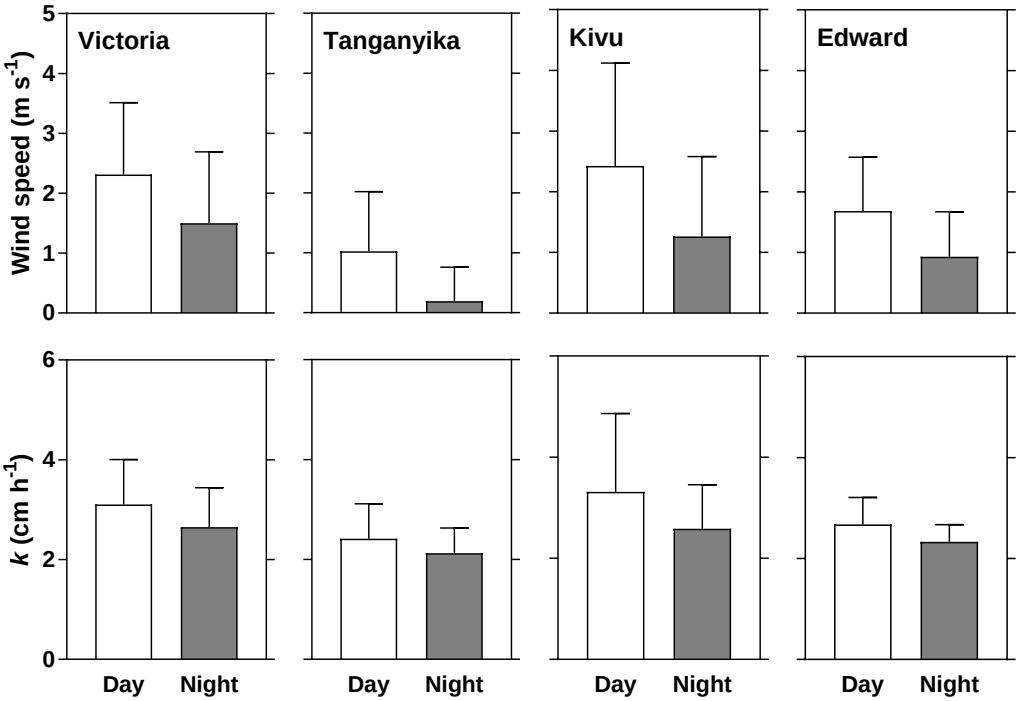

Fig. S13.

Day-time and night-time averages of wind speed and gas transfer velocity (*k*) computed with the parameterization of (*64*) in Lakes Victoria (Buzika Island, 29/01/2018 to 27/11/2018), Tanganyika (Kigoma, 28/02/2002 to 29/09/2006), Kivu (Bukavu, 01/01/2003 to 31/12/2011), and Lake Edward (Mweya, 22/03/2017 to 04/02/2018). These plots provide information on the wind speed variability at the measurement site, and do not necessarily represent absolute differences among the four lakes. Wind speed was higher during day-time because wind is in part forced by the gradient of air temperature between the lake surface and the surrounding land that is stronger during day-time.

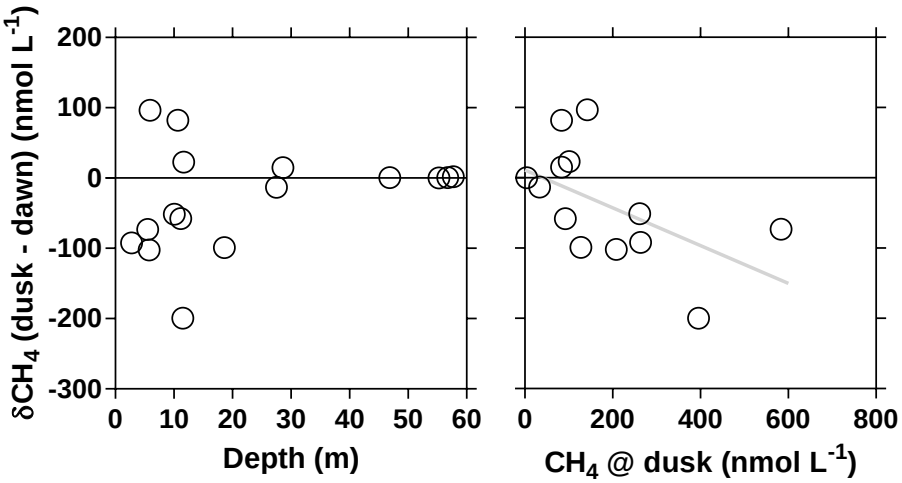

Fig. S14.

Difference of dissolved CH_4 concentration (δCH_4) in surface waters between dusk and dawn as a function of bottom depth and CH_4 at dusk in Lake Victoria during three cruises (Table S7). Sampling was carried out during day-time and the ship anchored during the night. The difference between dusk and dawn provides an estimate of the maximum daily amplitude. The δCH_4 values ranged between -200 and 97 nmol L^{-1}, with a median of -6 nmol L^{-1}. A δCH_4 signal was measureable for bottom depths < 30 m. In 8 out 12 cases, δCH_4 was negative, possibly related to an enhanced removal of CH_4 by MOX due to the absence during night-time of light inhibition of microbial methane oxidation (MOX) (*15*). This explanation was also consistent with the general tendency of a stronger night-time decrease of CH_4 with increasing CH_4 levels at dusk, since MOX is a first order process, dependent upon substrate concentration (*106*). The positive δCH_4 signal might be indicative of input of CH_4 from bottom waters due to night-time convection. Solid grey line is a linear fit to the data (Table S3).

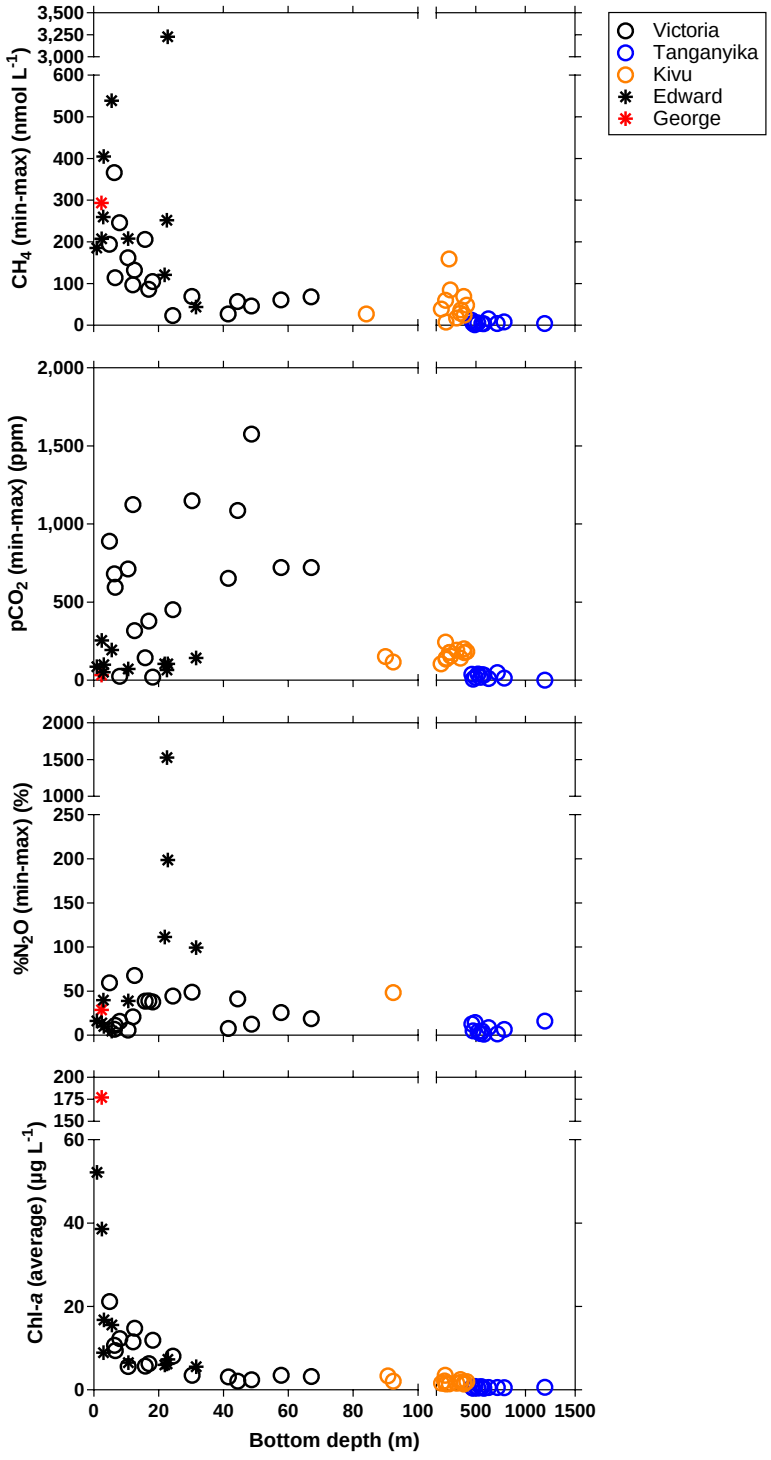

Fig. S15.

Maximal amplitude at stations repeatedly sampled during consecutive cruises (*n*) of dissolved CH_4 concentration, partial pressure of CO_2 (pCO_2) and N_2O saturation level ($\%N_2O$) in surface waters, and chlorophyll-*a* (Chl-*a*) concentration average for all cruises as a function of bottom depth in Lakes Victoria (*n*=3), Tanganyika (*n*=2), Kivu (*n*=4), Edward (*n*=4), and George (*n*=4). $\%N_2O$ showed extreme variability at 20 m in Lake Edward, due to strong mixing events induced by storms (not shown).

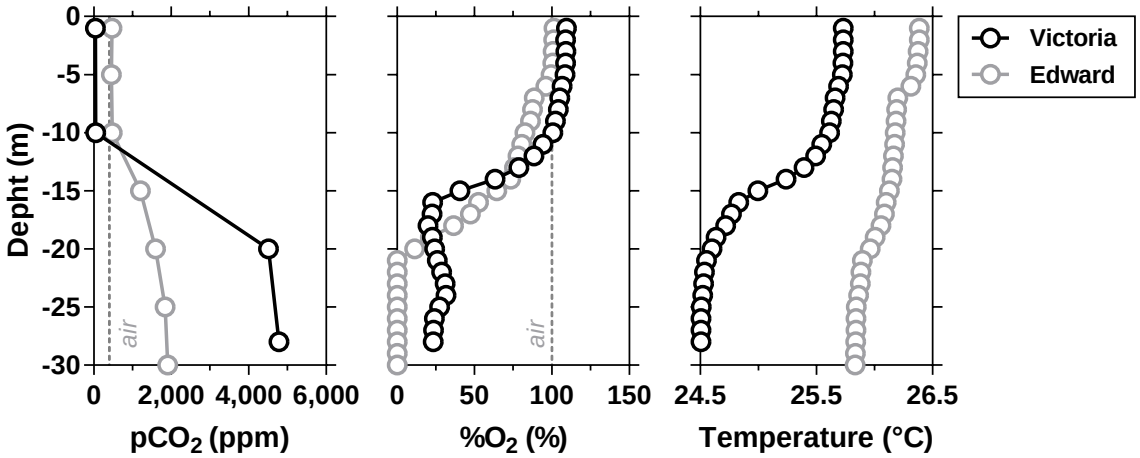

Fig. S16.

Vertical profiles of the partial pressure of CO_2 (pCO_2), oxygen saturation level ($\%O_2$), and water temperature in Lakes Victoria (26/10/2018) and Edward (27/03/2017) during the periods of maximal observed stratification at stations with equivalent bottom depth (30 and 32 m, respectively). Horizontal dotted lines indicate equilibrium with the atmosphere. Note that in Lake Victoria bottom waters were still oxygenated unlike Lake Edward where they were anoxic. The maximum pCO_2 value measured in bottom waters of Lake Victoria was 6,507 ppm at 68 m depth in the deepest central part of the lake. We do not have a clear explanation for the higher pCO_2 values in bottom water of Lake Victoria compared to Lake Edward at similar depths. Vertical thermal stratification was weaker in Lake Edward than Lake Victoria, allowing more frequent vertical mixing (by storms for example) and lesser accumulation of CO_2 in bottom waters. Lower pCO_2 and higher $\%O_2$ in surface waters indicated a higher primary production in surface waters of Lake Victoria than Edward, possibly sustaining a higher degradation of organic matter in bottom waters. In Lake Victoria, there could also be an important degradation in sediments of organic matter remnants of past periods with intense eutrophication (*54,107*).

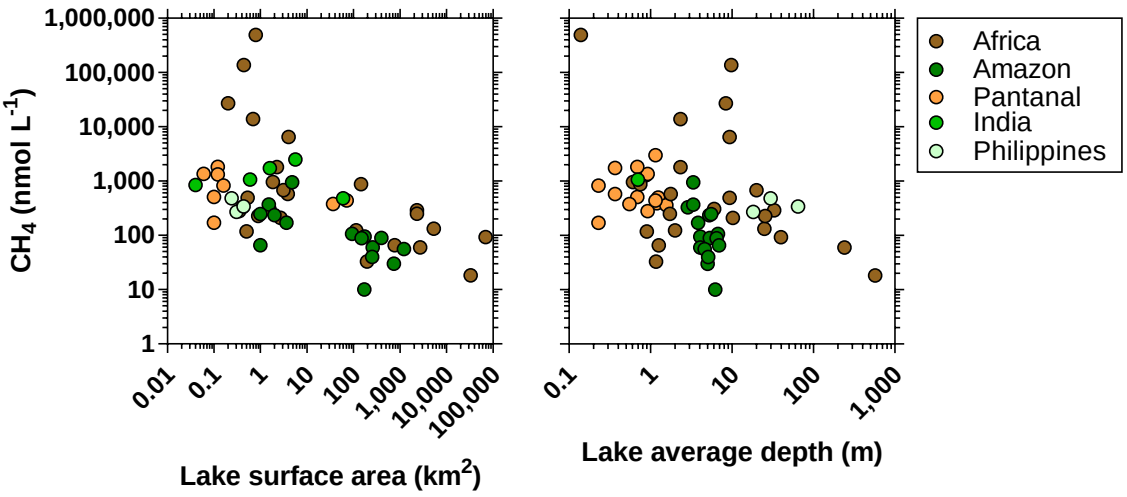

Fig. S17.

Dissolved CH_4 concentration in surface waters versus lake surface area and lake average depth in lakes in Africa (this study), Amazon floodplains (*108*, *109*), Pantanal (*99*), India (*105*,*110*), and Philippines (*111*).

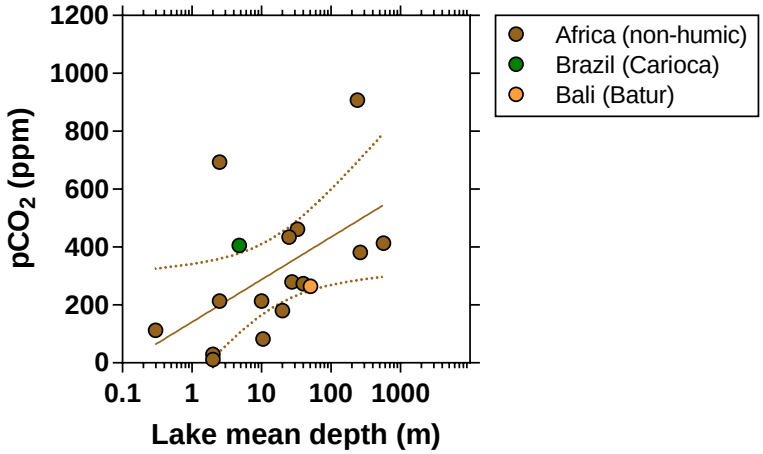

Fig. S18.

Partial pressure of CO_2 (pCO_2) in surface waters versus lake mean depth in non-humic African lakes (this study), Lake Carioca in Brazil (*112*) and Lake Batur in Bali (*113*). Solid line and dotted lines represent the linear regression and the 95% confidence interval based on the African lakes only. The fact that the two non-African lakes fall within (or very close) to the 95% confidence interval is indicative that depth is a good predictor of CO_2 dynamics in non-humic tropical lakes, because depth drives levels of primary productivity (Fig. 2H), although, admittedly based only on two lakes. For consistency, only studies based on direct measurements of pCO_2 were selected, excluding data derived from the computation of pCO_2 from pH and total alkalinity, as this computation can provide erroneous and unrealistically high pCO_2 values (*28*).

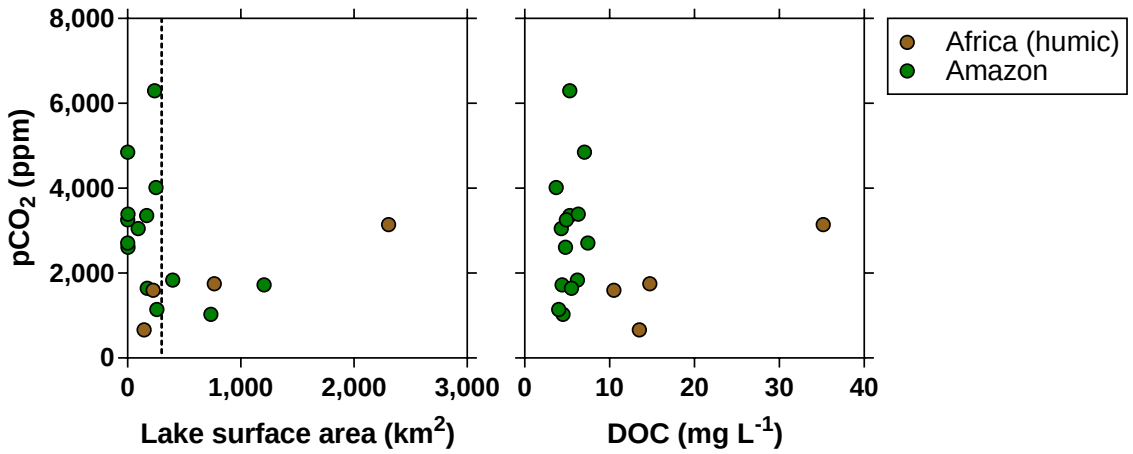

Fig. S19.

Partial pressure of CO_2 (pCO_2) in surface waters versus lake surface area and dissolved organic carbon (DOC) concentration in humic African lakes (this study) and Amazon floodplain lakes (*109*,*114*,*115*). For consistency, only studies based on direct measurements of pCO_2 were selected, excluding data derived from the computation of pCO_2 from pH and total alkalinity, as this computation provides erroneous and unrealistically high pCO_2 values (*28*). We did not find reports of pCO_2 measured directly in humic tropical lakes other than in the Amazon basin. We only selected seasonally resolved studies, so we excluded an additional study reporting pCO_2 measured directly in Amazon floodplain lakes based on single cruise (*116*). The vertical dotted line indicates the threshold surface area (260 km^2) used separate the lakes in HydroLAKES to which different ΔpCO_2 values were used for the scaling of FCO_2. Note that at equivalent DOC values, pCO_2 in the Amazon lakes are higher than in African humic lakes. This might reflect the stronger hydrological connectivity of the Amazon floodplain lakes with the Amazon River, while the sampled African humic lakes were not floodplain lakes, hence more disconnected hydrological isolated from river networks.

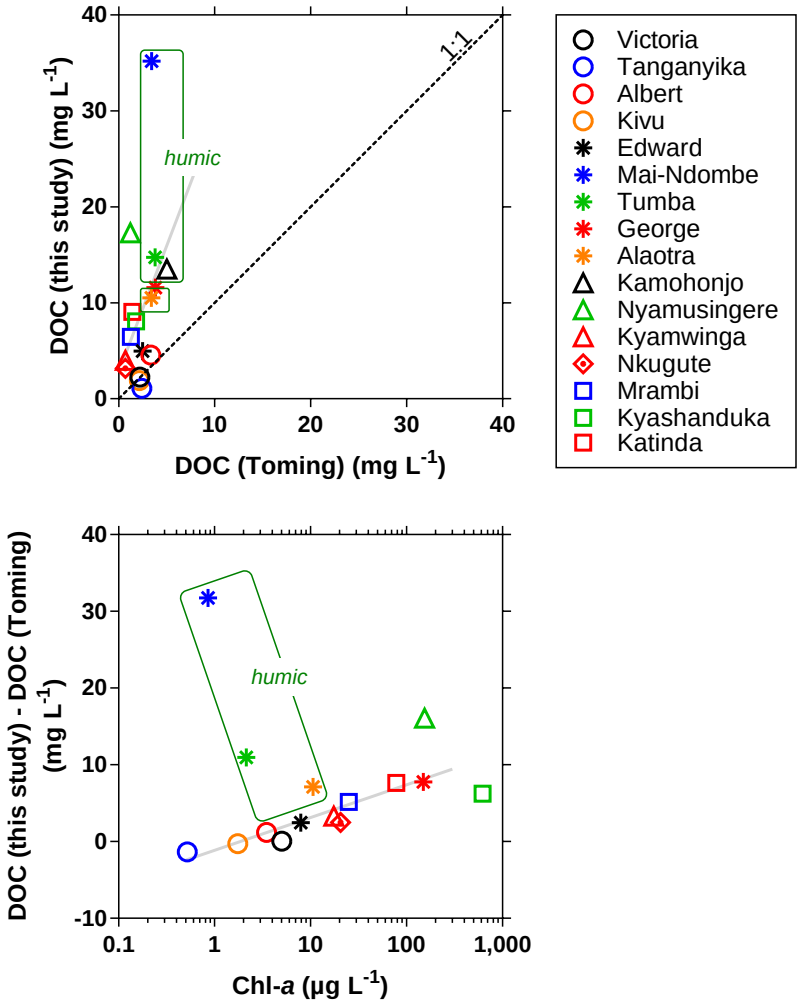

Fig. S20.

Comparison of dissolved organic carbon (DOC) concentration measured in several African tropical lakes ("DOC(this study)") versus modelled DOC ("DOC(Toming)") (*38*) and difference of measured DOC and modelled DOC as function of measured chlorophyll-*a* (Chl-*a*) concentration. The model used as predictors of DOC a combination of precipitation and radiation data from WorldClim (*63*) and lake morphological attributes of HydroLAKES (*29*) and was trained with DOC observations (*117*) almost exclusively from boreal and temperate regions (only 1 tropical lake versus 7,513 boreal and temperate lakes). In African tropical lakes, the model fails to account for DOC inputs from wetlands in humic lakes and for phytoplankton exudation in productive non-humic lakes. Dotted line is the 1:1 line, solid lines are fitted to the data (Table S3).

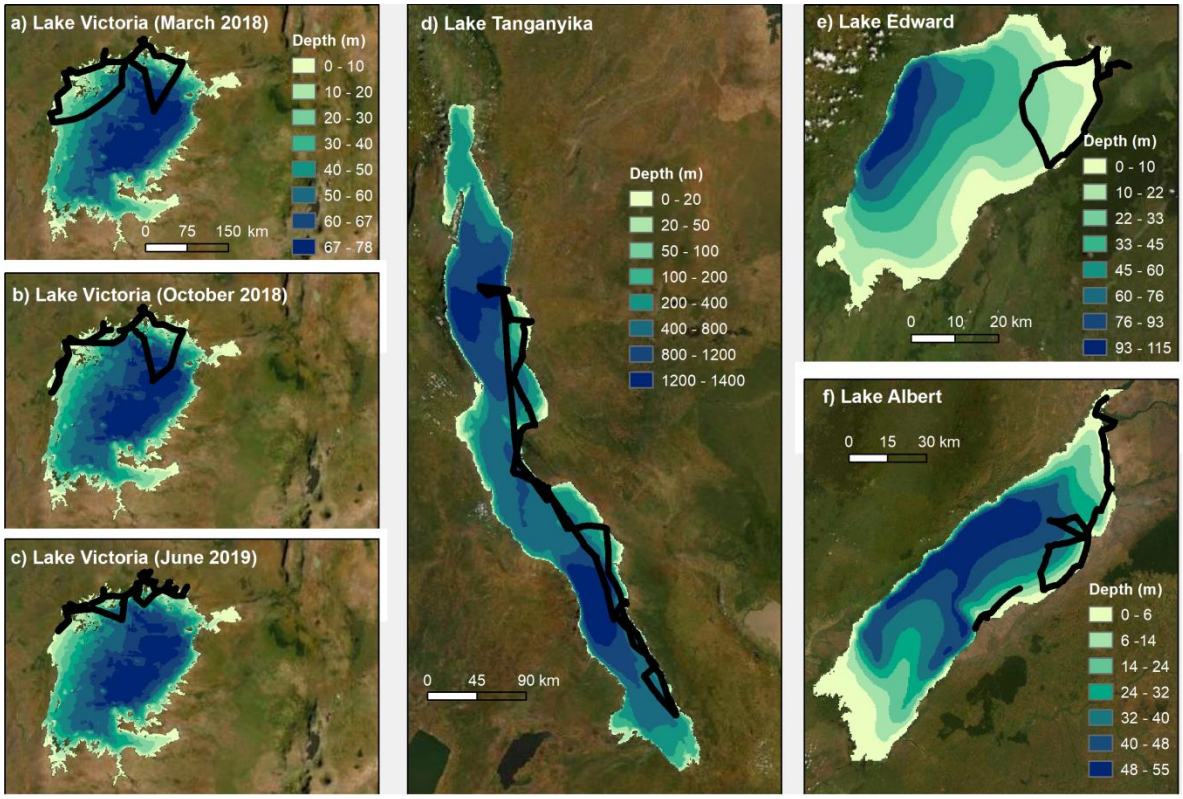

Fig. S21.
Ship tracks during which continuous measurements of partial pressure of CO_2 (pCO_2) and dissolved CH_4 concentration were made in surface waters with an equilibrator (*118*) connected to a laser spectrometer in Lakes Victoria, Tanganyika, Albert and Edward (Table S7).

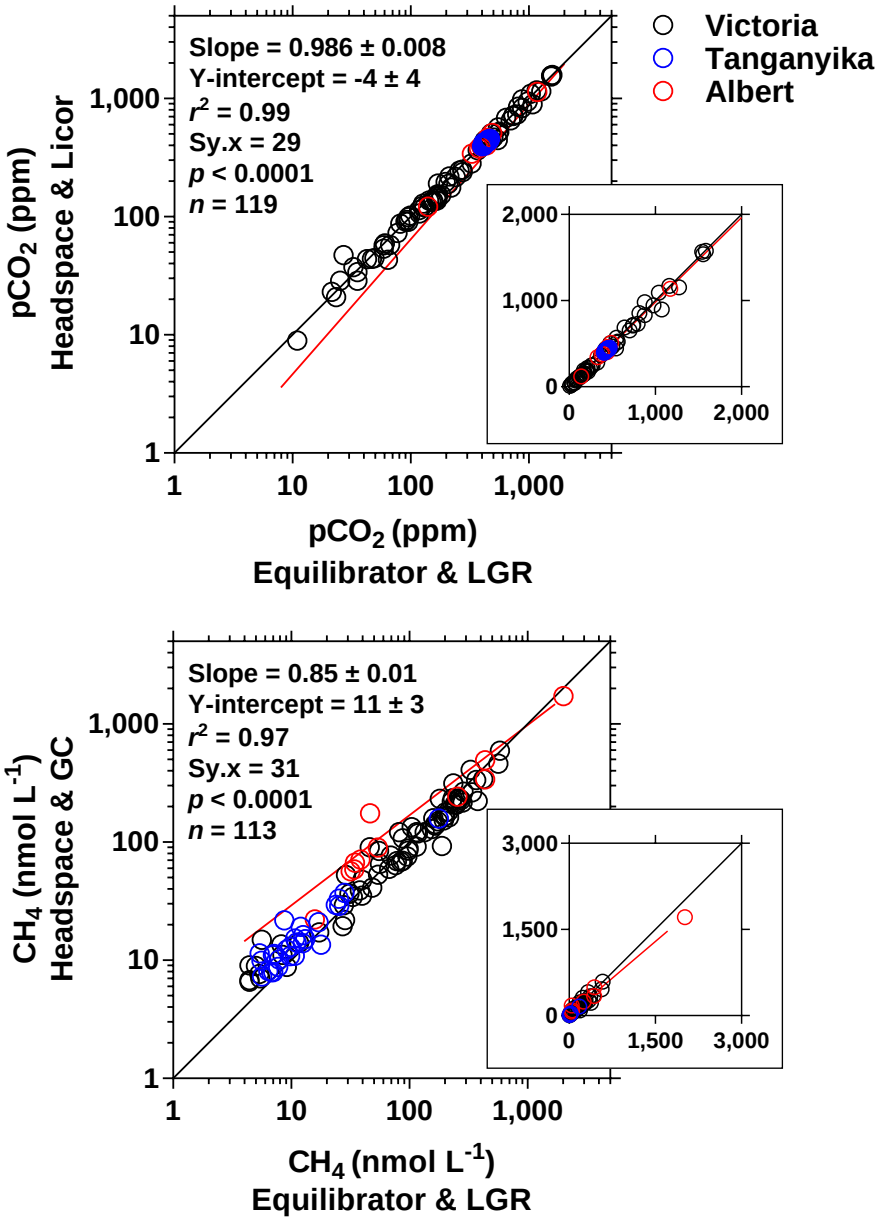

Fig. S22.
Comparison of partial pressure of CO_2 (pCO_2) and dissolved CH_4 concentration measured by two techniques in surface waters of Lakes Victoria, Tanganyika and Albert. On the X-axis, measurements of both pCO_2 and CH_4 with a LGR off-axis integrated cavity output spectroscopy analyzer coupled to an equilibrator (*118*) through which surface water was continuously pumped. On the Y-axis, measurements by headspace from samples collected in surface waters with a Niskin bottle, on-site with an infra-red gas analyzer (Li-cor Li-840) for pCO_2, and in the home laboratory by gas chromatography for CH_4. Insets show data on a linear scale, main panel shows data on a log-log scale. Solid black line shows 1:1 line, solid red line shows the linear regression.

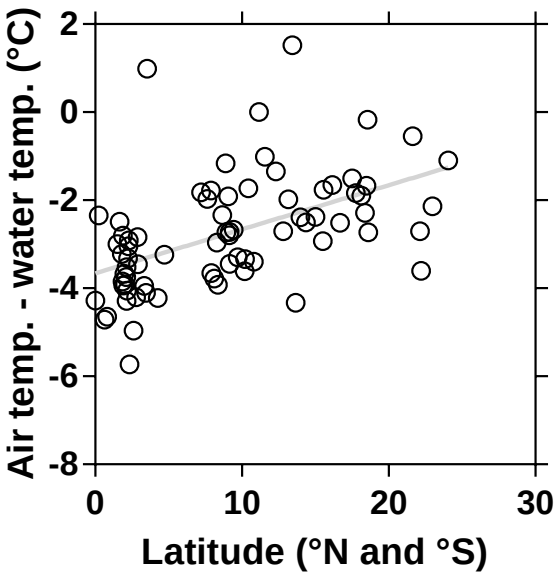

Fig. S23.

Difference of lake surface water temperature in 76 tropical lakes (*67*) and air temperature from WorldClim (*63*) as a function of absolute latitude. Solid line is the fit to the data (Table S3).

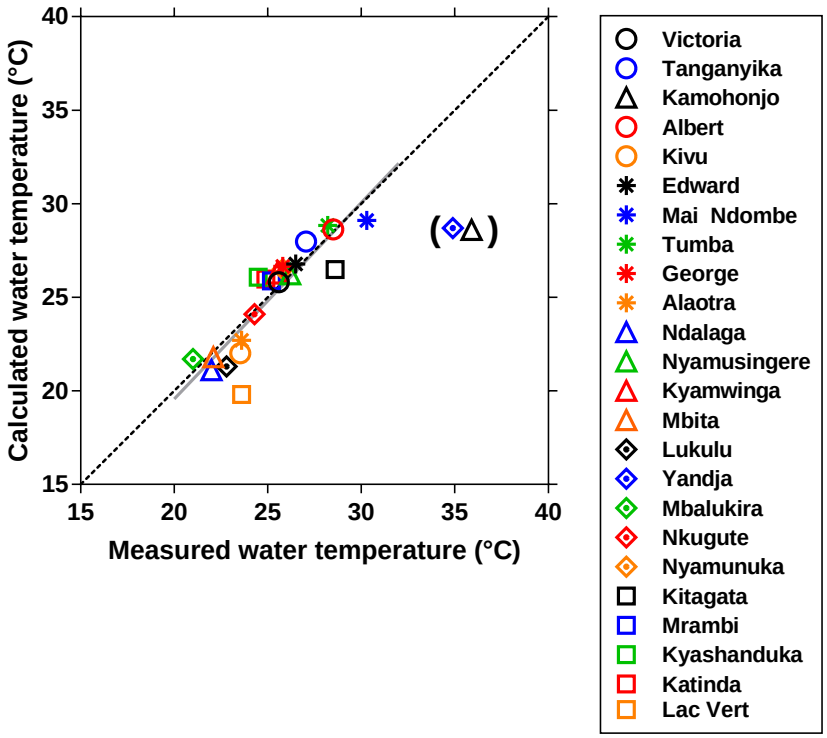

Fig. S24.

Comparison of lake surface water temperature calculated from a relation with air temperature from WorldClim (*63*) (refer to Fig. S23) and average measured water temperature. Solid line is the fit to the data (Table S3).

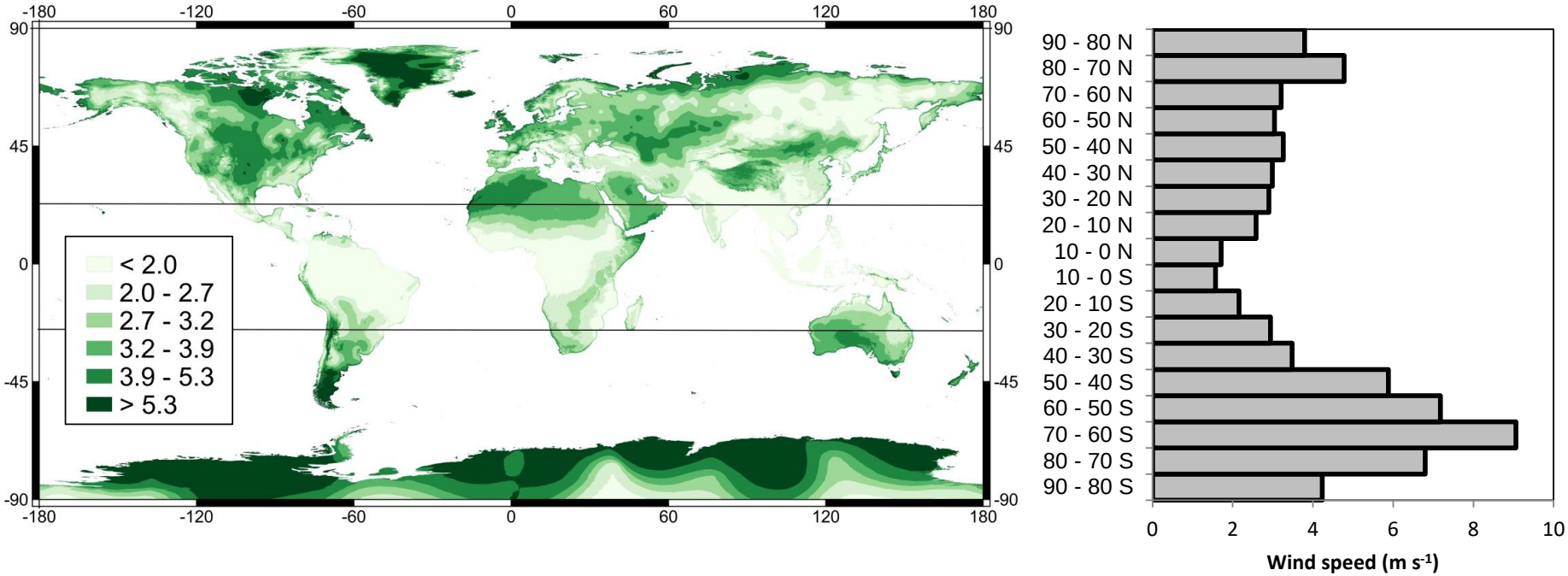

Fig. S25.

Spatial variation of long-term average of wind speed over land from WorldClim (*63*).

Table S1: Morphological and catchment characteristics of the studied lakes, including the 24 sampled African lakes, plus Lake Malawi (*48*). Drainage area and catchment slope were derived from HydroSHEDS (*65*), catchment vegetation biomass from a pantropical national level carbon stock data-set (*97*), and catchment land cover from the Global Land Cover 2000 database of Africa (*98*). The relative coverage of flooded dense forest is indicative of the importance of wetland coverage on the catchment.

Name	Longitude	Latitude	Average depth	Maximum depth	Lake surface elevation	Lake area	Drainage area	Catchment slope	Catchment vegetation biomass	Catchment land cover								
										Cropland	Mosaic veg./croplands	Dense forest	Flooded dense forest	Forest (open)	Mosaic Forest-Shrubland/Grassland	Grasslands	Flooded grasslands	Shrublands
	°E	°N	m	m	m	km^2	km^2	°	Mg km^{-2}	%	%	%	%	%	%	%	%	%
Victoria	32.839	-1.077	40	79	1135	67,075	196,993	2.5	223	13.1	52.1	6.0	0.9	10.2	0.8	8.7	0.1	8.1
Tanganyika	29.485	-6.484	572	1470	774	32,821	208,474	2.3	374	0.6	18.7	19.6	2.1	42.6	0.7	1.6	0.5	13.8
Malawi	34.568	-11.77	264	700	474	29,252	104,722	3.6	301	1.0	26.6	33.0	0.0	17.4	0.9	3.7	0.1	17.4
Albert	30.884	1.622	25	58	615	5,402	53,841	2.1	385	16.0	57.4	14.6	1.8	3.7	0.3	0.1	0.0	6.0
Kivu	29.149	-2.045	240	485	1461	2,371	5,020	6.1	456	3.5	29.5	43.6	1.1	19.5	0.2	0.8	0.0	1.8
Edward	29.565	-0.371	33	117	912	2,253	24,454	4.0	419	14.6	46.7	28.2	2.1	5.6	0.1	1.1	0.0	1.6
Mai Ndombe	18.313	-2.085	2.0	3.7	292	1,955	46,802	0.5	1041	0.0	2.5	51.1	46.2	0.1	0.0	0.0	0.0	0.2
Tumba	18.014	-0.776	1.5	2.9	295	694	6,174	0.4	964	0.0	9.1	50.3	40.6	0.0	0.0	0.0	0.0	0.1
George	30.219	-0.001	2.0	3.0	912	273	9,401	3.2	400	22.4	53.4	16.7	3.6	1.9	0.0	0.6	0.0	1.5
Kamohonjo	45.831	-16.156	0.7	1.6	9	255	2,769	1.3	163	0.0	1.3	17.1	0.1	0.0	2.3	46.9	0.0	32.3
Alaotra	48.521	-17.476	1.2	2.5	2536	195	7,503	2.0	234	0.0	1.8	19.3	0.0	0.0	1.1	44.5	0.0	33.4
Ndalaga	29.007	-1.281	9	20	1712	4.1	12.6	3.9	656	0.0	60.4	39.6	0.0	0.0	0.0	0.0	0.0	0.0
Nyamusingere	30.030	-0.288	1.8	3.8	983	4.0	7.9	0.9	1134	0.0	8.0	86.4	0.0	3.4	0.0	2.3	0.0	0.0
Kyamwinga	30.145	-0.188	20	43	1023	3.1	19.3	2.8	207	30.6	14.6	48.5	0.0	6.3	0.0	0.0	0.0	0.0
Mbita	29.014	-1.215	10	22	1613	2.8	43.7	6.8	642	0.0	91.1	8.9	0.0	0.0	0.0	0.0	0.0	0.0
Lukulu	29.029	-1.261	2.3	5.0	1706	2.2	5.4	1.4	745	0.0	55.2	44.8	0.0	0.0	0.0	0.0	0.0	0.0
Yandja	24.281	0.714	0.6	1.3	375	1.6	160.4	0.3	1011	0.0	35.9	21.0	43.2	0.0	0.0	0.0	0.0	0.0
Mbalukira	29.025	-1.226	6	13	1612	1.6	16.3	4.4	659	0.0	93.9	6.1	0.0	0.0	0.0	0.0	0.0	0.0
Nkugute	30.099	-0.324	26	55	1409	0.9	8.5	7.5	474	20.0	4.2	71.6	0.0	4.2	0.0	0.0	0.0	0.0
Nyamunuka	29.987	-0.090	0.1	0.3	904	0.9	2.8	1.8	192	0.0	36.6	4.9	0.0	19.5	0.0	7.3	0.0	31.7
Kitagata	29.975	-0.064	2.3	5.0	918	0.7	1.5	5.6	141	0.0	0.0	60.0	0.0	40.0	0.0	0.0	0.0	0.0
Mrambi	30.106	-0.230	9	20	1084	0.6	1.1	4.7	382	60.0	6.7	33.3	0.0	0.0	0.0	0.0	0.0	0.0
Kyashanduka	30.050	-0.290	0.9	2.0	1012	0.5	9.1	10.8	683	21.0	15.0	63.0	0.0	1.0	0.0	0.0	0.0	0.0
Katinda	30.106	-0.221	10	21	1041	0.4	0.8	4.9	248	33.3	0.0	66.7	0.0	0.0	0.0	0.0	0.0	0.0
Lac Vert	29.135	-1.614	8	18	1469	0.2	0.3	n.d.	n.d.	0.0	0.0	37.5	0.0	62.5	0.0	0.0	0.0	0.0

Table S2: Seasonally and spatially averaged water temperature (Wat. Temp.), partial pressure of CO_2 (pCO_2), air-water gradient of pCO_2 (ΔpCO_2), dissolved CH_4 concentration, dissolved N_2O concentration, N_2O saturation level ($\%N_2O$) in surface waters, wind speed (sp.) from WorldClim (*63*), air-water flux of CO_2 (*F*CO_2), CH_4 (*F*CH_4, diffusive) and N_2O (*F*N_2O) in 24 African Lakes.

Name	Wat. temp.	pCO_2	ΔpCO_2	CH_4	N_2O	$\%N_2O$	Wind sp.	*F*CO_2	*F*CH_4	*F*N_2O
	°C	ppm	ppm	nmol L^{-1}	nmol L^{-1}	%	m s^{-1}	mmol m^{-2} d^{-1}	mmol m^{-2} d^{-1}	µmol m^{-2} d^{-1}
Victoria	25.6	274	-118	54	7.8	112.6	2.3	-3.2	0.04	0.70
Tanganyika	27.1	412	21	19	5.4	82.4	2.2	0.8	0.01	-0.81
Albert	28.5	435	45	73	8.2	130.0	2.0	1.1	0.06	1.5
Kivu	23.5	907	536	62	7.3	105.0	2.0	13.8	0.04	0.27
Edward	26.5	461	72	145	8.1	122.1	1.9	1.8	0.11	1.1
Mai Ndombe	30.3	3143	2764	250	22.0	381.2	1.1	60.2	0.18	12.1
Tumba	28.2	1752	1373	66	14.1	227.0	1.0	29.0	0.04	5.4
George	25.8	30	-363	124	5.4	78.6	2.1	-9.4	0.09	-1.1
Kamohonjo	35.9	615	231	874	5.3	107.4	2.5	7.6	1.1	0.48
Alaotra	23.6	1628	1232	33	6.5	88.3	2.1	32.1	0.02	-0.64
Ndalaga	22.0			6,491	4.8	63.0	1.8		4.3	-2.0
Nyamusingire	26.2	213	-174	580	4.4	65.9	2.0	-4.5	0.44	-1.8
Kyamwinga	25.5	180	-212	680	5.2	76.2	2.1	-5.5	0.52	-1.3
Mbita	22.1			209	7.6	99.2	1.9		0.14	-0.04
Lukulu	22.8			1,808	5.2	69.2	1.8		1.2	-1.6
Yandja	34.9			960	4.7	97.1	1.1		0.81	-0.13
Mbalukira	21.0			309	17.9	224.0	1.9		0.20	6.7
Nkugute	24.3	280	-109	229	4.9	68.3	2.0	-2.8	0.16	-1.7
Nyamunuka	25.8	112	-276	490,749	0.6	8.1	2.0	-7.1	371.4	-4.8
Kitagata	28.6	693	303	13,858	0.6	10.0	2.0	7.8	11.2	-4.6
Mrambi	25.2	213	-176	494	4.7	67.4	2.1	-4.5	0.37	-1.7
Kyashanduka	24.5	11	-384	118	4.3	60.9	2.0	-9.9	0.08	-2.1
Katinda	24.9	83	-306	136,508	2.6	36.8	2.1	-7.9	101.6	-3.4
Lac Vert	23.6			26,980	4.1	56.7	1.7		18.1	-2.2

Table S3: Equations and statistics at 0.05 level of curve fits of data given in Figures.

Figure	Function	Equation	r^2	*n*	*p*	Comment
2	log (CH_4) versus log (surface area)	y = -0.406x + 3.3742	0.40	24	0.0009	
2	log (CH_4) versus log (mean depth)	y = -0.5245x + 3.2096	0.16	24	0.0561	
2	pCO_2 versus log (surface area)	y = 38.258x + 222	0.14	15	0.1719	excluding 4 humic lakes
2	pCO_2 versus log (mean depth)	y = 110.21x + 167	0.27	15	0.0464	excluding 4 humic lakes
2	$\%N_2O$ versus log (surface area)	y = 10.944x + 58.80	0.44	19	0.0021	excluding 4 humic lakes
2	$\%N_2O$ versus log (mean depth)	y = 18.045x + 55.53	0.28	19	0.0204	excluding 4 humic lakes
2	log (Chl-*a*) versus log (surface area)	y = -0.3292x + 1.7398	0.49	20	0.0004	excluding 4 humic lakes
2	log (Chl-*a*) versus log (mean depth)	y = -0.7764x + 2.066	0.62	20	<0.0001	excluding 4 humic lakes
3	log(pCO_2) versus log (primary production)	y = -1.0125x + 5.4839	0.81	15	<0.0001	
3	log(pCO_2) versus log (Chl-*a*)	y = -0.3872x + 2.9466	0.41	17	0.0068	
3	pCO_2 versus log ($\%O_2$)	y = -8276x + 17244	0.66	15	0.0002	excluding 2 hypersaline lakes
3	pCO_2 versus cyanobacteria abundance	$y = 2980.6e^{-0.034x}$	0.63	17		
3	pCO_2 versus δ^{13}C-DIC	y = -67.536x + 511.16	0.70	17	<0.0001	
3	pCO_2 versus DOC	y = 77.661x + 364	0.74	4	0.1395	humic lakes alone
3	pCO_2 versus DOC	y = -21.7752x + 396	0.28	12	0.0767	excluding 4 humic lakes
3	log(pCO_2) versus log (CDOM SR)	y = -1.8939x + 2.7666	0.25	17	0.0359	
4	CH_4 versus depth (L. Tanganyika <160 m)	y = -27.829ln(x) + 150	0.84	16		
4	CH_4 versus depth (L. Edward)	y = -48.845ln(x) + 169	0.99	3		
4	CH_4 versus depth (L. Albert)	y = -104.622ln(x) + 401	0.83	5		
4	CH_4 versus depth (L. Victoria)	y = -110.535ln(x) + 451	0.96	8		
6	log (CH_4) versus log (Chl-*a*)	y = 0.6981x + 1.9221	0.28	23	0.0088	
6	log (CH_4:CO_2) versus log (Chl-*a*)	y = 1.1226x - 2.7975	0.58	23	0.0004	
8	DOC versus log (Chl-*a*)	y = 4.2116x + 0.8315	0.6	12	0.0028	excluding 3 humic lakes
8	log(DOC) versus cyanobacteria abundance	y = 0.0123x - 0.2676	0.75	12	0.0003	excluding 3 humic lakes
S1	$\%N_2O$ versus $\%NO_3^-$	1.4064x + 52.706	0.23	14	0.0827	
S1	$\%N_2O$ versus $\%NH_4^+$	y = -1.4571x + 196.11	0.24	14	0.0765	
S1	log($\%N_2O$) versus log (primary production)	y = -0.3182x + 2.9195	0.57	14	0.0011	
S1	$\%N_2O$ versus log (Chl-*a*)	y = -55.885x + 169.88	0.35	23	0.0028	
S1	$\%N_2O$ versus DOC	y = 6.1599x + 46.678	0.47	17	0.0025	
S1	$\%N_2O$ versus CDOM SR	y = -94.39x + 250.61	0.32	16	0.0186	
S7	CO_2 versus HCO_3^-	y = 0.0016x + 1.166	0.65	12	0.0016	excluding 4 humic and 2 hypersaline lakes
S11	%CV versus Chl-*a*	y = 2.7709x + 23.609	0.36	18	0.0084	
S14	δCH_4 (dusk - dawn) versus CH_4 @ dusk	y = -0.2691x + 11.197	0.34	16	0.0182	
S18	pCO_2 versus log (mean depth)	y = 110.21x + 167	0.27	15	0.0464	non-humic lakes only
S20	DOC (this study) versus DOC (Toming)	y = 2.6277x + 2.8232	0.15	16	0.1355	
S20	[DOC (this study) - DOC (Toming)] versus Chl-*a*	y = 4.277x - 1.1499	0.64	16	0.0019	
S23	[Air temp - water temp] versus absolute Latitude	y = 0.104x - 3.8563	0.39	72	<0.0001	
S24	Calculated versus measured water temperature	y = 1.0513x - 1.4701	0.79	22	<0.0001	excluding Lakes Yandja and Kamohonjo

Table S4: Air-water flux of CO_2 (*F*CO_2), CH_4 (*F*CH_4, diffusive) and N_2O (*F*N_2O) per m^2 and integrated for African tropical and pan-tropical lakes scaled from relations between air-water gradient of the partial pressure of CO_2 (ΔpCO_2), CH_4 and N_2O saturation level ($\%N_2O$) as a function of depth and based on HydroLAKES data-base of lakes that were classified into humic and non-humic, plus area-averaged extrapolated pCO_2, CH_4, $\%N_2O$, as well as, surface areas (SA), gas transfer velocity (*k*) compared to previous estimates (*1*,*2*,*3*,*4*,*9*,*31*,*47*). Cole et al (*1*) provided an average pCO_2 for African lakes but did not provide estimates regionalized for the tropics. Note that the "African lakes" reported by Cole *et al.* (1) correspond to 39 lakes located in Cameroon formed in volcanic basins (*83*), some of which strongly enriched in magmatic and volcanic CO_2 (*119*). The unrealistic surface area used by (*47*) combines natural lakes and reservoirs. Values with a single asterisk (*) correspond to a scaling using the original HydroLAKES (*29*) surface area, including an unrealistic surface area value of 18,752 km^2 for Lake Chad. Values with a double asterisk (**) were obtained with a more recent surface area value of 2603 km^2 for Lake Chad (*30*). IQR = inter-quartile range.

	SA km^2	*k* cm h^{-1}	pCO_2 ppm	F_{CO2} gC m^2 yr^{-1}	F_{CO2} TgC yr^{-1}	CH_4 nmol L^{-1}	diffusive F_{CH4} gCH_4 m^2 yr^{-1}	diffusiveF_{CH4} $TgCH_4$ yr^{-1}	$\%N_2O$	F_{N2O} mgN_2O-N m^{-2} yr^{-1}	F_{N2O} GgN_2O-N yr^{-1}
African tropical lakes											
This study (*) (L. Chad SA = 18,752 km^2)											
Non-humic	***187,481***	***2.9***	***394***	***0.4 ± 9.7***	***0.08 ± 1.9***	***321***	***1.6 ± 0.4***	***0.3 ± 0.1***	***91***	***-2.7 ± 2.7***	***-0.5 ± 0.5***
Strongly humic	***38,061***	***3.1***	***1,691***	***165.5 ± 42.5***	***6.3 ± 1.6***	***4683***	***26.9 ± 6.1***	***1.0 ± 0.2***	***167***	***19.9 ± 8.1***	***0.8 ± 0.3***
Total	***225,543***	***3.0***	***613***	***28.3 ± 8.4***	***6.4 ± 1.9***	***1057***	***5.8 ± 1.5***	***1.3 ± 0.3***	***104***	***1.1 ± 0.7***	***0.3 ± 0.2***
This study (**) (L. Chad SA = 2603 km^2)											
Non-humic	***187,481***	***2.9***	***394***	***0.4 ± 10.4***	***0.08 ± 2.0***	***321***	***1.6 ± 0.4***	***0.3 ± 0.1***	***91***	***-2.7 ± 2.6***	***-0.5 ± 0.5***
Strongly humic	***21,913***	***3.1***	***1,691***	***147.9 ± 38.0***	***3.2 ± 0.8***	***2205***	***6.8 ± 1.5***	***0.1 ± 0.0***	***167***	***17.9 ± 7.3***	***0.4 ± 0.2***
Total	***209,394***	***3.0***	***530***	***15.9 ± 4.7***	***3.3 ± 1.0***	***518***	***2.1 ± 0.5***	***0.4 ± 0.1***	***99***	***-0.5 ± 0.3***	***-0.1 ± 0.1***
(*4*)	222,062	5.6	934	160.3	35.6						
(*1*)		2.1	2,296	124.0							
(*21*)	229,000									16.1	3.7
Pan-tropical lakes											
This study (*) (L. Chad SA = 18,752 km2)											
Non-humic	***246,925***	***2.9***	***367***	***-2.9 ± 5.9***	***-0.7 ± 1.4***	***334***	***1.6 ± 0.4***	***0.4 ± 0.1***	***86***	***-4.0 ± 3.0***	***-1.0 ± 0.7***
Strongly humic	***92,129***	***3.0***	***2,336***	***230.5 ± 59.9***	***21.2 ± 5.5***	***2255***	***12.7 ± 2.3***	***1.2 ± 0.2***	***167***	***18.9 ± 7.6***	***1.7 ± 0.7***
Total	***339,054***	***2.9***	***902***	***60.5 ± 31.5***	***20.5 ± 10.7***	***856***	***4.6 ± 1.2***	***1.6 ± 0.4***	***108***	***2.3 ± 4.1***	***0.8 ± 1.4***
This study (**) (L. Chad SA = 2603 km2)											
Non-humic	***246,925***	***2.9***	***367***	***-2.9 ± 5.9***	***-0.7 ± 1.5***	***334***	***1.6 ± 0.4***	***0.4 ± 0.4***	***86***	***-4.0 ± 3.0***	***-1.0 ± 1.0***
Strongly humic	***75,980***	***3.0***	***2,336***	***239.3 ± 62.2***	***18.2 ± 4.7***	***1024***	***3.8 ± 0.7***	***0.3 ± 0.3***	***167***	***18.1 ± 7.3***	***1.4 ± 0.6***
Total	***322,905***	***2.9***	***830***	***54.1 ± 28.2***	***17.5 ± 9.1***	***496***	***2.1 ± 0.5***	***0.7 ± 0.7***	***105***	***1.2 ± 2.2***	***0.4 ± 0.2***
(*9*)	585,536	2.1	1,804	176.0	103.1						
(*47*)	1,840,000	4.0	1,900	240.0	441.6						
(*4*)	400,906	5.6	1,906	261.0	104.5						
(*3*)	585,536						5.3	3.1			
(*31*)	345,870									18.7	6.47

Table S5: Ebullitive CH_4 fluxes (FCH_4) measured with inverted funnels (trapping surface area of 0.04 m^2) and diffusive CH_4 fluxes derived from CH_4 concentration and gas transfer velocity (k) computed from wind speed.

Name	Date	Trap deployement duration	Number of traps	Bottom depth	Water temperature	Wind speed	Chl-*a*	CH_4 (surface water)	Diffusive FCH_4	Ebullitve FCH_4
	dd/mm/yyyy	d		m	°C	m s^{-1}	µg L^{-1}	nmol L^{-1}	µmol m^{-2} d^{-1}	µmol m^{-2} d^{-1}
Edward	21-03-2019	2.0	2	10.2	27.0	0.5	33.0	62	36	198 ± 84
George	25-03-2019	1.3	4	2.5	29.2	0.5	57.4	578	363	8,547 ± 395
Nyamusingire	28-03-2019	0.8	6	3.0	25.7	0.5	59.9	1575	909	21,324 ± 788
Victoria	16-06-2019	0.5	1	5.9	25.4	1.5	23.4	220	150	10

Table S6: Median and inter-quartile range of ebullitive CH_4 flux (FCH_4) upscaled to the littoral zone over two depth zones (0-4 and 4-10 m) derived from morphometric relations (*74*) and the mean depth from HydroLAKES (*29*), using the median of ebullitive *F*CH4 measured in African lakes (Table S5) and compiled from literature (Fig. S10) in African tropical lakes and pan-tropical lakes, as well as previously published estimates (*3*). Values with a single asterisk (*) correspond to a scaling using the original HydroLAKES (*29*) surface area, including an unrealistic surface area value of 18,752 km^2 for Lake Chad. Values with a double asterisk (**) were obtained with a more recent surface area value of 2603 km^2 for Lake Chad (*30*).

	Surface area km^2	Median (IQR) Ebullitive FCH_4 $TgCH_4\ yr^{-1}$
African tropical lakes (*)		
This study (0-4 m)	52,133	1.7 (0.6-4.0)
This study (4-10 m)	20,078	0.2 (0.1-0.8)
This study (0-10 m)	72,211	1.9 (0.7-4.6)
Pan-tropical lakes (*)		
This study (0-4 m)	106,951	3.6 (1.2-7.9)
This study (4-10 m)	44,403	0.5 (0.1-1.7)
This study (0-10 m)	151,354	4.0 (1.4-9.7)
African tropical lakes (**)		
This study (0-4 m)	35,985	1.2 (0.4-2.7)
This study (4-10 m)	20,078	0.2 (0.1-0.8)
This study (0-10 m)	56,063	1.4 (0.5-3.5)
Pan-tropical lakes (**)		
This study (0-4 m)	90,803	3.0 (1.1-6.7)
This study (4-10 m)	44,403	0.5 (0.1-1.7)
This study (0-10 m)	135,206	3.5 (1.2-8.5)
Previous studies	585,536	22.2 ± 12.7

Table S7: Sampling dates and number of samples (*n*) collected in surface waters for partial pressure of CO_2 (pCO_2), CH_4 and N_2O concentrations in surface waters in 24 tropical African lakes. Italicized numbers in brackets correspond to continuous measurements in surface waters with an equilibrator and a laser analyzer, other numbers to discrete samples analyzed by headspace technique. All data are unpublished except for the 2007-2009 cruises in Lake Kivu (*49*,*55*).

Name	Sampling dates	pCO_2	CH_4	N_2O
	dd/mm-dd/mm/yyyy	*n* =	*n* =	*n* =
Victoria	29/03-08/04/2018	26 (*7379*)	26 (*7379*)	26
	25/10-04/11/2018	23 (*5976*)	23 (*5976*)	23
	07/06-17/06/2019	30 (*6579*)	30 (*6579*)	30
Tanganyika	08/10-18/10/2019	30 (*7334*)	30 (*7334*)	30
	01/05-07/05/2021	22	22	22
Albert	20/06-23/06/2019	12 (*1364*)	12 (*1364*)	12
Kivu	15/03-29/03/2007	14	14	*nd*
	28/08-10/09/2007	14	14	*nd*
	21/06-03/07/2008	14	14	*nd*
	21/04-05/05/2009	14	14	*nd*
	19/10-27/10/2010	9	9	9
Edward	20/10-04/11/2016	14	14	14
	23/03-31/03/2017	14	14	14
	18/01-02/02/2018	14	14	14
	21/03-30/03/2019	4 (*504*)	4 (*504*)	4 (*504*)
Mai Ndombe	03/05-03/05/2015	1	1	1
Tumba	24/06-24/06/2014	1	1	1
George	24/10-24/10/2016	1	1	1
	01/04-01/04/2017	3	3	3
	28/01-28/01/2018	2	2	2
	25/03-25/03/2019	1	1	1
Kamohonjo	01/10-02/10/2019	9	9	9
Alaotra	23/05-23/05/2019	4	4	4
	19/01-01/02/2019	6	6	6
	26/08-01/09/2019	5	5	5
Ndalaga	30/06-30/06/2011	*nd*	1	1
	01/02-01/02/2012	*nd*	1	1
Nyamusingere	02/11-02/11/2016	5	5	5
	04/04-04/04/2017	1	1	1
	25/01-25/01/2018	1	1	1
	28/03-28/03/2019	2	2	2
Kyamwinga	06/04-06/04/2017	1	1	1
Mbita	02/07-02/07/2011	*nd*	1	1
	02/02-02/02/2012	*nd*	1	1
Lukulu	01/02-01/02/2012	*nd*	1	1
Yandja	06/05-06/05/2010	*nd*	1	1
Mbalukira	01/07-01/07/2011	*nd*	1	1
	31/01-31/01/2012	*nd*	1	1
Nkugute	01/11-01/11/2016	1	1	1
	03/04-03/04/2107	1	1	1
	30/01-30/01/2018	1	1	1
Nyamunuka	02/11-02/11/2016	1	1	1
Kitagata	08/04-08/04/2017	1	1	1
Mrambi	07/04-07/04/2017	1	1	1
Kyashanduka	25/01-25/02/2018	1	1	1
Katinda	06/11-07/11/2016	3	3	3
	05/04-05/04/2017	1	1	1
	31/01-31/01/2018	1	1	1
Lac Vert	28/06-28/06/2011	*nd*	1	1
	29/01-29/01/2012	*nd*	1	1

Table S8: Alternative upscaling of air-water gradient of the partial pressure of CO_2 (ΔpCO_2) and corresponding air-water CO_2 flux (FCO_2) in African lakes using surface areas from Hydrolakes (*29*) but with the more recent and realistic surface area of Lake Chad (*30*). N°1: surface area weighted average for available 25 lakes of ΔpCO_2 = 12 ppm for both humic and non-humic lakes; N°2: ΔpCO_2 = 71.126 x DOC - 367 (r^2=0.53, *p*= 0.0012, *n*=16), where DOC is dissolved organic carbon concentration for both humic and non-humic lakes, and applied to modelled DOC (*35*) for HydroLAKES (*25*), N°3: for non-humic lakes ΔpCO_2 = 50.509 x log(lake surface area) – 165 (r^2=0.17, *p*= 0.1263, *n*=15); for humic lakes ΔpCO_2 = 0.9578 x lake surface area + 583 (r^2=0.86, *p*= 0.0731, *n*=4).

	Surface area km^2	FCO_2 $gC\ m^{-2}\ yr^{-1}$	FCO_2 $TgC\ yr^{-1}$
Alternative up-scaling N°1			
Non-humic African lakes	187,481	1.4	0.3
Strongly humic African lakes	21,913	1.4	0.03
Total African lakes	209,394	1.4	0.3
Alternative up-scaling N°2			
Non-humic African lakes	187,481	-22.5	-4.2
Strongly humic African lakes	21,913	-6.8	-0.1
Total African lakes	209,394	-20.9	-4.4
Alternative up-scaling N°3			
Non-humic African lakes	187,481	5.4	1.02
Strongly humic African lakes	21,913	214.7	4.7
Total African lakes	209,394	27.3	5.7

REFERENCES AND NOTES

1. J. J. Cole, N. F. Caraco, G. W. Kling, T. K. Kratz, Carbon dioxide supersaturation in the surface waters of lakes. *Science* **265**, 1568–1570 (1994).

2. S. Sobek, L. J. Tranvik, J. J. Cole, Temperature independence of carbon dioxide supersaturation in global lakes. *Global Biogeochem. Cycles* **19**, GB2003 (2005).

3. D. Bastviken, L. J. Tranvik, J. A. Downing, P. M. Crill, A. Enrich-Prast, Freshwater methane emissions offset the continental carbon sink. *Science* **331**, 50–50 (2011).

4. P. A. Raymond, J. Hartmann, R. Lauerwald, S. Sobek, C. McDonald, M. Hoover, D. Butman, R. Striegl, E. Mayorga, C. Humborg, P. Kortelainen, H. Dürr, M. Meybeck, P. Ciais, P. Guth, Global carbon dioxide emissions from inland waters. *Nature* **503**, 355–359 (2013).

5. T. DelSontro, J. J. Beaulieu, J. A. Downing, Greenhouse gas emissions from lakes and impoundments: Upscaling in the face of global change. *Limnol. Oceanogr. Lett.* **3**, 64–75 (2018).

6. W. M. Lewis Jr. Tropical limnology. *Annu. Rev. Ecol. Syst.* **18**,159–184 (1987).

7. J. Langeveld, A. F. Bouwman, W. J. van Hoek, L. Vilmin, A. H. W. Beusen, J. M. Mogollón, J. J. Middelburg, Estimating dissolved carbon concentrations in global soils: A global database and model. *SN Appl. Sci.* **2**, 1626 (2020).

8. J. F. Lapierre, P. A. del Giorgio, Geographical and environmental drivers of regional differences in the lake pCO_2 versus DOC relationship across northern landscapes, *J. Geophys. Res.* **117**, G03015 (2012).

9. H. Marotta, C. M. Duarte, S. Sobek, A. Enrich-Prast, Large CO_2 disequilibria in tropical lakes. *Global Biogeochem. Cycles* **23**, GB4022 (2009).

10. S. Kosten, F. Roland, D. M. L. Da Motta Marques, E. H. Van Nes, N. Mazzeo, L. da S. L. Sternberg, M. Scheffer, J. J. Cole, Climate-dependent CO_2 emissions from lakes. *Global Biogeochem. Cycles* **24**, GB2007 (2010).

11. J. R. Helms A. Stubbins, J. D. Ritchie, E. C. Minor, D. J. Kieber, K. Mopper, Absorption spectral slopes and slope ratios as indicators of molecular weight, source, and photobleaching of chromophoric dissolved organic matter. *Limnol. Oceanogr.* **53**, 955–969 (2008).

12. P. A. del Giorgio, R. H. Peters, Patterns in planktonic *P:R* ratios in lakes: Influence of lake trophy and dissolved organic carbon. *Limnol. Oceanogr.* **39**, 772–787 (1994).

13. S. Sobek, G. Algesten, A.-K. Bergström, M. Jansson, L. Tranvik, The catchment and climate regulation of pCO_2 in boreal lakes. *Glob. Change Biol.* **9**, 630–641 (2003).

14. J. P. Casas-Ruiz, J. Jakobsson, P. A. del Giorgio, The role of lake morphometry in modulating surface water carbon concentrations in boreal lakes. *Environ. Res. Lett.* **16**, 074037 (2021).

15. K. Sand-Jensen, P. A. Staehr, Scaling of pelagic metabolism to size, trophy and forest cover in small Danish lakes. *Ecosystems* **10**, 128–142 (2007).

16. R. Wanninkhof, Relationship between wind speed and gas exchange over the ocean. *J. Geophys. Res.* **97**, 7373–7382 (1992).

17. A. V. Borges, F. Darchambeau, T. Lambert, C. Morana, G. H. Allen, E. Tambwe, A. Toengaho Sembaito, T. Mambo, J. Nlandu Wabakhangazi, J.-P. Descy, C. R. Teodoru, S. Bouillon, Variations in dissolved greenhouse gases (CO_2, CH_4, N_2O) in the Congo River network overwhelmingly driven by fluvial-wetland connectivity. *Biogeosciences* **16**, 3801–3834 (2019).

18. C. S. Reynolds, *The Ecology of Phytoplankton* (Cambridge Univ. Press, 2006).

19. M. J. Bogard, P. A. del Giorgio, L. Boutet, M. C. G. Chaves, Y. T. Prairie, A. Merante, A. M. Derry, Oxic water column methanogenesis as a major component of aquatic CH_4 fluxes. *Nat. Commun.*, **5**, 5350 (2014).

20. M. Bižić, T. Klintzsch, D. Ionescu, M. Y. Hindiyeh, M. Günthel, A. M. Muro-Pastor, W. Eckert, T. Urich, F. Keppler, H.-P. Grossart, Aquatic and terrestrial cyanobacteria produce methane. *Sci. Adv.* **6**, eaax5343 (2020).

21. H.-P. Grossart, K. Frindte, C. Dziallas, W. Eckert, K. W. Tang, Microbial methane production in oxygenated water column of an oligotrophic lake. *Proc. Natl. Acad. Sci. U.S.A.* **108**, 19657–19661 (2011).

22. C. Morana, S. Bouillon, V. Nolla-Ardèvol, F. A. E. Roland, W. Okello, J.-P. Descy, A. Nankabirwa, E. Nabafu, D. Springael, A. V. Borges, Methane paradox in tropical lakes? Sedimentary fluxes rather than pelagic production in oxic conditions sustain methanotrophy and emissions to the atmosphere. *Biogeosciences* **17**, 5209–5221 (2020).

23. R. I. Jones, The influence of humic substances on lacustrine planktonic food chains. *Hydrobiologia* **229**, 73–91 (1992).

24. G. Yvon-Durocher, A. P. Allen, D. Bastviken, R. Conrad, C. Gudasz, A. St-Pierre, N. Thanh-Duc, P. A. del Giorgio, Methane fluxes show consistent temperature dependence across microbial to ecosystem scales. *Nature* **507**, 488–491 (2014).

25. P. Kankaala, J. Huotari, T. Tulonen, A. Ojala, Lake-size dependent physical forcing drives carbon dioxide and methane effluxes from lakes in a boreal landscape, *Limnol. Oceanogr.* **58**, 1915–1930 (2013).

26. M. A. Holgerson, P. A. Raymond, Large contribution to inland water CO_2 and CH_4 emissions from very small ponds, *Nat. Geosci.* **9**, 222–226 (2016).

27. S. R. Alin, T. C. Johnson, Carbon cycling in large lakes of the world: A synthesis of production, burial, and lake-atmosphere exchange estimates, *Global Biogeochem. Cycles* **21**, GB3002 (2007).

28. G. Abril, S. Bouillon, F. Darchambeau, C. R. Teodoru, T. R. Marwick, F. Tamooh, F. O. Omengo, N. Geeraert, L. Deirmendjian, P. Polsenaere, A. V. Borges, Technical note: Large overestimation of pCO_2 calculated from pH and alkalinity in acidic, organic-rich freshwaters. *Biogeosciences* **12**, 67–78 (2015).

29. M. L. Messager, B. Lehner, G. Grill, I. Nedeva, O. Schmitt, Estimating the volume and age of water stored in global lakes using a geo-statistical approach. *Nat. Commun.* **7**, 13603 (2016).

30. B. Pham-Duc, F. Sylvestre, F. Papa, F. Frappart, C. Bouchez, J.-F. Crétaux, The Lake Chad hydrology under current climate change. *Sci. Rep.* **10**, 5498 (2020).

31. R. Lauerwald, P. Regnier, V. Figueiredo, A. Enrich-Prast, D. Bastviken, B. Lehner, T. Maavara, P. Raymond, Natural lakes are a minor global source of N_2O to the atmosphere. *Global Biogeochem. Cycles*, **33**, 1564–1581 (2019).

32. J. M. Melack, L. L. Hess, M. Gastil, B. R. Forsberg, S. K. Hamilton, I. B. T. Lima , E. M. L. M. Novo, Regionalization of methane emissions in the Amazon Basin with microwave remote sensing. *Glob. Change Biol.* **10**, 530–544 (2004).

33. M. Saunois, P. Bousquet, B. Poulter, A. Peregon, P. Ciais, J. G. Canadell, E. J. Dlugokencky, G. Etiope, D. Bastviken, S. Houweling, G. Janssens-Maenhout, F. N. Tubiello, S. Castaldi, R. B. Jackson, M. Alexe, V. K. Arora, D. J. Beerling, P. Bergamaschi, D. R. Blake, G. Brailsford, V. Brovkin, L. Bruhwiler, C. Crevoisier, P. Crill, K. Covey, C. Curry, C. Frankenberg, N. Gedney, L. Höglund-Isaksson, M. Ishizawa, A. Ito, F. Joos, H.-S. Kim, T. Kleinen, P. Krummel, J.-F. Lamarque, R. Langenfelds, R. Locatelli, T. Machida, S. Maksyutov, Kyle C. Mc Donald, J. Marshall, J. R. Melton, I. Morino, V. Naik, S. O'Doherty, F.-J. W. Parmentier, P. K. Patra, C. Peng, S. Peng, G. P. Peters, I. Pison, C. Prigent, R. Prinn, M. Ramonet, W. J. Riley, M. Saito, M. Santini, R. Schroeder, I. J. Simpson, R. Spahni, P. Steele, A. Takizawa, B. F. Thornton, H. Tian, Y. Tohjima, N. Viovy, A. Voulgarakis, M. van Weele, Guido R. van der Werf, R. Weiss, C. Wiedinmyer, D. J. Wilton, A. Wiltshire, D. Worthy, D. Wunch, X. Xu, Y. Yoshida, B. Zhang, Z. Zhang, Q. Zhu, The global methane budget. *Earth Syst. Sci. Data* **8**, 697–751 (2016).

34. A. V. Borges, F. Darchambeau, C. R. Teodoru, T. R. Marwick, F. Tamooh, N. Geeraert, F. O. Omengo, F. Guérin, T. Lambert, C. Morana , E. Okuku, S. Bouillon, Globally significant greenhouse gas emissions from African inland waters. *Nat. Geosci.* **8**, 637–642 (2015).

35. A. V. Borges, G. Abril, F. Darchambeau, C. R. Teodoru, J. Deborde, L. O. Vidal, T. Lambert, S. Bouillon, Divergent biophysical controls of aquatic CO_2 and CH_4 in the World's two largest rivers. *Sci. Rep.* **5**, 15614 (2015).

36. J. F. Talling, The annual cycle of stratification and phytoplankton growth in Lake Victoria (East Africa). *Int. Rev. gesamten Hydrobiol., Syst. Beih.* **51**, 545–621 (1966).

37. L. Pinho, C. M. Duarte, H. Marotta, A. Enrich-Prast, Temperature dependence of the relationship between pCO_2 and dissolved organic carbon in lakes. *Biogeosciences* **13**, 865–871 (2016).

38. K. Toming, J. Kotta, E. Uuemaa, S. Sobek, T. Kutser, L. J. Tranvik, Predicting lake dissolved organic carbon at a global scale. *Sci. Rep.* **10**, 8471 (2020).

39. C. Verpoorter, T. Kutser, D. A. Seekell, L. J. Tranvik, A global inventory of lakes based on high-resolution satellite imagery. *Geophys. Res. Lett.* **41**, 6396–6402 (2014).

40. T. W. Drake, P. A. Raymond, R. G. M. Spencer, Terrestrial carbon inputs to inland waters: A current synthesis of estimates and uncertainty. *Limnol. Oceanogr. Lett.* **3**, 132–142 (2018).

41. J. J. Cole, Y. T. Prairie, N. F. Caraco, W. H. McDowell, L. J. Tranvik, R. G. Striegl, C. M. Duarte, P. Kortelainen, J. A. Downing, J. J. Middelburg, J. Melack, Plumbing the global carbon cycle: Integrating inland waters into the terrestrial carbon budget. *Ecosystems* **10**, 172–185 (2007).

42. R. Kindler, J. Siemens, K. Kaiser, D. C. Walmsley, C. Bernhofer, N. Buchmann, P. Cellier, W. Eugster, G. Gleixner, T. Grunwald, A. Heim, A. Ibrom, S. K. Jones, M. Jones, K. Klumpp, W. Kutsch, L. K. Steenberg, S. Lehuger, B. Loubet, R. McKenzie, E. Moors, B. Osborne, K. Pilegaard, C. Rebmann, M. Saunders, M. W. I. Schmidt, M. Schrumpf, J. Seyfferth, U. Skiba, J.-F. Soussana, M. A. Sutton, C. Tefs, B. Vowinckel, M. J. Zeeman, M. Kaupenjohann, Dissolved carbon leaching from soil is a crucial component of net ecosystem carbon balance. *Glob. Change Biol.* **17**, 1167–1185 (2011).

43. W. Liang, W. Zhang, Z. Jin, J. Yan, Y. Lü, S. Wang, B. Fu, S. Li, Q. Ji, F. Gou, S. Fu, S. An, F. Wang, Estimation of global grassland net ecosystem carbon exchange using a model tree ensemble approach. *J. Geophys. Res. Biogeosci.* **125**, e2019JG005034 (2020).

44. J. Zeng, T. Matsunaga, Z.-H. Tan, N. Saigusa, T. Shirai, Y. Tang, S. Peng, Y. Fukuda, Global terrestrial carbon fluxes of 1999–2019 estimated by upscaling eddy covariance data with a random forest. *Sci. Data* **7**, 313 (2020).

45. W. Ludwig, J. L. Probst, S. Kempe, Predicting the oceanic input of organic carbon by continental erosion, *Global Biogeochem. Cycles* **10**, 23–41 (1996).

46. G. Abril, A. V. Borges, Ideas and perspectives: Carbon leaks from flooded land: Do we need to replumb the inland water active pipe? *Biogeosciences* **16**, 769–784 (2019).

47. A. K. Aufdenkampe, E. Mayorga, P. A. Raymond, J. M. Melack, S. C. Doney, S. R. Alin, R. E. Aalto, K. Yoo, Riverine coupling of biogeochemical cycles between land, oceans, and atmosphere. *Front. Ecol. Environ.* **9**, 53–60 (2011).

48. M. J. Ngochera, H. A. Bootsma, Spatial and temporal dynamics of pCO_2 and CO_2 flux in tropical Lake Malawi. *Limnol. Oceanogr.* **65**, 1594–1607 (2020).

49. A. V. Borges, G. Abril, B. Delille, J.-P. Descy, F. Darchambeau, Diffusive methane emissions to the atmosphere from Lake Kivu (Eastern Africa), *J. Geophys. Res.* **116**, G03032 (2011).

50. P. Kortelainen, T. Larmola, M. Rantakari, S. Juutinen, J. Alm, P. J. Martikainen, Lakes as nitrous oxide sources in the boreal landscape. *Glob. Change Biol.* **26**, 1432–1445 (2020).

51. E. O. Okuku, S. Bouillon, M. Tole, A. V. Borges, Diffusive emissions of methane and nitrous oxide from a cascade of tropical hydropower reservoirs in Kenya, *Lakes Reserv.* **24**, 127–135 (2019).

52. C. R. Teodoru, F. C. Nyoni, A. V. Borges, F. Darchambeau, I. Nyambe, S. Bouillon, Spatial variability and temporal dynamics of greenhouse gas (CO_2, CH_4, N_2O) concentrations and fluxes along the Zambezi River mainstem and major tributaries. *Biogeosciences* **12**, 2431–2453 (2015).

53. G. Abril, F. Guérin, S. Richard, R. Delmas, C. Galy-Lacaux, P. Gosse, A. Tremblay, L. Varfalvy, M. Aurelio Dos Santos, B. Matvienko, Carbon dioxide and methane emissions and the carbon budget of a 10-year old tropical reservoir (Petit Saut, French Guiana). *Global Biogeochem. Cycles* **19**, GB4007 (2005).

54. L. Deirmendjian, J.-P. Descy, C. Morana, W. Okello, M. P. Stoyneva-Gärtner, S. Bouillon, A. V. Borges, Limnological changes in Lake Victoria since the mid-20th century, *Freshw. Biol.* **66**, 1630–1647 (2021).

55. A. V. Borges, C. Morana, S. Bouillon, P. Servais, J.-P. Descy, F. Darchambeau, Carbon cycling of Lake Kivu (East Africa): Net autotrophy in the epilimnion and emission of CO_2 to the atmosphere sustained by geogenic inputs. *PLOS ONE* **9**, e109500 (2014).

56. S. Yamamoto, J. B. Alcauskas, T. E. Crozier, Solubility of methane in distilled water and seawater. *J. Chem. Eng. Data* **21**, 78–80 (1976).

57. R. F. Weiss, B. A. Price, Nitrous oxide solubility in water and seawater. *Mar. Chem.* **8**, 347–359 (1980).

58. C. W. Hunt, L. Snyder, J. E. Salisbury, D. Vandemark, W. H. McDowell, SIPCO2: A simple, inexpensive surface water pCO_2 sensor. *Limnol. Oceanogr. Methods* **15**, 291–301 (2017).

59. M. D. Mackey, D. J. Mackey, H. W. Higgins, S. W. Wright, CHEMTAX—A program for estimating class abundances from chemical markers: Application to HPLC measurements of phytoplankton. *Mar. Ecol. Progr. Ser.* **144**, 265–283. (1996).

60. APHA, *Standard Methods For The Examination Of Water And Wastewater* (American Public Health Association, 1998).

61. Standing Committee Of Analysts, *Ammonia in Waters: Methods for the Examination of Waters and Associated Materials* (H.M.S.O., 1981), 16 pp.

62. E. Fluet-Chouinard, B. Lehner, L.-M. Rebelo, F. Papa, S. K. Hamilton, Development of a global inundation map at high spatial resolution from topographic downscaling of coarse-scale remote sensing data. *Remote Sens Environ.* **158**, 348–361 (2015).

63. S. E. Fick, R. J. Hijmans, WorldClim 2: New 1km spatial resolution climate surfaces for global land areas. *Int. J. Climatol.* **37**, 4302–4315 (2017).

64. J. J. Cole, N. F. Caraco, Atmospheric exchange of carbon dioxide in a low-wind oligotrophic lake measured by the addition of SF_6. *Limnol. Oceanogr.* **43**, 647–656 (1998).

65. B. Lehner, K. Verdin, A. Jarvis, New global hydrography derived from spaceborne elevation data. *Eos*, **89**, 93–94 (2008).

66. J.-F. Lapierre, D. A. Seekell, C. T. Filstrup, S. M. Collins, C. Emi Fergus, P. A. Soranno, K. S. Cheruvelil, Continental-scale variation in controls of summer CO2 in United States lakes. *J. Geophys. Res. Biogeosci.* **122**, 875–885 (2017).

67. S. C. Maberly R. A. O'Donnell, R. I. Woolway, M. E. J. Cutler, M. Gong, I. D. Jones, C. J. Merchant, C. A. Miller, E. Politi, E. M. Scott, S. J. Thackeray, A. N. Tyler, Global lake thermal regions shift under climate change, *Nat. Commun.* **11**:1232 (2020).

68. J. Verbeke, Recherches écologiques sur la faune des grands lacs de l'est du Congo belge. Bulletin de l'Institut royal des Sciences naturelles de Belgique : Résultats scientifiques de l'exploration hydrobiologique (1952-1954) des lacs Kivu, Edouard et Albert (1957).

69. S. E. Hamilton, "Creation of a bathymetric map of Lake Victoria, Africa" (2016); http://dx.doi.org/10.7910/DVN/SOEKNR.

70. S. MacIntyre, A. T. Crowe, A. Cortés, L. Arneborg, Turbulence in a small arctic pond. *Limnol. Oceanogr.* **63**, 2337–2358 (2018).

71. D. Vachon, Y. T. Prairie, The ecosystem size and shape dependence of gas transfer velocity versus wind speed relationships in lakes. *Can. J. Fish. Aquat. Sci.* **70**, 1757–1764 (2013).

72. T. DelSontro, L. Boutet, A. St-Pierre, P. A. del Giorgio, Y. T. Prairie, Methane ebullition and diffusion from northern ponds and lakes regulated by the interaction between temperature and system productivity, *Limnol. Oceanogr.* **61**, S62–S77 (2016)

73. M. Wik, P. M. Crill, R. K. Varner, D. Bastviken, Multiyear measurements of ebullitive methane flux from three subarctic lakes. *J. Geophys. Res. Biogeosci.* **118**, 1307–1321 (2013).

74. J. Håkan, A. A. Brolin, L. Håkanson, New approaches to the modelling of lake basin morphometry, *Environ. Model. Assess.* **12**, 213–228 (2007).

75. R. G. Wetzel, *Limnology: Lake & River Ecosystems* (Academic Press, ed. 3, 2001), p. 429.

76. P. A. del Giorgio, J. J. Cole, N. F. Caraco, R. H. Peters, Linking planktonic biomass and metabolism to net gas fluxes in northern temperate lakes. *Ecology* **80**, 1422–1431 (1999).

77. K. Finlay, P. R. Leavitt, A. Patoine, B. Wissel, Magnitudes and controls of organic and inorganic carbon flux through a chain of hardwater lakes on the northern Great Plains, *Limnol. Oceanogr.* **55**, 1551–1564 (2010).

78. H. Marotta, C. M. Duarte, L. Pinho, A. Enrich-Prast, Rainfall leads to increased pCO_2 in Brazilian coastal lakes, *Biogeosciences* **7**, 1607–1614 (2010).

79. M. A. Xenopoulos, D. M. Lodge, J. Frentress, T. A. Kreps, S. D. Bridgham, E. Grossman, C. J. Jackson, Regional comparisons of watershed determinants of dissolved organic carbon in temperate lakes from the Upper Great Lakes region and selected regions globally, *Limnol. Oceanogr.* **48**, 2321–2334 (2003).

80. J. A. Zwart, Z. J. Hanson, J. Vanderwall, D. Bolster, A. Hamlet, S. E. Jones, Spatially explicit, regional-scale simulation of lake carbon fluxes, *Global Biogeochem. Cycles* **32**, 1276–1293 (2018).

81. P. A. Staehr, L. Baastrup-Spohr, K. Sand-Jensen, C. Stedmon, Lake metabolism scales with lake morphometry and catchment conditions, *Aquat. Sci.* **74**, 155–169 (2012)

82. J. P. Casas-Ruiz, R. H. S. Hutchins, P. A. del Giorgio, Total aquatic carbon emissions across the boreal biome of Québec driven by watershed slope. *J. Geophys. Res. Biogeosci.* **126**, e2020JG005863 (2021).

83. G. W. Kling, Comparative transparency, depth of mixing, and stability of stratification in lakes of Cameroon, West Africa, *Limnol. Oceanogr.* **33**, 27–40 (1988).

84. E. G. Stets, D. Butman, C. P. McDonald, S. M. Stackpoole, M. D. DeGrandpre, R. G. Striegl, Carbonate buffering and metabolic controls on carbon dioxide in rivers, *Global Biogeochem. Cycles* **31**, 663–677 (2017).

85. J. Schenk, H. O. Sawakuchi, A. K. Sieczko, G. Pajala ,D. Rudberg, E. Hagberg, K. Fors, H. Laudon, J. Karlsson, D. Bastviken, Methane in lakes: Variability in stable carbon isotopic composition and the potential importance of groundwater input *Front. Earth Sci.* **9**, 722215 (2021).

86. W. E. West, K. P. Creamer, S. E. Jones, Productivity and depth regulate lake contributions to atmospheric methane, *Limnol. Oceanogr.***61**, S51-S61 (2016).

87. Bastviken, D., J. Cole, M. Pace, L. Tranvik, Methane emissions from lakes: Dependence of lake characteristics, two regional assessments, and a global estimate. *Global Biogeochem. Cycles* **18**, GB4009 (2004).

88. F. A. E. Roland, F. Darchambeau, C. Morana, A. V. Borges, Nitrous oxide and methane seasonal variability in the epilimnion of a large tropical meromictic lake (Lake Kivu, East-Africa), *Aquat. Sci.* **79**, 209–218 (2017).

89. K. Desrosiers, T. DelSontro, P. A. del Giorgio, Disproportionate contribution of vegetated habitats to the CH_4 and CO_2 budgets of a boreal lake. *Ecosystems* (2021).

90. E. S. Oliveira Junior, T. J. H. M. van Bergen, J. Nauta, A. Budiša, R. C. H. Aben, S. T. J. Weideveld, C. A. de Souza, C. C. Muniz, J. Roelofs, L. P. M. Lamers, S. Kosten, Water hyacinth's effect on greenhouse gas fluxes: A field study in a wide variety of tropical water bodies, *Ecosystems* **24**,988–1004 (2021).

91. J. E. Fernández, F. Peeters, H. Hofmann, On the methane paradox: Transport from shallow water zones rather than in situ methanogenesis is the major source of CH4in the open surface water of lakes. *J. Geophys. Res. Biogeosci.* **121**, 2717–2726 (2016).

92. T. DelSontro, P. A. del Giorgio, Y. T. Prairie, No longer a paradox: The interaction between physical transport and biological processes explains the spatial distribution of surface water methane within and across lakes, *Ecosystems*, **21**, 1073–1087 (2018).

93. H. Wang, L. Yang, W. Wang, J. Lu, C. Yin, Nitrous oxide (N_2O) fluxes and their relationships with water-sediment characteristics in a hyper-eutrophic shallow lake, China. *J. Geophys. Res.* **112**, G01005 (2007).

94. C. Soued, P. A. del Giorgio, R. Maranger, Nitrous oxide sinks and emissions in boreal aquatic networks in Quebec. *Nat. Geosci.* **9**, 116–120 (2015).

95. M. Mengis, R. Gächter, B. Wehrli, Sources and sinks of nitrous oxide (N_2O) in deep lakes. *Biogeochemistry* **38**, 281–301, (1997).

96. K. Finlay, P. R. Leavitt B. Wissel, Y. T. Prairie, Regulation of spatial and temporal variability of carbon flux in six hard-water lakes of the northern Great Plains, *Limnol. Oceanogr.* **54**, 2553–2564 (2009).

97. A. Baccini, N. Laporte, S. J. Goetz, M. Sun, H. Dong, A first map of tropical Africa's above-ground biomass derived from satellite imagery. *Environ. Res. Lett.* **3**, 045011 (2008).

98. P. Mayaux, E. Bartholomé, S. Fritz, A. Belward, A new land-cover map of Africa for the year 2000. *J. Biogeogr.* **31**, 861–877 (2004).

99. D. Bastviken, A. L. Santoro, H. Marotta, L. Q. Pinho, D. F. Calheiros, Patrick Crill, A. Enrich-Prast, Methane emissions from Pantanal, South America, during the low water season: Toward more comprehensive sampling, *Environ. Sci. Technol.* **44**, 5450–5455 (2010).

100. P. M. Barbosa, J. M. Melack, J. H. F. Amaral, S. MacIntyre, D. Kasper, A. Cortés, V. F. Farjalla, B. R. Forsberg, Dissolved methane concentrations and fluxes to the atmosphere from a tropical floodplain lake, *Biogeochemistry* **148**, 129–151 (2020).

101. P. M. Crill, K. B. Bartlett, J. O. Wilson, D. I. Sebacher, R. C. Harriss, J. M. Melack, S. MacIntyre, L. Lesack, L. Smith-Morrill, Tropospheric methane from an Amazonian floodplain lake, *J. Geophys. Res.* **93**, 1564–1570 (1988).

102. D. Engle, J. M. Melack, Methane emissions from an Amazon floodplain lake: Enhanced release during episodic mixing and during falling water, *Biogeochemistry* **51**,71–90 (2000).

103. A. H. Devol, J. E. Richey, W. A. Clark, S. L. King, L. A. Martinelli, Methane emissions to the troposphere from the Amazon Floodplain, *J. Geophys. Res.* **93**, 1583–1592 (1988).

104. L. K. Smith, W. M. Lewis, J. P. Chanton, G. Cronin, S. K. Hamilton, Methane emissions from the Orinoco River floodplain, Venezuela. *Biogeochemistry* **51**, 113–140 (2000).

105. K. Attermeyer, S. Flury, R. Jayakumar, P. Fiener, K. Steger, V. Arya, F. Wilken, R. van Geldern, K. Premke, Invasive floating macrophytes reduce greenhouse gas emissions from a small tropical lake, *Sci. Rep.* **6**, 20424 (2016)

106. P. M. Barbosa, V. F. Farjalla, J. M. Melack, J. H. F. Amaral, J. S. da Silva, B. R. Forsberg, High rates of methane oxidation in an Amazon floodplain lake. *Biogeochemistry* **137**, 351–365 (2018).

107. R. E. Hecky, R. Mugidde, P. S. Ramlal, M. R. Talbot, G. W. Kling , Multiple stressors cause rapid ecosystem change in Lake Victoria. *Freshw. Biol.* **55**, 19–42 (2010).

108. P. M. Barbosa, J. M. Melack, V. F. Farjalla, J. H. F. Amaral, V. Scofield, B. R. Forsberg, Diffusive methane fluxes from Negro, Solimões and Madeira rivers and fringing lakes in the Amazon basin. *Limnol. Oceanogr.* **61**, S221–S237 (2016).

109. G. Abril, J.-M. Martinez, L. F. Artigas, P. Moreira-Turcq, M. F. Benedetti , L. Vidal, T. Meziane, J.-H. Kim, M. C. Bernardes, N. Savoye, J. Deborde, P. Albéric, M. F. L. Souza, E. L. Souza, F. Roland, Amazon river carbon dioxide outgassing fuelled by wetlands, *Nature* **505**, 395–398 (2014).

110. B. Panneer Selvam, S. Natchimuthu, L. Arunachalam, D. Bastviken, Methane and carbon dioxide emissions from inland waters in India - implications for large scale greenhouse gas balances. *Glob. Change Biol.* **20**, 3397–3407 (2014).

111. M. U. Mendoza-Pascual, M. Itoh, J. I. Aguilar, K. S. A. R. Padilla, R. D. S. Papa, N. Okuda, Controlling factors of methane dynamics in tropical lakes of different depths. *J. Geophys. Res. Biogeosci.* **126**, e2020JG005828 (2021).

112. D. Tonetta, P. A. Staehr, B. Obrador, L. P. Mello Brandão, L. Silva Brighenti, M. Mello Petrucio, F. A. Rodrigues Barbosa, J. F. Bezerra-Neto, Effects of nutrients and organic matter inputs in the gases CO_2 and O_2: A mesocosm study in a tropical lake, *Limnologica* **69**, 1–9 (2018).

113. P. A. Macklin, I. G. N. A. Suryaputra, D. T. Maher, I. R. Santos, Carbon dioxide dynamics in a lake and a reservoir on a tropical island (Bali, Indonesia). *PLOS ONE* **13**, e0198678 (2018).

114. P. Albéric, M. A. P. Pérez, P. Moreira-Turcq, M. F. Benedetti, S. Bouillon, G. Abril, Variation of the isotopic composition of dissolved organic carbon during the runoff cycle in the Amazon River and the floodplains. *C. R. Geosci.* **350**, 65–75 (2018).

115. J. H. F. Amaral, J. M. Melack, P. M. Barbosa, S. MacIntyre, D. Kasper, A. Cortés, T. S. Freire Silva, R. Nunes de Sousa, B. R. Forsberg, Carbon dioxide fluxes to the atmosphere from waters within flooded forests in the Amazon basin. *J. Geophys. Res. Biogeosci.* **125**, e2019JG005293 (2020).

116. M. Call, C. J. Sanders, A. Enrich-Prast, L. Sanders, H. Marotta, I. R. Santos , D. T. Maher, Radon-traced pore-water as a potential source of CO_2 and CH_4 to receding black and clear water environments in the Amazon Basin, *Limnol. Oceanogr. Lett.* **3**, 375–383 (2018).

117. S. Sobek, L. J. Tranvik, , Y. P. Prairie, P. Kortelainen, J. J. Cole Patterns and regulation of dissolved organic carbon: An analysis of 7,500 widely distributed lakes. *Limnol. Oceanogr.* **52**, 1208–1219 (2007).

118. M. Frankignoulle, A. Borges, R. Biondo, A new design of equilibrator to monitor carbon dioxide in highly dynamic and turbid environments. *Water Res.* **35**, 1344–1347 (2001).

119. G. W. Kling, M. A. Clark, G. N. Wagner, H. R. Compton, A. M. Humphrey, J. D. Devine, W. C. Evans, J. P. Lockwood, M. L. Tuttle, E. J. Koenigsberg, The 1986 Lake Nyos gas disaster in Cameroon, West Africa. *Science* **236**, 169–175 (1987).